-TR-58-276
Document No. AD-209171

N

AD-209171

GEOPHYSICAL RESEARCH PAPERS
No. 61

A NUMERICAL INVESTIGATION OF THE BAROTROPIC DEVELOPMENT OF EDDIES

MANFRED M. HOLL

20030528114

December 1958

GRD

GEOPHYSICS RESEARCH DIRECTORATE
AIR FORCE CAMBRIDGE RESEARCH CENTER
AIR RESEARCH AND DEVELOPMENT COMMAND
UNITED STATES AIR FORCE
BEDFORD, MASSACHUSETTS

Requests for additional copies by Agencies of the Department of Defense, their contractors, and other government agencies should be directed to the:

Armed Services Technical Information Agency
Arlington Hall Station
Arlington 12, Virginia

Department of Defense contractors must be established for ASTIA services, or have their 'need-to-know' certified by the cognizant military agency of their project or contract.

All other persons and organizations should apply to the:

U. S. DEPARTMENT OF COMMERCE
OFFICE OF TECHNICAL SERVICES,
WASHINGTON 25, D. C.

AFCRC-TR-58-276
ASTIA Document No. AD 209171

Geophysical Research Papers
No. 61

A NUMERICAL INVESTIGATION OF THE BAROTROPIC DEVELOPMENT OF EDDIES

Manfred M. Holl

December 1958

Atmospheric Circulations Laboratory
GEOPHYSICS RESEARCH DIRECTORATE
AIR FORCE CAMBRIDGE RESEARCH CENTER
AIR RESEARCH AND DEVELOPMENT COMMAND
UNITED STATES AIR FORCE
Bedford, Mass.

ABSTRACT

This paper deals with the formation of eddies in a straight parallel or zonal flow and with the subsequent modification of the flow profile. The fluid is taken to be homogeneous and inviscid. Numerical analogues for the physical equations are developed in detail and are analyzed.

The work begins with the linear theory of dynamic stability. Numerical analogues are developed to determine the evolution of perturbations, sinusoidal along the flow, which are initially prescribed with arbitrary wave number, amplitude, and tilt variations, and which are superimposed on arbitrary flows. These flows are straight-parallel and are unbounded, or are half-bounded or bounded by plane surfaces. Integrations are carried out for an unbounded flow profile with an inflection point. Unstable perturbations are isolated and the unstable spectrum is determined.

A numerical analogue for the finite-amplitude problem, by which one can study the transfer of energy from the mean flow to the eddy is then developed. The most unstable perturbation, linearly determined, is taken as a small but finite disturbance. The integration is carried out and reveals the continued growth of the eddy and the modification of the mean flow.

This method of investigation with added lapse rate and compressibility is discussed as an approach to turbulence, and to the modification of wind shear and lapse rate by the developed eddies. The general problem of numerical analogues for integrations requiring finite time-steps is also briefly discussed.

CONTENTS

ILLUSTRATIONS

A NUMERICAL INVESTIGATION OF THE BAROTROPIC DEVELOPMENT OF EDDIES

1. INTRODUCTION

The study of the behavior of small disturbances superimposed on straight parallel flow originated in classical hydrodynamics in connection with the stability of laminar flow. (For a review of the literature and an excellent bibliography the reader is referred to Lin.[6]) In the present investigation, we treat two-dimensional motions of an inviscid homogeneous fluid.

A straight parallel flow is said to be dynamically stable if all superimposed infinitesimal perturbations die out or remain bounded at all times. Otherwise the flow is unstable and the profile must be considered a transitory state. Rayleigh[8] showed that an inflection point in the flow profile is a necessary condition for instability. Sufficient conditions have been established for flow profiles of certain general types; however, no complete theory has yet been developed.

Considering flow profiles with a point of inflection, Tollmien[9] showed that for symmetrical profiles the existence of a neutral oscillation implies a transition from stable to unstable solutions. In an investigation of unbounded broken profiles, Holmboe[3] found that those having maximum vorticity at the inflection point are unstable, whereas those having minimum vorticity at the inflection point are stable. This condition is apparently not sufficient for flow in a channel. An example which does not conform is a sinusoidal profile in a channel whose width is less than half a wave length of the profile. In this system the boundaries inhibit the development of unstable disturbances. However, if the channel is wider than half a wave length the current is unstable.

(Author's manuscript approved 24 October 1958)

In the present work a method of testing the dynamic stability of arbitrary profiles is developed. Initial value problems are solved by direct numerical integration.

2. THE SYSTEM

The fluid is homogeneous, incompressible, and nonviscous. The model is two-dimensional in the sense that there is no motion--and no variation in any of the fields or boundaries—along the third dimension. The effect of gravity in the model is trivial since we shall not be dealing with any free surfaces, and the gravity field is herewith dismissed. However, for orientation we may refer to the straight parallel flow as being horizontal, parallel to the x-axis, with the speed varying in the vertical along the z-axis, although some applications of the models to meteorological problems may be otherwise orientated.

The total velocity field, $\mathbb{V}$, is considered to be the resultant of two component fields. One of these is the straight parallel flow, $U\mathbf{i}$, which would be a steady state if it existed alone. The other component, $\mathbb{v}$, shall be called the disturbance or perturbation velocity. Only in special cases is the resultant field a steady state. In general the flow evolves. Its evolution shall be absorbed by $\mathbb{v}$, the straight parallel flow being maintained constant by choice. Thus

$$\mathbb{V} = U(z)\mathbf{i} + \mathbb{v}(x,z,t) \qquad (1)$$

Because $\mathbb{v}$ is the difference between two nondivergent fields, we may represent it by a stream function,

$$\mathbb{v} = \mathbf{j} \times \nabla\Psi = u\mathbf{i} + w\mathbf{k} \qquad (2)$$

The total vorticity is given by

$$\nabla \times \mathbb{V} = \nabla \times \left(U\mathbf{i} + \mathring{\mathbf{j}} \times \nabla \psi\right)$$
$$= \left(U' + \nabla^2\psi\right)\mathring{\mathbf{j}} = Q\mathring{\mathbf{j}}$$

The accent, whenever used, denotes differentiation with respect to z. Henceforth the term "vorticity" will be applied only to the scalar magnitude of the vorticity vector since the orientation is always along the unit-vector. The total vorticity is then given by

$$Q = U' + \nabla^2 \psi = U' + q \;, \qquad (3)$$

where q has been written for $\nabla^2\psi$, the perturbation vorticity.

The models to be included are (a) an unbounded fluid, (b) a fluid with a boundary surface below, and (c) a fluid with boundary surfaces below and above. Hereafter these will be called the <u>unbounded</u>, <u>half-bounded</u>, and <u>bounded</u> models, respectively. In any of these, the vorticity field (with boundary conditions) provides a unique determination of the velocity field, and the perturbation vorticity field is chosen as the principal dependent variable.

$$q = q\,(x, z, t) \cdot$$

The mechanism of the evolution is contained in Helmholtz' principle of individual vorticity conservation, $DQ/Dt = 0$. This is developed with the aid of Eqs. (1), (2), and (3) into

$$\frac{\partial q}{\partial t} = \frac{\partial}{\partial x}\left(-Uq + U''\psi\right) - \mathbf{v}\cdot\nabla q$$

(In treating zonal flow, $U''(z)$ is replaced by $U''(z) + f'(z)$ where $f(z)$ is the Coriolis vorticity. $U(z)\hat{i}$ then represents a westerly current, and X and Z are the eastward and northward coordinates, respectively.)

We linearize at this point by considering the flow as zero-order state and the perturbation as first order in smallness.

$$\frac{\partial}{\partial t} q = \frac{\partial}{\partial X}\left(-Uq + U''\Psi\right) . \tag{4}$$

Consequently, we shall be able to consider elements of an x-dependency spectrum singly. The perturbation vorticity of such an element is given by the real part of

$$q\,(z,t)\ e^{ikx} \tag{5}$$

where $q\,(z,t)$ is complex.

The boundary surfaces need not be smooth but, for consistency in this linear treatment, any departure from smooth must necessarily be of the first order in smallness. Furthermore, the boundary deformations must be analyzed and paired element for element with the perturbation. Accompanying Eq. (5), the boundaries are given by the real part of

$$S\ e^{ikx} \tag{6}$$

where S is a complex amplitude factor. So paired, the mechanism will not generate other wave numbers. Completeness is achieved by considering the entire real positive range of k .

At a boundary surface the slope of the streamline must be the same as the slope of the boundary. This condition, integrated with respect to X , gives the linearized relationship

$$\left[\psi = -US \right] e^{ikx} \tag{7}$$

at the boundary levels. In the unbounded and half-bounded models, the additional requirement that the perturbation velocity-field be upper-bounded is imposed.

Applied to the arbitrary element, Eq. (4) becomes

$$\left\{ \frac{\partial}{\partial t} q(z,t) = ik\left[-U(z)q(z,t) + U''(z)\psi(z,t) \right] \right\} e^{ikx} , \tag{8}$$

and the perturbation stream-function is then given by

$$\left\{ \psi''(z,t) - k^2 \psi(z,t) = q(z,t) \right\} e^{ikx} \tag{9}$$

together with the boundary conditions stated in the preceding paragraph.

Since the x-dependency factors out of the system, we shall subsequently omit the e^{ikx} addendum unless specific reference is desired.

The stream-function which satisfies Eq. (9) can be expressed by a Green's function integral*

$$\psi(z,t) = I(z,t) , \tag{10}$$

where

$$I(z,t) \equiv \int \frac{e^{-k|z-\zeta|}}{-2k} q(\zeta,t)\, d\zeta . \tag{11}$$

---

*The integral can be deduced by quasi-physical reasoning based on the superposition of Rayleigh Waves. See Holl.

For the general solution we add the solutions of the reduced equation and get

$$\Psi(z,t) = I(z,t) + C_+ e^{kz} + C_- e^{-kz} ;$$

the complex coefficients, C_+ and C_-, of the harmonic fields are determined by the boundary condtions.

In the unbounded model the fields extend from $z = -\infty$ to $z = \infty$. Arguing that the perturbation velocity field remains finite at $z = \pm\infty$ leads to

$$C_+ = C_- = 0 .$$

The perturbation stream-function for the unbounded model is thus given by

$$\Psi(z,t) = I_{-\infty}^{\infty}(z,t) , \tag{12}$$

in which the subscript denotes the lower—and the superscript the upper—limit of the integral.

In the half-bounded model the fields extend from the boundary at $z = a$ to $z = \infty$. The condition of finiteness leads to $C_+ = 0$. At the boundary surface Eq. (7) must be satisfied.

$$I_a^{\infty}(a,t) + C_- e^{-ka} = -U(a) S ,$$

which determines C_-. The perturbation stream-function for the half-bounded model is thus given by

$$\Psi(z,t) = I_a^{\infty}(z,t) - \left[U(a) S + I_a^{\infty}(a,t) \right] e^{-k(z-a)} \tag{13}$$

In the bounded model the fields extend from the boundary at $z = a$ to the boundary at $z = b$. At both boundary levels Eq. (7) must be satisfied. This gives a pair of simultaneous equations which, when solved for C_+ and C_-, yield:

$$C_+ = \frac{1}{e^{2ka} - e^{2kb}} \Big\{ -e^{ka} I_a^b(a,t) + e^{kb} I_a^b(b,t) - U(a) S_a e^{ka} + U(b) S_b e^{kb} \Big\} , \tag{14}$$

$$C_- = \frac{1}{e^{-2ka} - e^{-2kb}} \Big\{ -e^{-ka} I_a^b(a,t) + e^{-kb} I_a^b(b,t) - U(a) S_a e^{-ka} + U(b) S_b e^{-kb} \Big\} . \tag{15}$$

The subscripts a and b have been attached to S so as to differentiate between the complex amplitude of the corrugation below and the complex amplitude of the corrugation above. The perturbation stream-function for the bounded model is thus given by

$$\psi(z,t) = I_a^b(z,t) + C_+ e^{kz} + C_- e^{-kz} \tag{16}$$

where C_+ and C_- are given by Eqs. (14) and (15), respectively.

Regarding the unbounded model, there is a special case which is of interest and which requires special treatment. This is the case of periodicity in z. The straight parallel flow and the initial disturbance are periodic in z, and they have the same period so that the periodicty will be maintained. The perturbation vorticity at all times satisfies the relationship

$$q(z,t) = q(z + nH,t) \tag{17}$$

where H is the period and $n = \ldots -2, -1, 0, 1, 2 \ldots$

To treat this problem we need focus our attention on only a single layer, from $z = a$ to $z = b$, of thickness $H = b - a$. We develop $\psi(z,t)$ in this layer, that is, where $a \leqq z \leqq b$, as follows:

$$\psi(z,t) = \int_{-\infty}^{\infty} \frac{e^{-k|z-\zeta|}}{-2k} q(\zeta,t)\, d\zeta$$

$$= \sum_n \int_{a+nH}^{b+nH} \frac{e^{-k|z-\zeta|}}{-2k} q(\zeta,t)\, d\zeta \, .$$

Put $\zeta = s + nH$, and, by virtue of Eq. (17),

$$\psi(z,t) = \sum_n \int_a^b \frac{e^{-k|z-s-nH|}}{-2k} q(s,t)\, ds \, .$$

Subsequently,

$$\psi(z,t) = \int_a^b \frac{e^{-k|z-s|}}{-2k} q(s,t)\, ds$$

$$+ \sum_{n=1}^{\infty} \int_a^b \frac{e^{-k(z+s+nH)}}{-2k} q(s,t)\, ds$$

$$+ \sum_{-n=1}^{\infty} \int_a^b \frac{e^{-k(z-s-nH)}}{-2k} q(s,t)\, ds$$

$$= I_a^b(z,t)$$

$$+ \; e^{-k(b-z)} \, I_a^b(a,t) \sum_{n=1}^{\infty} e^{-k(n-1)H}$$

$$+ \; e^{-k(z-a)} \, I_a^b(b,t) \sum_{-n=1}^{\infty} e^{k(n+1)H}$$

Whereupon, summing the series,

$$\psi(z,t) = I_a^b(z,t) + \frac{I_a^b(a,t)}{1-e^{-kH}} \, e^{-k(b-z)} \tag{18}$$

$$+ \; \frac{I_a^b(b,t)}{1-e^{-kH}} \, e^{-k(z-a)}$$

These boundary-fitting solutions of the stream-function, Eqs. (12), (13), (16), and (18), when introduced in the tendency equation, Eq. (3), give, in each case, a single all-inclusive governing equation. The equation is sufficiently complicated to make the finding of even very special analytic solutions exceedingly difficult. Besides, what is desired here is a solution method which is applicable to any arbitrary initial disturbance superimposed on any arbitrary profile. To at least partially achieve this, we must use numerical methods; and we shall find that the expressions we have developed are well suited for numerical treatment.

3. NUMERICAL METHODS, AN INTRODUCTION

Finite-region fields in general cannot be completely specified by a finite number of pieces of data. In fact not even is the exact value at a point relayable. However, for numerical tractability, fields must be defined (that is, approximated) by a finite set of rounded-off numbers necessarily accompanied by an interpretation scheme. This discretization can be accomplished in characteristically different ways.

The most common method, that associated with direct measurement, is to give the value of a field, by a rounded number, at each of a finite number of points in the region and, in addition, to specify some interpolation scheme. Usually there is some order in the spacing of these points.

In another common method the field is expressed as a linear combination of a given finite set of analytic functions. The value and derivatives of each of these functions can be computed, from its analytic form, to any desired accuracy at any point in the region. The field is defined by a set of rounded numbers which are interpreted, in a prescribed order, as the combination coefficients of the analytic functions in the linear combination.

A fixed number of pieces of data represents only so much information no matter which method is used. One method may give a better approximation than another in particular cases, but basically one method is as capable as any other. In fact, the two methods are equivalent if interpolation in the first is based on the fitting of the functions, used in the second, to the data at the given points. The choice of method rests on peculiarities of the particular problem. If functions can be found which are indigenous to the system of equations, such that their use makes the problem more tractable, then the second method may be preferable.

Generally the first method, with a uniform spacing of points (called a grid) is used. And it is often used with mixed interpolations (low-order polynomials) even at the same place in a particular field. It is up to numerical analysis to determine if such inconsistency is permissible. It is numerical analysis, the investigation of the method for accuracy and economy, which gives confidence in the method and results therefrom.

We shall use the grid discretization. The equations and boundary conditions which define the continuous fields must be transformed so that they define the discrete fields. This is generally done by evaluating the equations at each of the grid points. Differentials in these equations are approximated by corresponding differences so that algebraic equations, called finite-difference equations, result. The error introduced by these approximations is called truncation error because it can be regarded as due to truncating series representations of the derivatives.

P. D. Thompson* indicated the merits in developing the finite-difference equations by an averaging of the differential equations over finite elemental regions referred to the grid points. He has shown that certain undesirable biases in the finite-difference equations are eliminated in this way.

A necessary condition which must be satisfied by the finite-difference equations is that they approach the equations which they approximate as the space and time increments tend toward zero. However, this is not sufficient to insure that the discrete fields computed from the finite-difference equations will approximate the behavior of the continuous fields defined by the differential equations; the usurper here is computational instability, an apparent "blowing up" of the round-off error.

Certain finite-difference equations are referred to as "marching" equations because of their use. They are similar to recurrence formulae. Values at successive points are given in terms of those that came before. The discretization of initial value problems always results in marching equations.

In well-behaved marching equations the round-off errors are random and largely self-cancelling, while in others they may grow rapidly and soon swamp out all significant digits. What happens in the latter is actually a systematic growth of error, due to a more or less complicated interplay of round-off errors.

*Private communication.

An elementary example of a marching equation which is computationally unstable is the recurrence formula for Bessel functions of increasing order at any fixed value of x,

$$J_{n+1}(x) = \frac{2n}{x} J_n(x) - J_{n-1}(x), \quad (n=1,2,\ldots).$$

In linear theory the mechanism of computational instability is relatively simple. Several forms are recognized. One is the admission of extraneous solutions which amplify more rapidly than the desired solution. This is the cause of instability in the above equation. The Neumann function of increasing order is also a solution of this recurrence formula. The least round-off error admits the Neumann function into the marching equation and, as the Bessel component decreases, the Neumann component amplifies rapidly. In addition, at each step, new round-off error changes the composition of the solution.

This recurrence formula is thus inadequate to compute more than just a few Bessel terms. On the other hand, as a recurrence formula for Neumann functions, the above is computationally stable. Now the Bessel functions are the extraneous solutions, but these dampen and are of less importance than the purely random round-off errors. We shall again encounter this problem of extraneous solutions later on.

Some problems in mathematical physics become tractable by only a partial discretization. We shall also encounter an example of this situation.

Discretization transforms fields into vectors. Each piece of specifying data can be interpreted as a component of this vector in some prescribed order. In a grid discretization the components are given by the values at the grid points. Hence a field which is unknown becomes a vector with as many unknown components as there are points in the field. And when the differential equation which determines this field is transformed, we get one algebraic equation per point—thus the same determinateness is maintained. The resulting system of algebraic equations can generally be written in matrix notation, a form which is also suitable for numerical analysis.

4. THE SPACE DISCRETIZATION

In this section we carry out the discretization of the z-dependency, the t-dependency being left continuous. The z continuum is replaced by the points $z = Mh$, $M = 0, \pm 1, \pm 2, \ldots$ where h is a fixed increment. The integer M will be called the "address" of the point $z = Mh$, and will be used as a labeling subscript. Our principal dependent field, $q(z,t)$, becomes a vector, $\underset{\sim}{q}(t)$, $q_M(t)$ being its M component.

Applied at the arbitrary point $z = Mh$, our governing equation, Eq. (8), tells us that

$$\frac{d}{dt} q_M(t) = ik \left[-U_M q_M(t) + U''_M \psi_M(t) \right] \tag{19}$$

We have developed four expressions for $\psi(z,t)$ depending on the boundary condtions. We are now going to develop the corresponding expressions for $\underset{\sim}{\psi}(t)$, to be given in terms of $\psi_M(t)$, its M component.

We begin this transformation by evaluating the integral $I_a^b(z,t)$ at the arbitrary point $z = Mh$. The grid is placed so that the level $z = a$ coincides with the point whose address is M_a. The fixed increment, h, is chosen so that the level $z = b$ coincides with another grid point, whose address shall be M_b, and so that the number of points in between captures the desired amount of detail.

By expressing the integral as the sum of two parts,

$$I_{M_a h}^{M_b h}(Mh,t) = I_{M_a h}^{Mh}(Mh,t) + I_{Mh}^{M_b h}(Mh,t),$$

we can remove the absolute value notation in the integrands.

We shall show the development of one of these (the second part) and proceed as follows:

$$I_{Mh}^{M_b h}(Mh,t) = \int_{Mh}^{M_b h} \frac{e^{k[Mh-\zeta]}}{-2k} q(\zeta,t)\, d\zeta$$

$$= \sum_{m=0}^{M_b-M-1} \int_{[M+m]h}^{[M+m+1]h} \frac{e^{k[Mh-\zeta]}}{-2k} q(\zeta,t)\, d\zeta$$

Next replace the dummy variable ζ by s where $\zeta = [M+m]h + s$. We get

$$I_{Mh}^{M_b h}(Mh,t) = \sum_{m=0}^{M_b-M-1} \frac{K^m}{-2k} \int_0^h e^{-ks} q(s,t)\, ds, \tag{20}$$

where $K = e^{-kh}$. At this point we must specify the interpolation scheme. For $q(s,t)$, in the interval $0 \leqq s \leqq h$ where q varies from $q_{M+m}^{(t)}$ to $q_{M+m+1}^{(t)}$, we introduce

$$q(s,t) = q_{M+m}^{(t)} + \frac{s}{h}\left[q_{M+m+1}^{(t)} - q_{M+m}^{(t)}\right] + \epsilon, \tag{21}$$

where ϵ is the so-called truncation error in this expression. The advantage in using linear interpolation will be seen in the resulting simplicity of the operational matrix, particularly when boundaries are involved.

If $q(z,t)$ is analytic in z, we can develop a series expression for the truncation error. We may write

$$q(s) = q_{M+m} + (q')_{M+m} s + (q'')_{M+m} s^2/2! + \ldots \tag{22}$$

which is a Maclaurin series expansion about $z = (M+m)h$. Successive derivatives can be eliminated by evaluating Eq. (22) at other grid points. We eliminate the first derivative by substituting for it from

$$q_{M+m+1} = q_{M+m} + (q')_{M+m} h + (q'')_{M+m} h^2/2! + \ldots$$

and get

$$q(s) = q_{M+m} + \frac{s}{h}\left(q_{M+m+1} - q_{M+m}\right) + (q'')_{M+m}\frac{s^2}{2!}\left(1 - \frac{h}{s}\right)$$

$$+ (q''')_{M+m}\frac{s^3}{3!}\left(1 - \frac{h^2}{s^2}\right) + \ldots$$

This gives

$$\epsilon = (q'')_{M+m}\frac{s^2}{2!}\left(1 - \frac{h}{s}\right) + (q''')_{M+m}\frac{s^3}{3!}\left(1 - \frac{h^2}{s^2}\right) + \ldots \qquad (23)$$

Proceeding with evaluating our integral, we introduce Eq. (21) into Eq. (20) which we develop as follows:

$$I_{Mh}^{M_b h}(Mh, t)$$

$$= \sum_{m=0}^{M_b - M - 1} \frac{K^m}{-2k} \int_0^h e^{-ks}\left\{ q_{M+m} + \frac{s}{h}\left[q_{M+m+1} - q_{M+m}\right] + \epsilon \right\} ds$$

$$= \sum_{m=0}^{M_b - M - 1} \frac{K^m}{-2k}\left\{ q_{M+m}\int_0^h e^{-ks}\,ds + \frac{q_{M+m+1} - q_{M+m}}{h}\int_0^h s e^{-ks}\,ds + \int_0^h \epsilon e^{-ks}\,ds \right\}$$

$$= \sum_{m=0}^{M_b-M-1} \frac{K^m}{-2k} \left\{ q_{M+m} K_1 + q_{M+m+1} K_2 + \epsilon_1 \right\}$$

where

$$K_1 = \frac{kh + e^{-kh} - 1}{hk^2} \; ; \qquad K_2 = \frac{1-(1+kh)e^{-kh}}{hk^2}, \tag{24}$$

and

$$\epsilon_1 = \int_0^h \epsilon \, e^{-ks} ds = -\frac{h^3}{12} (q'')_{M+m} + \left[\begin{matrix}\text{terms of higher} \\ \text{order in } h\end{matrix}\right]$$

In numerical analysis, the value of judging truncation error on the basis of a few terms of the error series is dubious and this practice can be carried too far. At the stage where truncation error becomes troublesome, the validity of such an approximation becomes questionable. Furthermore, there is a tendency for such approximations to give a false sense of security in higher-order interpolation schemes, whereas, in practice the arrival of intolerable gross-truncation-error in computations is probably little delayed by such schemes. More consideration should be given to the use of tighter grids (that is, smaller h) which results in a more significant actual reduction of truncation error.

In making real predictions from initial data, some investigators object to the use of tighter grids. They feel the number of grid points should not exceed the number of initial observations of the field. They also feel that computations should be carried out with no more than the number of significant digits in the observations. We believe these notions are incorrect.

It is important to distinguish between the types of error with which we are dealing. The initial error in the fields is due to limited observations. Truncation error is due to the disparity between finite-difference equations and differential equations. Because we are trying to duplicate a differential process it behooves us to use as tight a grid as is economically feasible; and, enough digits to give a significant difference between neighbouring grid points should be carried.

In the absence of any subjective analysis skill, the initial values of the fields at the grid points are computed from some objective interpolation scheme. Extra grid points thus do not add to the specification of the fields at the initial moment but at moments after the initial. The values at the extra grid points are not redundant and play a significant role in holding down truncation error.

If it could be shown that physical differential processes are transformable into algebraic relationships between values at grid points without differentially dependent truncation error, then the comments of the preceding two paragraphs could be ruled out.

Returning from this digression to our problem, we accept the truncation error by dropping ϵ. This error can be estimated by visually superimposing linear interpolation on a plot of q vs. z.

In our development we have reached

$$I_{Mh}^{M_b h}(Mh,t) = \frac{K_1}{-2k}\sum_{m=0}^{M_b-M-1} K^m q_{M+m} + \frac{K_2}{-2k}\sum_{m=0}^{M_b-M-1} K^m q_{M+m+1} .$$

In the second summation, put $m = \bar{m} - 1$.

$$I_{Mh}^{M_b h}(Mh,t) = \frac{K_1}{-2k}\sum_{m=0}^{M_b-M-1} K^m q_{M+m} + \frac{K_2}{-2kK}\sum_{\bar{m}=1}^{M_b-M} K^{\bar{m}} q_{M+\bar{m}} .$$

Since $\bar{m}$ is only a dummy, we can drop the bar, that is, we can replace $\bar{m}$ by m. If we now express the first term of the first summation separately and add and subtract an extra term on its end,

$$\int_{Mh}^{M_b h}(Mh,t) = \frac{K_1}{-2k} q_M + \frac{K_1}{-2k}\sum_{m=1}^{M_b-M} K^m q_{M+m} - \frac{K_1}{-2k} K^{M_b-M} q_{M_b} + \frac{K_2}{-2kK}\sum_{m=1}^{M_b-M} K^m q_{M+m},$$

then we can recombine the two summations. Thus

$$\int_{Mh}^{M_b h}(Mh,t) = \frac{K_1}{-2k} q_M + \frac{K_3}{-2k}\sum_{m=1}^{M_b-M} K^m q_{M+m} - \frac{K_1}{-2k} K^{M_b-M} q_{M_b},$$

where

$$K_3 = K_1 + \frac{K_2}{K} = \left[e^{kh} + e^{-kh} - 2\right] \Big/ hk^2 . \tag{25}$$

By a similar treatment we find

$$\int_{M_a h}^{Mh}(Mh,t) = \frac{K_1}{-2k} q_M + \frac{K_3}{-2k}\sum_{m=1}^{M-M_a} K^m q_{M-m} - \frac{K_1}{-2k} K^{M-M_a} q_{M_a} .$$

Adding the two parts of the integral completes its evaluation at the arbitrary point $z = Mh$.

$$\int_{M_a h}^{M_b h}(Mh,t) = \frac{1}{-2k}\Bigg[2K_1 q_M + K_3 \sum_{m=1}^{M_b-M} K^m q_{M+m} \tag{26}$$

$$+ K_3 \sum_{m=1}^{M-M_a} K^m q_{M-m} - K_1 K^{M_b-M} q_{M_b} - K_1 K^{M-M_a} q_{M_a}\Bigg]$$

The two other integrals which need be evaluated can readily be found from this one. The first results when M_b goes to infinity. Eq. (26) becomes

$$I_{M_a h}^{\infty}(Mh,t) = \frac{1}{-2k}\left[2K_1 q_M + K_3 \sum_{m=1}^{\infty} K^m q_{M+m} + K_3 \sum_{m=1}^{M-M_a} K^m q_{M-m} - K_1 K^{M-M_a} q_{M_a}\right]. \tag{27}$$

The second results when in addition we let M_a go to minus infinity.

$$I_{-\infty}^{\infty}(Mh,t) = \frac{1}{-2k}\left[2K_1 q_M + K_3 \sum_{m=1}^{\infty} K^m q_{M+m} + K_3 \sum_{m=1}^{\infty} K^m q_{M-m}\right]. \tag{28}$$

We may now readily complete the four expressions for $\psi_M(t)$ corresponding to the different boundary conditions. We already have it for the unbounded model. According to Eq. (12) page 6, it is given by Eq.(28):

$$\psi_M(t) = \frac{1}{-2k}\left[2K_1 q_M + K_3 \sum_{m=1}^{\infty} K^m q_{M+m} + K_3 \sum_{m=1}^{\infty} K^m q_{M-m}\right] \tag{29}$$

At this point we should make some remark as to what is going to be done with the infinite series. In computing, these must of course be terminated; and, in practice, one can at most compute the evolution throughout a finite layer of the fluid (with the exception of the z-periodic case). This necessarily restricts the type of profiles that can be handled with this method if there is to be any standard of accuracy. Since the stream function at any level in the layer is to be computed only from the vorticity in the layer, it is required that the ignored vorticity, q, outside of the layer we are considering is—and is expected to remain—negligible in comparison with the vorticity in the layer. The method is valid if this is initially so, and will remain valid the longer the smaller U'' is outside the layer. Fortunately the condition can be checked quite simply. The vorticity at the end points of the layer may be regarded as an indicator of the magnitude of the neglected outside vorticity. If these end vorticities become appreciable, again by comparison, then the method begins to break down as increasing error flows in from the outside.

In the absence of boundaries, the addresses of the extreme points of the layer shall be given by M_U for the upper and M_L for the lower. The upper limits of the summations are thus replaced by $M_U - M$ for ∞ and by $M - M_L$ for $-\infty$. We shall also at this point introduce the notation

$$\sum_{m=1}^{M_U - M} K^m q_{M+m} = (q_M)_u \; ; \; \sum_{m=1}^{M-M_L} K^m q_{M-m} = (q_M)_l \tag{30}$$

where the subscripts u and l indicate that the weighted summation is to be taken over all the upper grid points and over all the lower grid points, respectively.

The stream function of the unbounded model is given, with this notation, by

$$\psi_M(t) = \frac{1}{-2k}\left[2K_1 q_M + K_3 (q_M)_u + K_3 (q_M)_l\right] , \tag{31}$$

in which it is understood that the q_M's are functions of time.

We now move on to the stream function of the half-bounded model as given by Eq. (13) page 6 . The discretization is accomplished with the help of Eq. (27) for the integrals. Substituting as before $z = Mh$, $a = M_a h$ and labeling the uppermost point by M_u , we find that

$$\psi_M(t) = \frac{1}{-2k}\left[2K_1 q_M + K_3 \sum_{m=1}^{M_u-M} K^m q_{M+m} + K_3 \sum_{m=1}^{M-M_a} K^m q_{M-m} - K_1 K^{M-M_a} q_{M_a}\right] + \frac{1}{2k}\left[-2kU(a)S + 2K_1 q_{M_a} + K_3 \sum_{m=1}^{M_u-M} K^m q_{M_a-m} - K_1 K^{M-M_a} q_{M_a}\right] ,$$

wherein the term $K_1 K^{M-M_a} q_{M_a}$ appears twice and cancels. Since the summations extend over all the grid points above or all the grid points below, we again adopt the notation, Eq. (30). Hence, for the <u>half-bounded</u> model,

$$\psi_M(t) = \frac{1}{-2k}\left[2K_1 q_M + K_3 (q_M)_u + K_3 (q_M)_l\right] + \frac{1}{2k}\left[-2kU(a)S + 2K_1 q_{M_a} + K_3 (q_{M_a})_u\right] K^{M-M_a} . \tag{32}$$

In the same way, with the help of Eq. (26), the stream function of the bounded model, as given by Eq. (16), page 7, and the stream function of the z-periodic case, as given by Eq. (18), are discretized.

If we introduce generalized star functions, $*_1$ and $*_2$, all four expressions for the stream function can be given by one expression:

$$\Psi_M(t) = \frac{1}{-2k}\left[2K_1 q_M + K_3 (q_M)_u + K_3 (q_M)_l\right] \tag{33}$$

$$+ \frac{K_3}{2k} *_1 K^{M_b - M} + \frac{K_3}{2k} *_2 K^{M - M_a} \quad .$$

The corresponding star functions are given as follows:

For the unbounded model,

$$*_1 = *_2 = 0 \quad . \tag{34}$$

For the half-bounded model,

$$\begin{aligned} *_1 &= 0 \\ *_2 &= K_4 q_{M_a} + (q_{M_a})_u + S_0 \quad . \end{aligned} \tag{35}$$

For the bounded model,

$$\begin{aligned} *_1 &= -K_b\left[K_4 q_{M_a} + (q_{M_a})_u\right] + K_a\left[K_4 q_{M_b} + (q_{M_b})_l\right] + S_1 \\ *_2 &= K_a\left[K_4 q_{M_a} + (q_{M_a})_u\right] - K_b\left[K_4 q_{M_b} + (q_{M_b})_l\right] + S_2 \quad . \end{aligned} \tag{36}$$

For the z-periodic unbounded model,

$$\begin{aligned} *_1 &= \frac{-1}{1 - K^{M_b - M_a}}\left[K_4 \frac{q_{M_a} - q_{M_b}}{2} + (q_{M_a})_u\right] \\ *_2 &= \frac{-1}{1 - K^{M_b - M_a}}\left[K_4 \frac{q_{M_b} - q_{M_a}}{2} + (q_{M_a})_l\right] \quad . \end{aligned} \tag{37}$$

The explanation of the new notations follows:

$$K_4 = \frac{2K_1}{K_3} = \frac{(e^{-kh}+2kh)+(e^{-kh}-2)}{e^{kh}+(e^{-kh}-2)} \tag{38}$$

$$\left.\begin{aligned} K_a &= K^{M_a}\, K^{M_a}/(K^{2M_a}-K^{2M_b}) \\ K_b &= K^{M_b}\, K^{M_a}/(K^{2M_a}-K^{2M_b}) \end{aligned}\right\} \tag{39}$$

$$S_0 = -2k\,U(a)\,S/K_3 \tag{40}$$

$$\left.\begin{aligned} S_1 &= K_a K^{M_b}\left[U(a)\,2k\,K^{-M_a} S_a - U(b)\,2k\,K^{-M_b} S_b\right]/K_3 \\ S_2 &= -K_a K^{-M_a}\left[U(a)\,2k\,K^{M_a} S_a - U(b)\,2k\,K^{M_b} S_b\right]/K_3 \end{aligned}\right\} . \tag{41}$$

Substitution of Eq. (33) into Eq. (19) yields the tendency of the arbitrary component $q_M(t)$:

$$\begin{aligned} \frac{d}{dt} q_M = -\iota\Big[\mu_M q_M + \nu_M\{(q_M)_u + (q_M)_l\} \\ - \nu_M *_1 K^{M_b-M} - \nu_M *_2 K^{M-M_a}\Big] , \end{aligned} \tag{42}$$

where

$$\mu_M = kU_M + U''_M K_1 \; ; \quad \nu_M = U''_M K_3/2 \quad . \tag{43}$$

It should be apparent that these formulae have been designed for simplicity in computing. For a given problem, the S's and K's are all constants; and μ_M and ν_M are components of constant vectors. The q_M's and the star functions are functions of time. The star functions are computed at any instant from the constants and from q_{M_a}, q_{M_b}, $(q_{M_a})_u$ and $(q_{M_b})_\ell$, and are independent of M.

There is an all-important feature on which rests the simplicity and economy of these formulae for computational purposes. As can be seen from Eq. (30):

$$
\begin{aligned}
(q_M)_u &= K\left[(q_{M+1})_u + q_{M+1}\right] \\
(q_M)_\ell &= K\left[(q_{M-1})_\ell + q_{M-1}\right] .
\end{aligned}
\tag{44}
$$

It is these recurrence formulae which make it possible to compute the tendency, at all grid points, by making at most only five computing traverses of the grid points, no matter how many points there are in all. The procedure is as follows:

a. Beginning with the top point and progressing downward, the contribution of the term containing $(q_M)_u$ is computed at each point with the help of Eq. (44).

b. Beginning at the bottom, the contribution of the term containing $(q_M)_\ell$ is computed at each point also making use of Eq. (44). Upon completion of these first two traverses the two star functions are evaluated.

c. Then, beginning at the top, the contribution of the term containing $*_1 \, K^{M_b - M}$ is computed at each point.

d. Beginning at the bottom, the contribution of the term containing $*_2 \, K^{M - M_a}$ is computed at each point. These latter two traverses require only a multiplication by K in progressing with the factor from one point to the next.

e. The contribution of the term containing q_M may be obtained by a separate traverse, or may be combined with one of the other traverses.

At this stage, we may ask about the applicability of this investigation method. For one thing, $U''(z)$ must be continuous. Should we desire to investigate particular profiles in which this is not the case, then we must either use a modified procedure or we can make an approximation to the flow profile by fitting to it a curve which has a continuous second derivative.

The perturbation vorticity distribution in z is being approximated by a linear interpolation between grid points. The magnitude of the space increment, h , must be sufficiently small so that linear interpolation will closely approximate the initial distribution. Whether the interpolation will yield a good approximation at later times depends also on the smoothness of $U(z)$ and $U''(z)$. Hence, h must be chosen sufficiently small to also capture the detail of these functions. Even with these precautions the linear interpolation of q during its evolution may become completely inadequate. This is called the arrival of the intolerable gross-truncation-error.

5. EIGENSOLUTIONS AND COMPUTATIONAL STABILITY

For purposes of numerical analysis the governing set of linear equations which is represented by Eq. (42) is written in matrix notation:

$$\frac{d}{dt}\, \underset{\sim}{q}(t) = -i\left[\underset{\approx}{C}\, \underset{\sim}{q}(t) + \underset{\sim}{d}\right] \tag{45}$$

The coefficient matrix, $\underset{\approx}{C}$, has only real constant elements. The constant vector, $\underset{\sim}{d}$, arises from the deformation of the boundary surfaces and may be complex. The presence of the boundary surfaces, but not their deformation, affects the elements of $\underset{\approx}{C}$.

The evolution of initial perturbations can be determined without discretizing the t continuum. Partial discretization has made the problem tractable but the work is prohibitive unless $\underset{\sim}{q}(t)$ has few components. The solution method is based on the expansion of the initial field into a linear combination of eigensolutions.

A particular solution of Eq. (45) is the steady state

$$\underset{\sim}{q}_s = -\underset{\approx}{C}^{-1}\underset{\sim}{d} \ . \tag{46}$$

This may not be the most general steady state with wave number $\underline{k}$.

For the complete solution of Eq. (45) we must add to $\underset{\sim}{q}_s$ the general solution of the reduced equation,

$$\frac{d}{dt}\underset{\sim}{q}(t) = -i\underset{\approx}{C}\,\underset{\sim}{q}(t) \ . \tag{47}$$

Introducing the eigensolution

$$\underset{\sim}{q}(t) = \hat{q}\,e^{-i\lambda t} \ , \tag{48}$$

into Eq. (47) leads to

$$-\lambda\hat{q} = -\underset{\approx}{C}\,\hat{q} \ .$$

This is equivalent to

$$\left(\underset{\approx}{C} - \lambda\underset{\approx}{I}\right)\hat{q} = \underset{\sim}{0} \ , \tag{49}$$

where $\underset{\approx}{I}$ is the identity (or unit) matrix.

This system of linear equations, Eq. (49), being homogeneous is overprescribed (thus cannot have any solution) unless the determinant of the coefficient matrix vanishes:

$$\left|\underset{\approx}{C} - \lambda\underset{\approx}{I}\right| = 0 \ . \tag{50}$$

This is a polynomial in λ and is called the characteristic polynomial of the matrix $\underset{\approx}{C}$. Its order is that of the matrix. Thus it has in general as many different roots as we have grid points. These are called the latent roots of $\underset{\approx}{C}$ and are the eigenvalues which we seek. Corresponding to each latent root λ_n there is a non-zero vector which satisfies

$$\underset{\approx}{C}\,\underset{\sim}{q}_n = \lambda_n \underset{\sim}{q}_n . \tag{51}$$

These are the latent vectors of $\underset{\approx}{C}$ and are the eigenvectors which we seek. They are indeterminate to the extent of an arbitrary factor. Thus we may add that they be normalized, that is, $|\underset{\sim}{q}_n| = 1$.

If Eq. (50) admits $\lambda = 0$ as a solution, then the corresponding eigenvector can be combined with $\underset{\sim}{q}_s$ to form a more general steady state.

Because, in general, there are as many different eigensolutions as there are grid points, the set of eigensolutions is complete. That is, by a proper choice of complex weighting coefficients, a linear combination of the eigensolutions added to $\underset{\sim}{q}_s$ can be made to fit <u>any</u> initial vector $\underset{\sim}{q}_0$ and thus will give its subsequent evolution.

Because $\underset{\approx}{C}$ has all real elements, its latent roots are either real or occur in complex conjugate pairs. If, as a special case, $\underset{\approx}{C}$ is symmetric as well, then all its roots must be real. However, the roots of an asymmetric matrix may also all be real.

For a real latent root it is clear that the corresponding latent vector can always be chosen so as to be real. If not so chosen, its real and imaginary parts must be parallel.

If $\underset{\sim}{q} = \underset{\sim}{A}_0 + i\underset{\sim}{B}_0$ corresponds to one latent root of a complex conjugate pair then $\underset{\sim}{q} = \underset{\sim}{A}_0 - i\underset{\sim}{B}_0$ corresponds to the other, $\underset{\sim}{A}_0$ and $\underset{\sim}{B}_0$ here being real and not parallel. These statements can be verified by substitution in Eq. (51).

The above remarks have a bearing on the "tilt" of the eigensolutions. To introduce the tilt concept we must first return our x dependency. The eigensolution is then given by

$$\underset{\sim}{q}(x,t) = R_e : \underset{\sim}{q}\, e^{-i\lambda t}\, e^{ikx} \tag{52}$$

The substitution of $\underset{\sim}{q} = \underset{\sim}{A}_o + i\underset{\sim}{B}_o$ and $\lambda = \mu + i\nu$, where $\underset{\sim}{A}_o$, $\underset{\sim}{B}_o$, μ and ν are real, leads to

$$\underset{\sim}{q}(x,t) = e^{\nu t}\left[\underset{\sim}{A}_o \cos(kx-\mu t) - \underset{\sim}{B}_o \sin(kx-\mu t)\right]$$

$$= e^{\nu t}\, \underset{\sim}{D}_o \cos(kx - \mu t - \underset{\sim}{\phi}_o) \; .$$

The components of $\underset{\sim}{D}_o$, the amplitude vector, and $\underset{\sim}{\phi}_o$, the phase-angle vector, are given by

$$D_{o_M} = \left(A^2_{o_M} + B^2_{o_M}\right)^{1/2}$$

$$\Phi_{c_M} = \arctan\left(-B_{o_M}/A_{o_M}\right) .$$

If ϕ_{c_M} varies with M (that is, with the height z) we say that the wave "tilts." The shape of the nodal "line" is given by the nodal vector $\underset{\sim}{x} = \underset{\sim}{\phi}_o / k$.

The eigensolution which has a real eigenvalue (a real latent root) yields a neutral wave which has no tilt. The eigensolution which has a complex eigenvalue (one of a complex conjugate pair of latent roots) yields a tilting wave.

A complex conjugate pair of eigenvalues yields one amplifying wave and one damping wave. These have parallel amplitude vectors and equal but opposite tilt. Where the nodal line of one tilts forward, the nodal line of the other tilts backward by the same amount.

The dynamic stability properties of the flow profile are revealed by the eigensolutions. In actual fluids, flow of smaller scale (down to and including Brownian motion) will generate them. Thus, if Eq. (50) admits any complex conjugate pair of latent roots, the perturbation will grow indefinitely as it contains an exponentially amplifying eigensolution. The profile must then be considered a transient state as it is dynamically unstable.

The eigensolution synthesis method of solving an initial-value problem presents a formidable task which might be entertained if we are dealing with a small number of components. It is more feasible to complete the discretization. Discretizing the time dependency results in a marching equation.

In proceeding to discretize, one discovers that for our system there are a number of finite-difference analogues which satisfy the necessary condition for validity mentioned on page 11. The choice among these is made according to which of the analogues <u>preserves the nature</u> of the time-continuous system as revealed by its eigensolutions. We shall examine some of the analogues in this manner which has been expounded by Hyman[4] and others.

The t continuum is replaced by the discrete values $t = N\tau$ where N is an integer and τ is the time increment. The integer N will be used as a labeling subscript. The continuously varying vector $\underset{\sim}{q}(t)$ is thus replaced by discrete values: $\underset{\sim}{q}_N$ at the time $t = N\tau$.

The resulting marching equation also has characteristic solutions. We shall call these the τ eigensolutions. They have the form

$$\underset{\sim}{q}_N = \underset{\sim}{q}\,\gamma^N , \tag{53}$$

whereas the eigensolutions evaluated at $t = N\tau$ are given by

$$\underset{\sim}{q}(N\tau) = \underset{\sim}{q}\,\left(e^{-i\lambda\tau}\right)^N . \tag{54}$$

We shall see that the eigenvectors are unchanged by the discretization. Hence the change suffered by a particular eigensolution is entirely revealed by the disparity between $e^{-i\lambda\tau}$ and γ.

All the valid analogues of Eq. (45), page 25,* have the same particular solution as has Eq. (45) as given by Eq. (46). For this reason we shall refer the analogues directly to the reduced system, Eq. (47), thus avoiding the repetitious reduction in each case.

The first analogue we shall examine results when a forward first-order difference is introduced for the derivative. The system, Eq. (47), becomes

$$\left[\underset{\sim}{q}_{N+1} - \underset{\sim}{q}_N\right]/\tau = -i\underset{\approx}{C}\,\underset{\sim}{q}_N \,.$$

Substitution of Eq. (53) results in

$$\left(\underset{\approx}{C} - \frac{1-\gamma}{i\tau}\underset{\approx}{I}\right)\underset{\sim}{q} = \underset{\sim}{0} \,. \qquad (55)$$

Hence

$$\left|\underset{\approx}{C} - \frac{1-\gamma}{i\tau}\underset{\approx}{I}\right| = 0 \,,$$

which restricts γ. Comparison with Eq. (50) reveals that $(1-\gamma)/i\tau$ can be identified with λ. That is, corresponding to each eigensolution with eigenvalue λ_N satisfying Eq. (50) we have a τ eigensolution whose τ eigenvalue, γ_n, is given by

$$\gamma_n = 1 - i\tau\lambda_n \,.$$

Also revealed by Eq. (55) is that the τ eigenvectors are the same as the corresponding eigenvectors.

Corresponding to a real λ, $|\gamma|^2 = 1 + (\tau\lambda)^2$, that is, the magnitude of γ is greater than one. This means that all neutral waves are converted into amplifying waves by the discretization. We need investigate no further; this analogue is computationally unstable.

We next examine the centered second-order analogue which has received such wide use for a first-order system that it can be called the "conventional" analogue. For Eq. (47) it takes the form

$$\left[\underset{\sim}{q}_{N+1} - \underset{\sim}{q}_{N-1} \right] / 2\tau = -i \underset{\approx}{C}\, \underset{\sim}{q}_N \tag{56}$$

Substitution of Eq. (53) results in

$$\left(\underset{\approx}{C} - \frac{1-\gamma^2}{i2\tau\gamma} \underset{\approx}{I} \right) \underset{\sim}{q} = \underset{\sim}{0} .$$

Thus, according to Eq. (50) the γ's are given by

$$(1-\gamma_n^2)/i2\tau\gamma_n = \lambda_n ;$$

that is

$$\gamma_n = \pm \left[1 - (\tau\lambda_n)^2 \right]^{1/2} - i\tau\lambda_n$$

Each λ gives rise to two values of γ for the same eigenvector —twice as many τ eigensolutions as there are eigensolutions! This multiplicity is needed for completeness because both the initial-value vector and the vector at $N = 1$ must be accommodated. Both these vectors must be specified before one can begin to march with Eq. (56).

This analogue hardly preserves the nature of the first-order tendency system which it purports to approximate. It actually has a nature corresponding to a second-order tendency equation.

Comparison with $e^{-i\lambda\tau}$ shows that the roots given by the plus sign,

$$\gamma_{n+} = +\left[1 - (\tau\lambda_n)^2\right]^{1/2} - i\tau\lambda_n , \tag{57}$$

are the proper roots. But we must attach a condition for the computational stability of this set of roots. For a real λ_n (neutral wave).

$$|\gamma_{n+}|^2 = 1 - (\tau\lambda_n)^2 + (\tau\lambda_n)^2 = 1$$

provided the square root of Eq. (57) is real, that is, provided

$$\tau \leq 1/|\lambda| \tag{58}$$

According to Rayleigh's theorem, neutral waves move with the speed of the basic current at some level in the flow.* The translation speed of the neutral wave is given by λ/k , hence

$$|\lambda|_{max} \leq k|U|_{max} .$$

Introduced into Eq. (58), this yields the possibly stronger condition (that is, sufficient but perhaps not necessary):

$$\tau \leq 1/k|U|_{max} .$$

For a given τ this defines a critical wave number:

$$k_c = 1/\tau|U|_{max} .$$

*See, e.g., Garcia[1], p. 90.

Neutral waves with a longer wave length ($k < k_c$) are preserved neutral but those with a shorter wave length ($k > k_c$) may be computationally amplified.

The presence of the extraneous roots is far more cause for alarm. Were it not for round-off, q_1 could be chosen in complete accord with $\underset{\sim}{q}_0$ and the proper $\tilde{\tau}$ eigensolutions. Unfortunately, the extraneous τ eigensolutions do enter into the computing as a result of round-off, or more rapidly by an incompatible first-time-step (for example, a forward step).

Corresponding to a propagating neutral wave (λ_n real) the extraneous τ eigensolution introduces an additional neutral wave, $|\gamma_{n-}| = 1$, travelling in the opposite direction.

Corresponding to an amplifying wave (one of a complex conjugate pair) the extraneous wave has the same tilt but dampens. Corresponding to a damping wave (the other of this conjugate pair) the extraneous wave has the same tilt but amplifies.

It is fortuitous that the latent roots in our case occur in complex conjugate pairs; otherwise the "conventional" analogue could introduce amplifying waves (from damping waves) where none with that wave length should be present. This could happen in other problems. As it is here, the main nuisance value of the extraneous τ eigensolutions is the distortion they can cause in the amplifying configurations.

The fact that the extraneous unstable component is oscillating (γ_{n-} negative), that is, changes sign with each step, may make this trouble readily detectable. The conventional analogue is further criticized in Section 10.

Extraneous τ eigensolutions appear whenever a finite-difference analogue relates more instances in time than are permitted by the order of the differential equation. A first-order differential equation by its nature permits only a two-point analogue.

A number of analogues which are composed of two operations have been prepared. These readily yield to analysis. One particular group has in common the second operation

$$\left[\underset{\sim}{q}_{N+1} - \underset{\sim}{q}_N \right] / \tau = -i \underset{\approx}{C} \left[\underset{\sim}{q}_N + \underset{\sim}{q}_{N+1}^{(e)} \right] / 2 \tag{59}$$

where $\underset{\sim}{q}_{N+1}^{(e)}$ is an estimate of the value being sought and which may be based on one of several different first operations.

The estimate may come from a simple linear extrapolation of the vector itself:

$$\underset{\sim}{q}_{N+1}^{(e)} = 2 \underset{\sim}{q}_N - \underset{\sim}{q}_{N-1} \; . \tag{60}$$

Substitution of Eq. (60) in Eq. (59) reveals the true form of this analogue:

$$\left[\underset{\sim}{q}_{N+1} - \underset{\sim}{q}_N \right] / \tau = -i \underset{\approx}{C} \left[3 \underset{\sim}{q}_N - \underset{\sim}{q}_{N-1} \right] / 2 \; .$$

It is a three-point formula which will have extraneous Υ eigen-solutions. Substitution of Eq. (53) leads to

$$\left(\underset{\approx}{C} - \frac{2}{i\tau} \; \frac{\Upsilon - \Upsilon^2}{3\Upsilon - 1} \underset{\approx}{I} \right) \underset{\sim}{q} = \underset{\sim}{0} \; .$$

Hence, according to Eq. (50), page 26, the corresponding Υ's are given by

$$\Upsilon_n = \frac{1}{2} - \frac{3}{4} i \tau \lambda_n \pm \left[\frac{1}{4} - \frac{9}{16} \tau^2 \lambda_n^2 - i \frac{\tau \lambda_n}{4} \right]^{1/2} \; . \tag{61}$$

Another possible combination results when the estimate comes from a forward time-step:

$$\left[\underset{\sim}{q}^{(e)}_{N+1} - \underset{\sim}{q}_N \right] / \tau = -i \underset{\approx}{C} \underset{\sim}{q}_N \ .$$

Combined with Eq. (59), the result is

$$\left[\underset{\sim}{q}_{N+1} - \underset{\sim}{q}_N \right] / \tau = -i \underset{\approx}{C} \left[2 \underset{\sim}{q}_N - i \tau \underset{\approx}{C} \underset{\sim}{q}_N \right] / 2 \ . \qquad (62)$$

Introduction of Eq. (53) leads to

$$\left(\tau^2 \underset{\approx}{C}^2 + i \tau \underset{\approx}{C} - (1-\gamma) \underset{\approx}{I} \right) \underset{\sim}{q} = \underset{\sim}{0} \ ,$$

and the condition on γ is

$$\left| \left(\tau^2 \underset{\approx}{C}^2 + i \tau \underset{\approx}{C} \right) - (1-\gamma) \underset{\approx}{I} \right| = 0 \ . \qquad (63)$$

According to a useful theorem* of matrix algebra, the latent roots of the matrix $\left(\tau^2 \underset{\approx}{C}^2 + i \tau \underset{\approx}{C} \right)$ are given by $(\tau^2 \lambda^2 + i \tau \lambda)$ and the latent vectors are those of $\underset{\approx}{C}$. Hence,

$$1 - \gamma_n = \tau^2 \lambda^2 + i \tau \lambda_n \ . \qquad (64)$$

A third combination results when the estimate for Eq. (59) comes from the conventional analogue:

$$\left[\underset{\sim}{q}^{(e)}_{N+1} - \underset{\sim}{q}_{N-1} \right] / 2\tau = -i \underset{\approx}{C} \underset{\sim}{q}_N \ .$$

---

*See, e.g., Milne,[7], p. 163.

This leads to

$$\gamma_n^2 + \left[\tau^2\lambda_n^2 - 1 + i\frac{\tau\lambda_n}{2}\right]\gamma_n + i\frac{\tau\lambda_n}{2} = 0 \quad . \tag{65}$$

None of these schemes is satisfactory. The reader may complete the critique by mapping their respective transforms, Eqs. (61), (64), and (65).

We now move on to the most natural finite-difference analogue of our first-order system. This is the "centered" first-order scheme:

$$\left[\underset{\sim}{q}_{N+1} - \underset{\sim}{q}_N\right]/\tau = -i\underset{\approx}{C}\left[\underset{\sim}{q}_N + \underset{\sim}{q}_{N+1}\right]/2 \quad . \tag{66}$$

The significant feature is that the difference is related to the tendency evaluated for a centered mean-value of the argument.

Introduction of Eq. (53) leads to

$$\left(\underset{\approx}{C} - \frac{2}{i\tau}\,\frac{1-\gamma}{1+\gamma}\,\underset{\approx}{I}\right)\underset{\sim}{q} = \underset{\sim}{0} \quad .$$

Hence,

$$\frac{2}{i\tau}\,\frac{1-\gamma_n}{1+\gamma_n} = \lambda_n \ ,$$

that is,

$$\gamma_n = \frac{1 - i\tau\lambda_n/2}{1 + i\tau\lambda_n/2} \quad ; \tag{67}$$

one value of γ_n corresponds to each λ_n for the same eigenvector.

To simplify the investigation we introduce $\lambda\tau/2 = \eta + i\omega$, where η and ω are real. γ becomes

$$\gamma = \frac{1+\omega-i\eta}{1-\omega+i\eta} \quad .$$
$$= \left[1 + \frac{4\omega}{(1-\omega)^2+\eta^2}\right]^{1/2} e^{i \arctan \frac{-2\eta}{1-\omega^2-\eta^2}} \tag{68}$$

This is to be compared with

$$e^{-i\lambda\tau} = e^{2\omega} \quad e^{i(-2\eta)} \quad .$$

Examination reveals excellent agreement and no computational instability. Neutral eigensolutions, $\omega = 0$, become neutral τ eigensolutions. Damping eigensolutions, $\omega < 0$, becomes damping τ eigensolutions. Amplifying eigensolutions, $\omega > 0$, become amplifying τ eigensolutions.

For $|\omega, \eta| << 1$, the quantitative agreements of the corresponding phase-speeds and the corresponding growth-rates are very good indeed. Therein lies the advantage of using small values of τ , the time increment.

Equation (68) can be used to compute η and ω from γ for a particular eigensolution.

This investigation reveals the centered first-order finite-difference analogue to be the most natural analogue of our first-order system. It will correctly detect the dynamic instability of flow profiles.

This is the analogue we shall use.

It may be feasible in special cases to transform a first-order system into a legitimate second-order system. This is necessarily accompanied by a corresponding reduction in the number of variables.

A second-order derivative has an easy-to-use analogue. Furthermore, the conventional analogue may be used for a first-order derivative when it appears in a second-order equation.

The desired transformation is not accomplished by merely raising the order of the system without losing variables in the process. If the same number of variables are maintained in the resulting higher-order system, then the nature of the system has thereby been corrupted and extraneous eigensolutions have entered. The extraneous eigensolutions are carried over into Υ eigensolutions and they would subsequently develop in the computations.

The variables lost in the desired transformation manifest themselves as initial tendencies and are related to the tendencies during the evolution.

Such a transformation is particularly simple in our system because $\underset{\approx}{C}$ is real. The differentiation of Eq. (45), page 25, and the subsequent substitution of Eq. (45) for the first derivative which appears on the right, leads to:

$$\frac{d^2}{dt^2}\,\underset{\sim}{q}(t) = -\underset{\approx}{C}\left[\underset{\approx}{C}\,\underset{\sim}{q}(t) + \underset{\sim}{d}\right] \qquad (69)$$

The real part of Eq. (69) and also the imaginary part thereof form two complete systems, each having half the number of variables of the former system, Eq. (45).

If we substitute $\underset{\sim}{q}(t) = \underset{\sim}{A}(t) + i\,\underset{\sim}{B}(t)$, where $\underset{\sim}{A}(t)$ and $\underset{\sim}{B}(t)$ are real, the real part of Eq. (69) is

$$\frac{d^2}{dt^2}\,\underset{\sim}{A}(t) = -\underset{\approx}{C}\left[\underset{\approx}{C}\,\underset{\sim}{A}(t) + \mathrm{Re}:\underset{\sim}{d}\right], \qquad (70)$$

for which we have an initial value, $\underset{\sim}{A}_o$, and according to Eq. (45), an initial tendency

$$\left(\frac{d}{dt}\,\underset{\sim}{A}(t)\right)_o = \underset{\sim}{B}_o + \mathrm{Im}:\underset{\sim}{d}\ .$$

The lost variables, the components of $\underset{\sim}{B}(t)$, are related to $\underset{\sim}{A}(t)$ at all times by

$$\frac{d}{dt}\underset{\sim}{A}(t) = \underset{\sim}{B}(t) + \ell m : \underset{\sim}{d} \quad ,$$

this relationship being the real part of Eq. (45).

In the same way we could deal with $\underset{\sim}{B}(t)$ as a principal dependent variable.

Equation (70) yields the same particular solution for $\underset{\sim}{A}(t)$ as did Eq. (45), namely, $\underset{\sim}{A}_s = -\underset{\approx}{C}^{-1}\, \Re\ell : \underset{\sim}{d}$. To determine the general solution we require a complete set of eigensolutions of the reduced equation

$$\frac{d^2}{dt^2}\underset{\sim}{A}(t) = -\underset{\approx}{C}^2\,\underset{\sim}{A}(t) \; . \tag{71}$$

If $\underset{\sim}{q}\, e^{-i\Gamma t}$ is a complex solution of Eq. (71) then the real and the imaginary parts thereof are separately real eigensolutions of Eq. (71). Substitutions of $\underset{\sim}{q}\, e^{-i\Gamma t}$ in Eq. (71) leads to

$$\left| \underset{\approx}{C}^2 - \Gamma^2 \underset{\approx}{I} \right| = 0 \; .$$

Thus, according to Eq. (50), page 26, $\Gamma = \pm \lambda_n$ are the latent roots which correspond to the latent vector, $\underset{\sim}{q}_n$ of $\underset{\approx}{C}$. The roots $-\lambda_n$ do not add anything alien or extraneous, they naturally belong. Their presence in Eq. (71) verifies that the complex latent roots of the real matrix $\underset{\approx}{C}$ must occur in conjugate pairs, or else the nature of the problem would indeed have changed.

The finite-difference analogue of Eq. (70) after reduction is

$$\left(\underset{\sim}{A}_{N+1} + \underset{\sim}{A}_{N-1} - 2\underset{\sim}{A}_N\right)/\tau^2 = -\underset{\approx}{C}^2 A_N \quad . \tag{72}$$

If $\underset{\sim}{q}\gamma^N$ is a complex solution of Eq. (72) then the real and the imaginary parts thereof are separately real τ eigensolutions of Eq. (72). Substitution of $\underset{\sim}{q}\gamma^N$ in Eq. (72) leads to

$$\left| \underset{\approx}{C}^2 - \frac{2\gamma - 1 - \gamma^2}{\tau^2 \gamma} \underset{\approx}{I} \right| = 0.$$

Thus, according to Eq. (50)

$$2\gamma_n - 1 - \gamma_n^2 = \gamma_n \tau^2 \lambda_n^2$$

which, solved for γ_n, yields

$$\gamma_n = 1 - \frac{1}{2}\tau^2\lambda_n^2 \pm i\left(\tau^2\lambda_n^2 - \frac{1}{4}\tau^4\lambda_n^4\right)^{1/2} \tag{73}$$

corresponding to the eigenvector $\underset{\sim}{q}_n$. The comparison of these two values of γ_n with $e^{\pm i\lambda_n \tau}$ shows the necessary qualitative as well as excellent quantitative agreement. The analogue is computationally stable.

The application of this analogue is quite straightforward. Each time-step requires the procedure described on page 24 to be performed twice with slight modification.

Although it is highly recommended, we shall not use this analogue of the cultivated second-order system because we made use of special features of our first-order system. We are interested in dealing directly with first-order systems for which we use the natural centered first-order analogue which we have analysed.

6. THE INTEGRATING PROCEDURE (LINEAR PROBLEM)

The centered first-order analogue,

$$\left[\underset{\sim}{q}_{N+1} - \underset{\sim}{q}_N\right]/\tau = -i\left\{\underset{\approx}{C}\left[\underset{\sim}{q}_N + \underset{\sim}{q}_{N+1}\right]/2 + \underset{\sim}{d}\right\} \quad , \tag{74}$$

can be made explicit as follows:

$$\left(2\underset{\approx}{I} + i\tau\underset{\approx}{C}\right)\underset{\sim}{q}_{N+1} = \left(2\underset{\approx}{I} - i\tau\underset{\approx}{C}\right)\underset{\sim}{q}_N - i2\tau\underset{\sim}{d}$$

$$\underset{\sim}{q}_{N+1} = \left(2\underset{\approx}{I} + i\tau\underset{\approx}{C}\right)^{-1}\left(2\underset{\approx}{I} - i\tau\underset{\approx}{C}\right)\underset{\sim}{q}_N - \left(2\underset{\approx}{I} + i\tau\underset{\approx}{C}\right)^{-1} i2\tau\underset{\sim}{d} \; .$$

In some cases it might be desirable to use this explicit formula. However, several objections may be raised: (a) the inversion and multiplication involve considerable calculation with accompanying inaccuracies; (b) the magnitude of the time step is frozen; and (c) the resulting coefficient matrix on the right hand side is generally far more complicated than the matrix $\underset{\approx}{C}$. Simplifying features such as exhibited by Eq. (44), page 24, are lost.

Because of Eq. (44), it may be more convenient to use an iterative method to achieve Eq. (74). This method is particularly interesting because of its applicability to nonlinear systems (see Section 11).

Equation (74) may be written

$$\underset{\sim}{q}_{N+1} = \underset{\sim}{q}_N - i\tau\left\{\underset{\approx}{C}\left[\underset{\sim}{q}_N + \underset{\sim}{q}_{N+1}\right]/2 + \underset{\sim}{d}\right\} \quad . \tag{75}$$

The iterative scheme for arriving at the solution of this equation is revealed by

$$\underset{\sim}{q}_{N+1}^{(r)} = \underset{\sim}{q}_N - i\tau\left\{\underset{\approx}{C}\left[\underset{\sim}{q}_N + \underset{\sim}{q}_{N+1}^{(r-1)}\right]/2 + \underset{\sim}{d}\right\} , \tag{76}$$

where the superscripts in parenthesis label the successive approximations of $\underset{\sim}{q}_{N+1}$.

To analyze the convergence of this scheme we set

$$\underset{\sim}{q}_{N+1}^{(r)} = \underset{\sim}{q}_{N+1} + \underset{\sim}{e}^{(r)}; \quad r = 0,1,2\ldots \tag{77}$$

and thereby define $\underset{\sim}{e}^{(r)}$ as the error of the r-th estimate. The subtraction of Eq. (75) from Eq. (76) reveals

$$\underset{\sim}{e}^{(r)} = -i\frac{\tau}{2}\underset{\approx}{C}\,\underset{\sim}{e}^{(r-1)} . \tag{78}$$

Hence by induction

$$\underset{\sim}{e}^{(r)} = \left(-i\frac{\tau}{2}\underset{\approx}{C}\right)^{r}\underset{\sim}{e}^{(0)} . \tag{79}$$

This scheme is convergent if $\underset{\sim}{e}^{(r)} \longrightarrow \underset{\sim}{0}$ as $r \longrightarrow \infty$. The necessary and sufficient condition for convergence is that all the latent roots of the matrix $\left(-i\frac{\tau}{2}\underset{\approx}{C}\right)$ be less than "one" in magnitude.

According to Eq. (50), page 26, the latent roots of the matrix, $\left(-i\frac{\tau}{2}\underset{\approx}{C}\right)$, are given by $\left(-i\frac{\tau}{2}\lambda_n\right)$, where $n = 1, 2 \ldots . n_0$ and n_0 is the order of the matrix. Its latent vectors are those of $\underset{\approx}{C}$:

$$\left(-i\frac{\tau}{2}\underset{\approx}{C}\right)\underset{\sim}{q}_n = \left(-i\frac{\tau}{2}\lambda_n\right)\underset{\sim}{q}_n \tag{80}$$

Let us impose that the latent roots be numbered in descending order of magnitude; and let us express $\underset{\sim}{e}^{(0)}$ as a linear combination of the latent vectors:

$$\underset{\sim}{e}^{(0)} = \sum_n \epsilon_n \underset{\sim}{q}_n \tag{81}$$

Thus, according to Eqs. (79) and (80),

$$\underset{\sim}{e}^{(r)} = \sum_n \epsilon_n \left(-i \frac{\tau}{2} \lambda_n\right)^r \underset{\sim}{q}_n \; . \tag{82}$$

This makes apparent the stated necessary and sufficient condition for convergence. Imposing this condition on Eq. (82) yields

$$\tau < 2/|\lambda_1| \; . \tag{83}$$

This is a definite limitation on the size of the time increment which may be used with this iterative scheme.

On page 32 we stated that according to Rayleigh

$$|\lambda_1| \leq k \, |U|_{max}$$

if λ_1 is real. If we assume that this also includes λ_1 complex, we are led from Eq. (83) to the sufficient condition

$$\tau < 2/k|U|_{max} \; . \tag{84}$$

The first guess, $\underset{\sim}{q}_{N+1}^{(0)}$, may be chosen objectively. Let us consider and compare choosing extrapolation (which we shall indicate by E:) with choosing persistence (which we shall indicate by P:).

$$E: \; \underset{\sim}{q}_{N+1}^{(0)} = 2\underset{\sim}{q}_N - \underset{\sim}{q}_{N-1} \; ,$$

$$P: \; \underset{\sim}{q}_{N+1}^{(0)} = \underset{\sim}{q}_N \; .$$

This yields

$$E: \underset{\sim}{e}^{(0)}_{N+1} = 2\underset{\sim}{q}_N - \underset{\sim}{q}_{N-1} - \underset{\sim}{q}_{N+1},$$

$$P: \underset{\sim}{e}^{(0)}_{N+1} = \underset{\sim}{q}_N - \underset{\sim}{q}_{N+1} \quad .$$

We can expand $\underset{\sim}{q}_N$ as a weighted sum of τ eigensolutions, Eq. (53), page 29,

$$\underset{\sim}{q}_N = \sum_n \sigma_n \underset{\sim}{q}_n \gamma_n^N \quad ,$$

where the σ 's are determined by fitting the initial vector $\underset{\sim}{q}_0$ and the γ 's are given by Eq. (67). It follows that the choices yield

$$\begin{aligned} E: \ (\epsilon_n)_{N+1} &= -\sigma_n (1-\gamma_n)^2 \gamma_n^{N-1} \quad , \\ P: \ (\epsilon_n)_{N+1} &= \sigma_n (1-\gamma_n)^2 \gamma_n^N \quad . \end{aligned} \tag{85}$$

It is of interest to determine which of the two choices yields smaller values for the ϵ_n 's. The ratio of the members of Eq. (85) yields

$$\left| E:/P: \right| = \left| (\gamma_n - 1)/\gamma_n \right| \quad .$$

This magnitude is $\lesseqqgtr$ 1 for Re: $\gamma_n \gtreqqless 1/2$. Thus Re: $\gamma_n = 1/2$ is critical. According to Eq. (68),

$$Re: \gamma = \frac{(1+\omega)(1-\omega) - \eta^2}{(1-\omega)^2 + \eta^2} \quad ,$$

where $\lambda\tau/2 = \eta + i\omega$; and the critical value lies on the circle

$$\eta^2 + (\omega - 1/3)^2 = (2/3)^2 .$$

For values of $\lambda_n\tau/2$ falling inside the circle, extrapolation yields a smaller value of ϵ_n than does persistence. That all values of $\lambda_n\tau/2$ fall inside the circle can be assured by the sufficient condition, $|\lambda_1|\tau/2 < 1/3$, that is, by

$$\tau < 2/3|\lambda_1| \tag{86}$$

In practice, the incidence of two successive estimates which differ in each component by less than some prescribed tolerance magnitude, T , shall be accepted as convergence. The iteration which achieves this is denoted by the subscript c , that is, by r_c , and the accepted solution is $q_{N+1}^{(r_c)}$.

If the matrix $\underset{\approx}{C}$ is symmetric, then its latent roots are mutually orthogonal and the analysis of the error extinction is rather elementary. However, this is too special a case to dwell on and we shall not be so restrictive.

If the matrix $\underset{\approx}{C}$ is asymmetric, then the magnitude of the error vector and its components do not <u>necessarily</u> decrease monotonically until the slowest decaying component of the error latent-vector expansion dominates.

After some minimum number of iterations, r_m ,

$$\underset{\sim}{e}^{(r)} \approx \epsilon_1 \left(-i\frac{\tau}{2}\lambda_1\right)^r \underset{\sim}{q}_1 , \quad r > r_m . \tag{87}$$

If $r_c > r_m$, the analysis of the rate of convergence can be based entirely on Eq. (87) because what happens to the other latent-vectors of the error expansion does not matter.

Equation (85) reveals that in both cases the weights of the error latent-vector expansion develop with the τ eigensolutions.

Corresponding to neutral waves, $|\gamma_n| = 1$ and the ϵ_n does not grow. But in the case of dynamic instability $|\gamma_i| > 1$ for some i, and the corresponding ϵ_i grows to progressively increase r_m. For this reason or more directly because T may have been chosen insufficiently small, r_c may occur before r_m. If this happens, an effective analysis, with $\underset{\approx}{C}$ asymmetric, depends on all particulars of the problem and is tantamount to solving the particular evolution. We restrict ourselves to $r_c > r_m$.

The reiteration is ended when

$$\underset{\sim}{\Delta}_{N+1}^{(r_c)} \equiv \underset{\sim}{q}_{N+1}^{(r_c)} - \underset{\sim}{q}_{N+1}^{(r_c-1)} \tag{88}$$

has all components less than T in magnitude. This limits the error because

$$\underset{\sim}{\Delta}_{N+1}^{(r_c)} = \underset{\sim}{e}_{N+1}^{(r_c)} - \underset{\sim}{e}_{N+1}^{(r_c-1)}$$

$$\approx \left(-i\frac{\tau}{2}\lambda_1 - 1\right)\epsilon_1\left(-i\frac{\tau}{2}\lambda_1\right)^{r_c-1}\underset{\sim}{q}_1 .$$

Up to this point we have not discussed the effect of round-off during the reiteration. Some comments are now called for. Round-off causes spurious variations which are usually confined to the last few binary digits of the components of $\underset{\sim}{q}_{N+1}^{(r)}$ during each iteration. Because of these variations the iterations may not lead to a steady value for $\underset{\sim}{q}_{N+1}$. Instead the reiteration may settle into a cycle of two or more iterations. It may happen that during such a cycle none of the successive differences satisfies the tolerance, and convergence will not occur. This bothersome phenomenon should not be mistaken for divergence. It causes oscillations, not "blow-up."

This is a shortcoming of the test method to determine satisfactory convergence. The probability of the occurrence of such oscillations is reduced by increasing T. On the other hand, it is undesirable to increase the tolerance not only because of reduced disparity in Eq. (74) but also because the terms of the centered first-order analogue will not have been met. In fact, if $\underset{\sim}{q}_{N+1}^{(o)}$ is being determined by extrapolation then our operation still relates three instances in time. The tolerance should be of the order of round-off so that only error which is practically random remains.

Instead of testing for convergence it may be preferable to simply carry out and accept the result of a fixed number of iterations for each and every time step. The number of iterations may be determined by fixing a maximum error-to-wave-amplitude ratio.

If extrapolation is used the error vector is given by

$$\underset{\sim}{e}_{N+1}^{(\lambda)} = \sum_{n} - \sigma_n (1-\gamma_n)^2 \gamma_n^{N-1} \left(-i \frac{\tau}{2} \lambda_n\right)^{\lambda} \underset{\sim}{q}_n ,$$

and the vector itself by

$$\underset{\sim}{q}_{N+1} = \sum_{n} \sigma_n \gamma_n^{N+1} \underset{\sim}{q}_n .$$

Consequently the error-to-wave-amplitude ratio for the n-th wave (n-th latent vector) is

$$- \left[(\gamma_n - 1)/\gamma_n\right]^2 \left(-i \frac{\tau}{2} \lambda_n\right)^{\lambda} .$$

We set the upper limit E on the magnitude of this ratio for all n. If Eq. (86) is satisfied, it is sufficient that $\left|\frac{\tau}{2} \lambda_1\right|^{\lambda} \leqq E$, or

$$\lambda \geqq \ln E / \ln \left|\frac{\tau}{2} \lambda_1\right| .$$

Both of these $\ln$'s are negative.

This method also takes on more significance if $\underset{\approx}{C}$ is symmetric, otherwise it also has its shortcomings. It is not as readily extensible to the iterative solution of nonlinear equations as is the test method. In the integrations to follow, the test method is used.

The amount of computing may be reduced by making use of the fact that $\underset{\approx}{C}$ has all real elements. We introduce $\underset{\sim}{q}_N = \underset{\sim}{A}_N + i\underset{\sim}{B}_N$, where $\underset{\sim}{A}_N$ and $\underset{\sim}{B}_N$ are real, into Eq. (76), page 42. The real and imaginary parts of Eq. (76) then yield

$$\begin{aligned} \underset{\sim}{A}^{(\lambda)}_{N+1} &= \underset{\sim}{A}_N + \tau\left\{\underset{\approx}{C}\left[\underset{\sim}{B}_N + \underset{\sim}{B}^{(\lambda-1)}_{N+1}\right]/2 + \mathrm{Im}:\underset{\sim}{d}\right\} \\ \underset{\sim}{B}^{(\lambda)}_{N+1} &= \underset{\sim}{B}_N - \tau\left\{\underset{\approx}{C}\left[\underset{\sim}{A}_N + \underset{\sim}{A}^{(\lambda-1)}_{N+1}\right]/2 + \mathrm{Re}:\underset{\sim}{d}\right\} . \end{aligned} \tag{89}$$

This reveals that it is redundant to compute all indicated successive estimates for both $\underset{\sim}{A}_{N+1}$ and $\underset{\sim}{B}_{N+1}$. The even λ estimates of $\underset{\sim}{A}_{N+1}$ and odd λ estimates of $\underset{\sim}{B}_{N+1}$ converge quite independently of the odd λ estimates of $\underset{\sim}{A}_{N+1}$ and the even λ estimates of $\underset{\sim}{B}_{N+1}$. Both sets converge to the same values, so it is necessary to compute only one set. The set which begins with $\underset{\sim}{B}^{(0)}_{N+1}$ is chosen and so as to reduce the number of coding instructions, persistence is chosen, $\underset{\sim}{B}^{(0)}_{N+1} = \underset{\sim}{B}_N$.

The convergence test may be satisfied by either succeeding values of $\underset{\sim}{B}_{N+1}$ or of $\underset{\sim}{A}_{N+1}$. The intervening value of the other part is then also accepted. For example, if $\underset{\sim}{B}^{(6)}_{N+1}$ lies within tolerance of $\underset{\sim}{B}^{(4)}_{N+1}$, then $\underset{\sim}{q}_{N+1} = \underset{\sim}{A}^{(5)}_{N+1} + i\,\underset{\sim}{B}^{(6)}_{N+1}$.

It may be possible to design iterative procedures for solving Eq. (74), page 41, which converge more rapidly than does Eq. (76). In this respect the techniques discussed in Section 10, in connection with the iterative method of solving the finite-difference analogue of Poisson's equation, might prove successful. However, the analysis by Young[10] does not apply because our matrix $\underset{\approx}{C}$ does not have the necessary property (property A).

7. THE COMPUTING PROCEDURE AND OUTPUT

According to Eq. (42), page 23, and the marching procedure, the equations which must be programmed are:

$$A^{(n)}_{M,N+1} = A_{M,N} + \tau\Big[\mu_M \bar{B}^{(n-1)}_M + \nu_M\Big\{(\bar{B}^{(n-1)}_M)_u + (\bar{B}^{(n-1)}_M)_\ell\Big\}$$
$$- \nu_M \ast_1 (\bar{B}^{(n-1)})\, K^{M_b-M} - \nu_M \ast_2 (\bar{B}^{(n-1)})\, K^{M-M_a}\Big] ,$$

$$B^{(n+1)}_{M,N+1} = B_{M,N} - \tau\Big[\mu_M \bar{A}^{(n)}_M + \nu_M\Big\{(\bar{A}^{(n)}_M)_u + (\bar{A}^{(n)}_M)_\ell\Big\}$$
$$- \nu_M \ast_1 (\bar{A}^{(n)})\, K^{M_b-M} - \nu_M \ast_2 (\bar{A}^{(n)})\, K^{M-M_a}\Big] ,$$

where

$$\bar{B}^{(n-1)}_M = \frac{1}{2}\left(B_{M,N} + B^{(n-1)}_{M,N+1}\right) ,$$

$$\bar{A}^{(n)}_M = \frac{1}{2}\left(A_{M,N} + A^{(n)}_{M,N+1}\right) .$$

The μ_M 's, ν_M 's, τ , K and the constants required by the ..ar functions are precalculated and are stored in the computer.

A consideration of the types of profiles to be investigated, of computer storage, and of the desirability to retain any symmetries, led to the approximation of the z continuum by 33 points, 32 intervals.

Regarding the <u>units</u> of dimension, both the length unit and time unit shall be selected from the straight parallel flow, thus keeping

k variable. Units which make

$$|U|_{max} = 1^{*} ,$$
$$|U'|_{max} = 1 , \tag{90}$$

are selected for each profile. In atmospheric considerations, a lower bound for the time unit is obtained by selecting extreme values for the shear. In the horizontal a representative high value is 10^{-4} seconds^{-1}, which yields a time unit of about 2 1/2 hours. This makes the length unit corresponding to about a U_{max} of 50 meters seconds^{-1}, 450 kilometers. In the vertical a representative high value of the shear is 10^{-2} seconds^{-1}, which yields a time unit of only about 1 1/2 minutes. This makes the length unit corresponding to a U_{max} of 50 meters seconds^{-1}, 4 1/2 kilometers.

To arrive at a graphical representation of the evolution we use $q(z,t) = A(z,t) + iB(z,t)$ and $\psi(z,t) = \alpha(z,t) + i\beta(z,t)$ where A, B, α and β are real functions of z and t. This leads to

$$\begin{aligned} q(x,z,t) &= A(z,t)\cos kx - B(z,t)\sin kx \\ &= D(z,t)\cos\left[kx - \phi(z,t)\right] , \\ \psi(x,z,t) &= \alpha(z,t)\cos kx - \beta(z,t)\sin kx \\ &= \chi(z,t)\cos\left[kx - \theta(z,t)\right] , \end{aligned} \tag{91}$$

where

$$\begin{aligned} D &= (A^2 + B^2)^{1/2} ; \qquad \phi = \arctan(-B/A) , \\ \chi &= (\alpha^2 + \beta^2)^{1/2} ; \qquad \theta = \arctan(-\beta/\alpha) . \end{aligned} \tag{92}$$

---

*In a frame of reference moving with the fluid at some level.

The computer* is instructed to output the set of 33 A's and the 33 B's for each time unit, that is, at intervals of $1/\tau$ time steps. A second code is later used to compute the 33 α 's and the 33 β 's from each set. According to Eq. (33), page 22, they are given by

$$\begin{aligned}\alpha_M &= \frac{-1}{2k}\left[2K_1 A_M + K_3 (A_M)_u + K_3 (A_M)_l\right] \\ &\quad + \frac{K_3}{2k} *_1(A)\, K^{M_b - M} + \frac{K_3}{2k} *_2(A)\, K^{M-M_a}, \\ \beta_M &= \frac{-1}{2k}\left[2K_1 B_M + K_3 (B_M)_u + K_3 (B_M)_l\right] \\ &\quad + \frac{K_3}{2k} *_1(B)\, K^{M_b - M} + \frac{K_3}{2k} *_2(B)\, K^{M-M_a}.\end{aligned} \tag{93}$$

In addition, this second code computes a figure representative of the perturbation kinetic energy, which will be used as an indication of the growth or decay of this quantity with time. This energy computation is based on a linear interpolation of ψ between points. A third code** computes D and ϕ from each A, B pair and χ and θ from each α, β pair according to Eq. (92). The D and χ retain all the significant digits of the A, B and α, β pairs, respectively. The ϕ and θ are obtained from a table-read routine and are accurate to 10^{-3} degrees.

* The Standards Western Automatic Computer (SWAC), Numerical Analysis Research (N.A.R.), University of California at Los Angeles.

** These codes are on file at the N.A.R. library.

8. APPLICATION TO AN UNBOUNDED HYPERBOLIC-TANGENT PROFILE

The straight parallel flow profile is given by

$$U(z) = -\tanh z^{*} \tag{94}$$

where z extends to $\pm\infty$.

This profile is one which is acceptable for the "contained" treatment discussed on page 19. By choosing a sufficiently deep layer about $z = 0$, $U''(z)$ can be made as small as desired in the neglected exterior.

This profile is skew-symmetric, that is,

$$U(z) = -U(-z)\,. \tag{95}$$

Hence also $U''(z) = -U''(-z)$. To preserve this property in our space-discretized system, we center our grid at the level $z = 0$ with 16 intervals above and below.

It is usual to order the components of our vector, $\underset{\sim}{q}$, and our set of equations in ascending order of the grid points (that is, ascending M). However it will serve us better to adopt the order

$$M = -16, -15, \ldots -1;\ 0;\ 16, 15, \ldots 1.$$

Because we have no boundaries, $\underset{\sim}{d}$ of Eq. (45), page 25, is zero, and the elements of $\underset{\approx}{C}$, which we shall label $C_{M,j}$, are given by

$$\begin{aligned} C_{M,M} &= \left(kU_M + U''_M K_1\right) \\ C_{M,j} &= \left(U''_M K_3/2\right) K^{|M-j|}, \quad j \neq M \end{aligned} \tag{96}$$

where the columns are labeled as the rows, in the order

$$j = -16, -15, \ldots -1;\ 0;\ 16, 15, \ldots 1.$$

---

* In arbitrary units, $U(z) = U \tanh \mathcal{K} z$, and we are free to add an arbitrary translation to our frame of reference.

By virtue of Eq. (95),

$$C_{o,j} = 0, \quad C_{M,j} = -C_{-M,-j} \quad . \tag{97}$$

To exhaust the relationships expressed by Eq. (97), we write the relationship which the eigensolutions must satisfy as follows

$$\begin{array}{c} \\ -16 \\ \vdots \\ -1 \\ 0 \\ 16 \\ \vdots \\ 1 \end{array} \begin{array}{c} -16 \cdots -1 \;\; 0 \;\; 16 \cdots 1 \\ \left(\begin{array}{c|c|c} \underset{\approx}{w} & \underset{\sim}{c} & \underset{\approx}{p} \\ \hline \underset{\approx}{0} & 0 & \underset{\approx}{0} \\ \hline -\underset{\approx}{p} & -\underset{\sim}{c} & -\underset{\approx}{w} \end{array} \right) \end{array} \begin{array}{c} \\ \left(\begin{array}{c} \underset{\sim}{q_\ell} \\ \hline q_o \\ \hline \underset{\sim}{q_u} \end{array} \right) \end{array} = \lambda \begin{array}{c} \\ \left(\begin{array}{c} \underset{\sim}{q_\ell} \\ \hline q_o \\ \hline \underset{\sim}{q_u} \end{array} \right) \end{array} \begin{array}{c} \\ -16 \\ \vdots \\ -1 \\ 0 \\ 16 \\ \vdots \\ 1 \end{array} \tag{98}$$

which is the same as

$$\begin{aligned} \underset{\approx}{w}\,\underset{\sim}{q_\ell} + q_o \underset{\sim}{c} + \underset{\approx}{p}\,\underset{\sim}{q_u} &= \lambda \underset{\sim}{q_\ell} \\ 0 &= \lambda q_o \\ -\underset{\approx}{p}\,\underset{\sim}{q_\ell} - q_o \underset{\sim}{c} - \underset{\approx}{w}\,\underset{\sim}{q_u} &= \lambda \underset{\sim}{q_u} \end{aligned} \tag{99}$$

We may note that if $\lambda \neq 0$ then $q_o = 0$.

It is apparent that one of the latent roots is $\lambda_1 = 0$. The corresponding vector satisfies

$$\begin{pmatrix} \underset{\approx}{w} & \underset{\approx}{p} \\ -\underset{\approx}{p} & -\underset{\approx}{w} \end{pmatrix} \begin{pmatrix} \underset{\sim}{q_\ell} \\ \underset{\sim}{q_u} \end{pmatrix} = q_o \begin{pmatrix} -\underset{\sim}{c} \\ \underset{\sim}{c} \end{pmatrix} ,$$

which shows this vector to be symmetric, that is,

$$\underset{\sim}{q_\ell} = \underset{\sim}{q_u} = -q_o (\underset{\approx}{w} + \underset{\approx}{p})^{-1} \underset{\sim}{c} \tag{100}$$

The latent roots in the case of skew-symmetric profiles occur in $\pm$ pairs. If $\lambda, \{\underset{\sim}{X}, q_o, \underset{\sim}{Y}\}$ satisfies Eq. (99), then also does $-\lambda, \{\underset{\sim}{Y}, q_o, \underset{\sim}{X}\}$. It follows from Eq. (99) that the sixteen admissible values of λ^2 satisfy

$$\left| (\underset{\approx}{w} + \underset{\approx}{p})(\underset{\approx}{w} - \underset{\approx}{p}) - \lambda^2 \underset{\approx}{I} \right| = 0. \tag{101}$$

This is a polynomial in λ^2 with real coefficients. Hence an admissible λ^2 is either real or is one of a complex conjugate pair. A complex conjugate pair of λ^2's give rise to two pairs of complex conjugate roots, $\lambda = \mu \pm i\nu$ and $\lambda = -(\mu \pm i\nu)$. To each such pair there corresponds a complex conjugate pair of latent vectors.

It follows from the preceding paragraph that if Eq. (101) admits a real λ^2 which is negative (that is, $\lambda = \pm i\nu$ where ν is real), then the corresponding pair of solutions may be expressed by

$$\begin{aligned} &i\nu, \{\underset{\sim}{P} + i\underset{\sim}{Q}, 0, \underset{\sim}{P} - i\underset{\sim}{Q}\} \\ &-i\nu, \{\underset{\sim}{P} - i\underset{\sim}{Q}, 0, \underset{\sim}{P} + i\underset{\sim}{Q}\} \end{aligned} \tag{102}$$

where $\underset{\sim}{P}$ and $\underset{\sim}{Q}$ are real.

The profile Eq. (94) has already been studied by Garcia.[1] He chose Ψ as the principal dependent variable and investigated the steady-state differential equation

$$-U(z)\left[\Psi''(z) - k^2\Psi(z)\right] + U''(z)\Psi(z) = 0 \tag{103}$$

This steady-state condition is readily obtained from Eq. (8), page 5, with substitution for q according to Eq. (9).

With $U = -\tanh z$, Eq. (103) has the solutions

$$\Psi_1 = \left[k - U(z)\right] e^{-kz} \; ; \quad \Psi_2 = \left[k + U(z)\right] e^{kz} .$$

To satisfy the boundary conditions (which neither one of the above can do) Garcia fitted these together (about the level $z = 0$) arriving at the solution

$$\psi_S = \left[k + |U(z)| \right] e^{-k|z|} \tag{104}$$

Since ψ' as well as ψ must be continuous, Garcia found $k = 1$ to yield the only possible stationary wave, no matter at which level the two solutions are fitted.

For $k \neq 1$, Eq. (104) has a discontinuity in ψ' (that is, in u) at $z = 0$. The harmonic field which is compatible with this slipping (sometimes called sliding vorticity) is

$$\psi_R = (k - 1/k)\, e^{-k|z|} \tag{105}$$

Removing ψ_R from Eq. (104) Garcia arrived at the continuous field

$$\psi = \psi_S - \psi_R = \left[1/k + |U(z)| \right] e^{-k|z|} \tag{106}$$

which is no longer stationary. From the initial phase speed at all levels, he found that for $k < 1$ an amplifying tilt develops and for $k > 1$ a damping tilt develops.* This indicates the imminent tendency. Garcia concluded that the short waves are stable while the long waves are unstable and $k_c = 1$.

For extremely short waves ($k \rightarrow \infty$), the determinant, Eq. (101), reduces to a diagonal with elements $(kU_M)^2 - \lambda^2$. This means that the components of $\underset{\sim}{q}$, that is, the q_M 's, are each advected by the straight parallel flow at their level, their influence on other levels being negligible.

*According to the Reynolds-Fjortoft criterion. See, e.g., Holmboe[3] p. 11.

Thus for large k, all $\lambda^2(k)$ are real and positive. In the light of Garcia's work we may expect one of the 16 values of $\lambda^2(k)$ to become zero in the vicinity of $k = 1$. This value of $\lambda^2(k)$ may become negative as k decreases further. The numerical results to follow agree with this conjecture.

Garcia's stream function, Eq. (106), is taken as the initial field. It is compatible with

$$q(z) = -2\left(k + |\tanh z|\right) \operatorname{sech}^2 z \; e^{-k|z|}, \tag{107}$$

which is symmetric and real.* The amplitude factor remains free because it drops out of the homogeneous linear system.

The space increment, h, was chosen to be 0.2. This extends our grid from $z = -3.2$ to $z = 3.2$. Figure 1 shows $U(z)$ and $U''(z)$ in this interval.

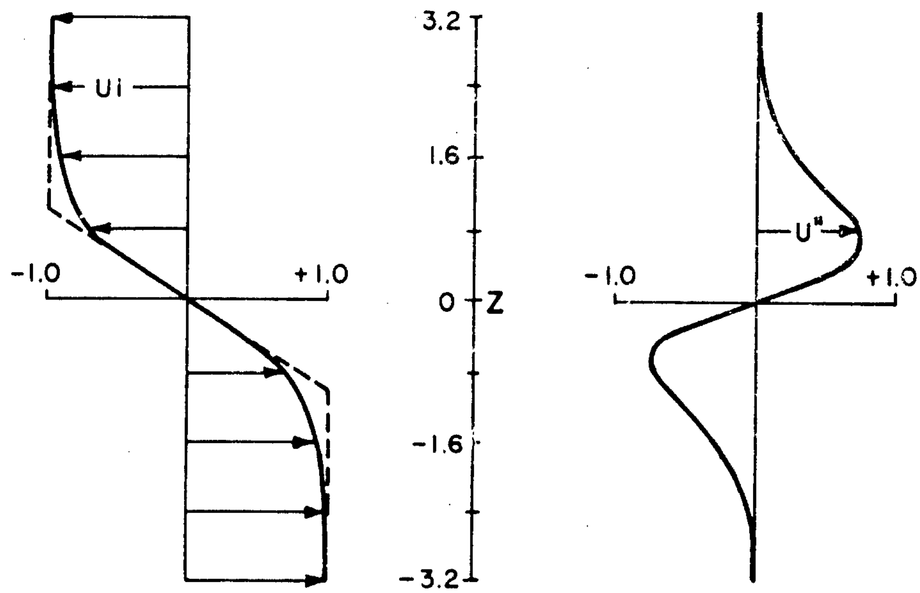

Fig. 1. The hyperbolic tangent profile.

*Such an initial value may prove to lack generality.

Integrations were made in steps $\tau = 1/20$ or less, from $t = 0$ to $t = 15$ for the values $k = 0.3, 0.5, 0.7$, and 2.0. The last of these, $k = 2.0$, was apparently stable. The others lying within $0 < k < 1$ were unstable.

In each of the three unstable cases, a single τ eigensolution corresponding to $\lambda = i\nu$ (ν positive) rapidly dominated the evolution. The growth rates were determined to be

$$\begin{array}{lllll} k & = & 0.3 & 0.5 & 0.7 \\ & & & & \\ \nu & = & 0.174 & 0.184 & 0.129 \end{array} \qquad (108)$$

These values of ν are considered to be accurate to within 2 percent.* In view of this wide margin the correction afforded us by Eq. (68), page 37, is trivial. On the basis of these values the solid curve in Fig. 2 was drawn.

The exact wave-number at which the negative λ^2 becomes zero is rather difficult to locate by integrations. These integrations would have to be extended for long periods to detect the presence or absence of slow growth rates.

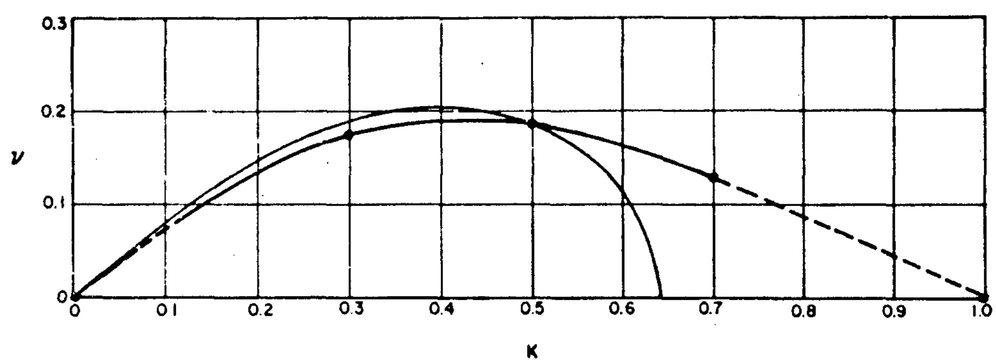

Fig. 2. The unstable band.

*More accuracy could have been attained by carrying each integration further, thereby purifying the unstable eigensolution.

The broken line extension of our curve has been drawn to the point $k = 1$, $\nu = 0$. It is not expected to be much in error.

It seems reasonable to assume that the other end of our curve (approaching infinite wave length) will asymptotically approach the dotted curve. This dotted curve represents the instability of the kinked profile (the dotted curve in Fig. 1), of the same dimensions, which has been investigated by Holmboe.[3]

We will assume that except for the one value of $\lambda^2(k)$ which passes through zero near $k = 1$ and which is negative for $0 < k < 1$, all other 15 values of $\lambda^2(k)$ are real and positive for $0 < k < \infty$. This assumption may be verified by numerically computing all λ^2 admitted by Eq. (101) for discrete values of k. However there is no indication why the assumption should not verify.

Because $k = 0.5$ is about the most unstable, only its evolvement from the initial state, Eq. (107), will be given in detail. The evolutions for $k = 0.3$ and 0.7 are basically similar. The evolution for $k = 2.0$ showed a rapid fall-off in energy to less than 1 percent of the initial by $t = 6$, at which time gross-truncation-error became evident.

The evolution for $k = 0.5$, wave length 4π, is shown in the following diagrams. The representation, Eq. (91), is used. Figure 3 shows the amplitude and phase of the perturbation vorticity at times $t = 0, 5, 10$, and 15. Figure 4 shows the same for the perturbation stream function. The "energy" growth of the perturbation is shown in Fig. 5.

To draw the total streamlines and total vorticity isopleths we must prescribe the amplitude of the perturbation. We may prescribe it arbitrarily large to show the features of the flow. The lateral displacement of a total streamline at a level z, consistent with the linearization, is given by

$$-\frac{X(z,t)}{U(z)} \cos\left[kx - \theta(z,t)\right] , \qquad (109)$$

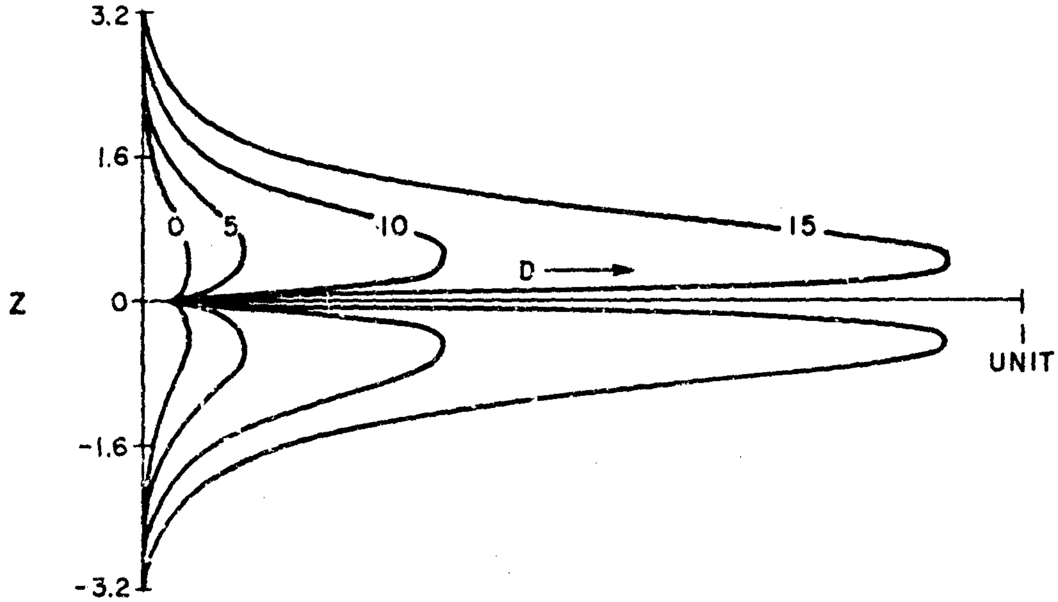

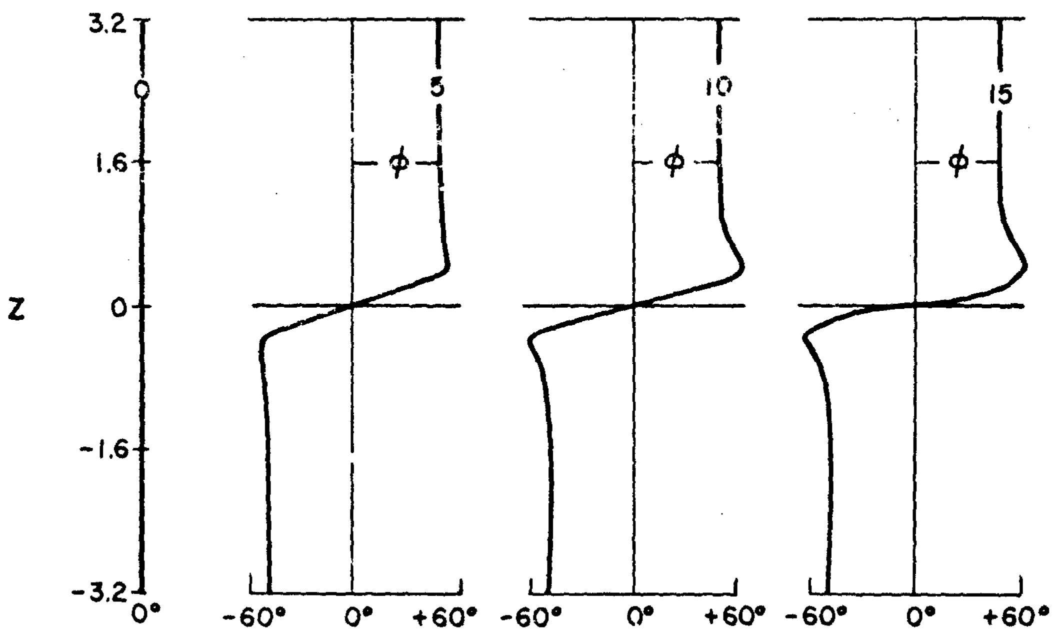

Fig. 3. The q-functions D (z) and ϕ (z), long wave case (k = 1/2) at times t = 0, 5, 10 and 15.

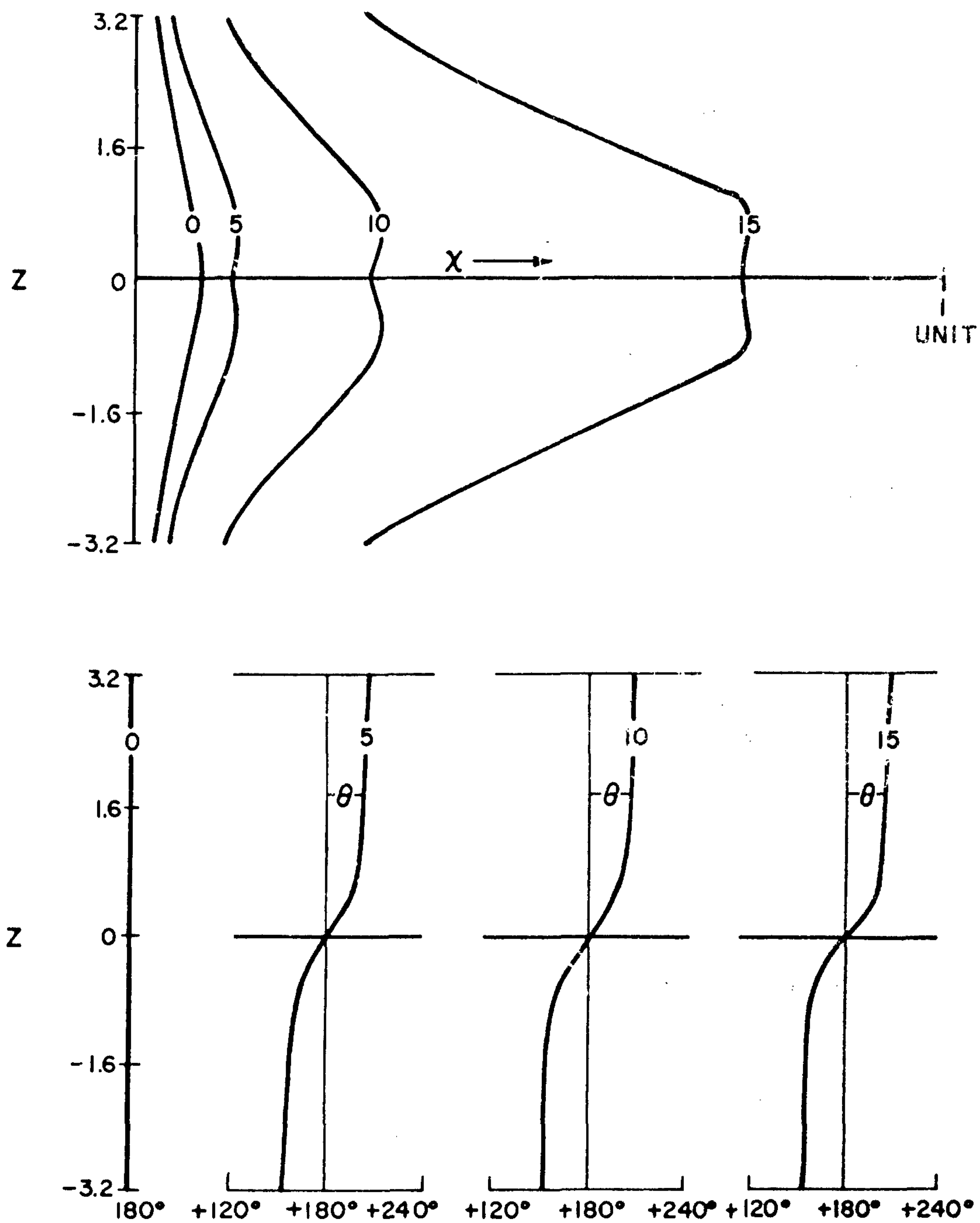

Fig. 4. The ψ-functions $\chi(z)$ and θ (z), long wave case ($k = 1/2$), at times $t = 0, 5, 10$ and 15.

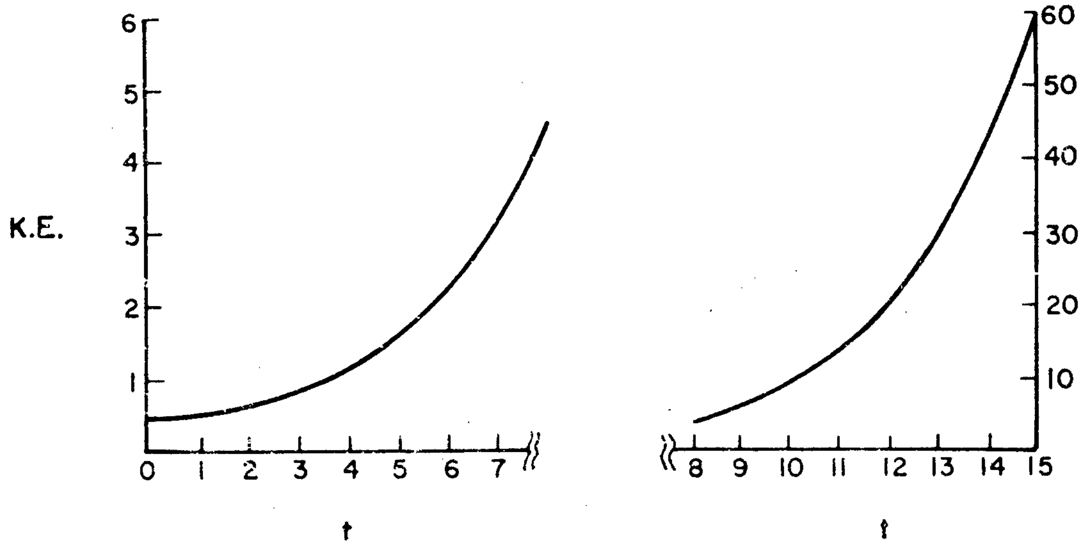

Fig. 5. Kinetic energy curve for K = 1/2.

and that of the total vorticity isopleth by

$$-\frac{D(z,t)}{U''(z)} \cos\left[kx - \phi(z,t)\right] \tag{110}$$

These expressions apply only at levels where the denominator, $U(z)$ or $U''(z)$, is an order of magnitude greater than the numerator. Figure 6 shows the total streamlines (solid curves) and total vorticity isopleths (broken curves), at selected levels, at time $t = 0$ above and $t = 15$ below. The exaggerated amplitude of the perturbation has been reduced by a factor of 10 in the lower diagram relative to that of the upper diagram.

At no time does it appear as if the vorticity in the neglected exterior has become significant.

All integrations and auxiliary computations carried out for this skew-symmetric profile, with symmetric initial values, retained their symmetries to the last digit. Some twenty hours of high-speed computing were involved. This speaks highly of SWAC. *

---

*See footnote, p. 51.

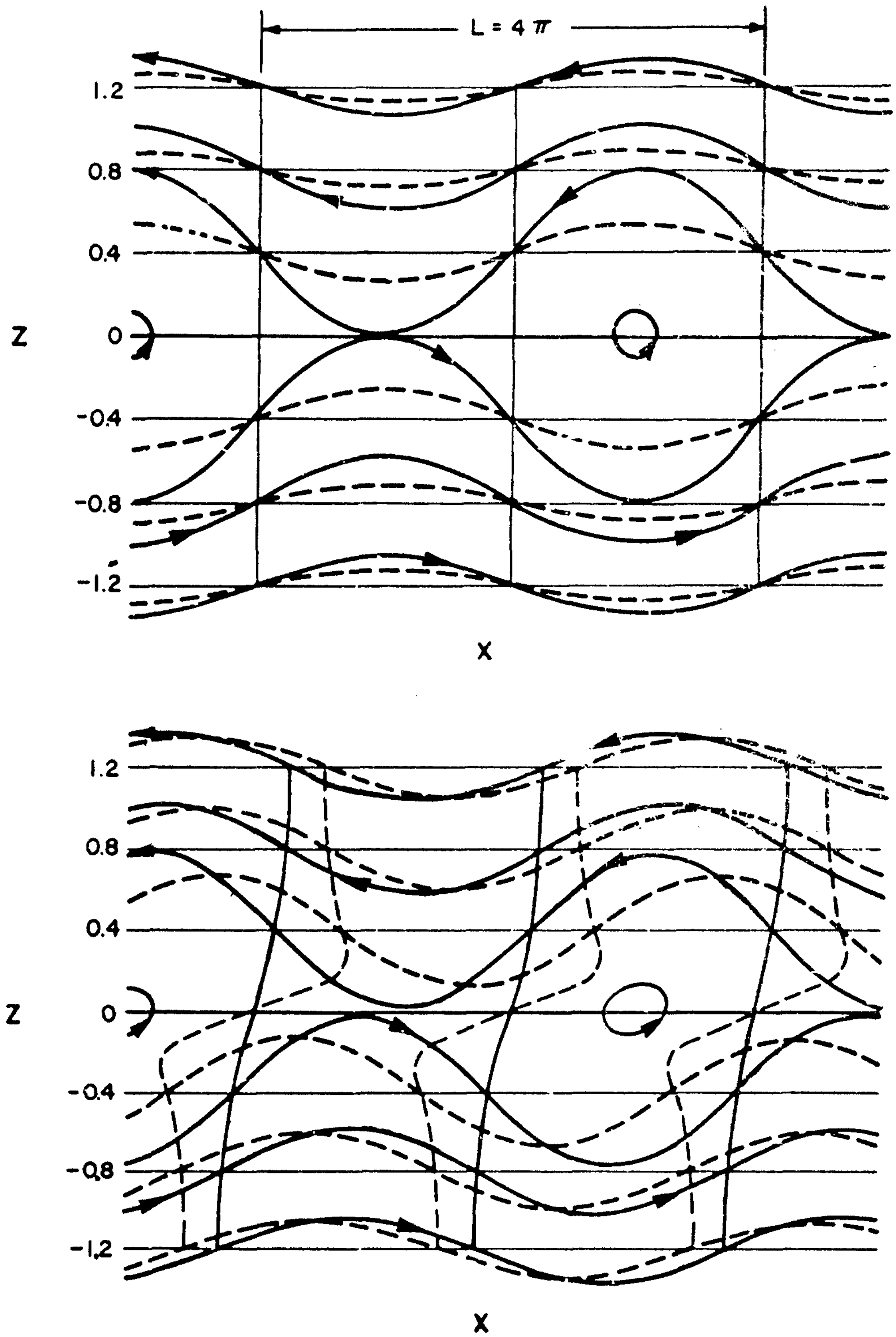

Fig. 6. The total streamlines and total vorticity isolines of selected selected levels, long wave case at t = 0 above and t = 15 below.

9. THE SIGNIFICANCE OF THE RESULTS

We have crossed three bridges to get to our numerical results. The first bridge connects the governing finite-amplitude system to the linearized system. The second connects the linearized system to the space-discretized system. And the third connects the latter to the space-and-time discretized system. If we are to consider that our numerical evolutions represent first-order (in amplitude) approximations to the evolutions of the finite-amplitude systems then we must reconcile these crossings.

The analysis of Section 5 has shown that the character of the system is unchanged by crossing the third bridge provided we use the centered first-order analogue. The eigensolution $\underset{\sim}{q}\, e^{i\lambda t}$, where $\lambda = \mu + i\nu$ becomes the τ eigensolution $\underset{\sim}{q}\, e^{i\lambda_\tau t}$. The vector is unchanged. According to Eq. (68), λ_τ is given by

$$\begin{aligned} \lambda_\tau &= \mu_\tau + i\nu_\tau \\ &= \frac{1}{\tau} \arctan \frac{\mu\tau}{1-R^2} + \frac{i}{2\tau} \ln \frac{1+R^2+\nu\tau}{1+R^2-\nu\tau} , \end{aligned} \qquad (111)$$

where

$$R^2 = (\tau/2)^2 \, (\mu^2 + \nu^2) .$$

It should be noted that each of the four quadrants of the complex λ is altered in the same way. That is, any symmetries in the occurence of eigenvalues are preserved.

We cannot as readily or as completely reconcile the second crossing.

Let us consider what is revealed by the eigensolutions of the linearized system. The eigensolution $q(z,t) = q(z)\, e^{-i\Gamma t}$ corresponds to $\underset{\sim}{q}\, e^{-i\lambda t}$ of the space-discretized system. Its introduction into Eq. (8), page 5, leads to

$$-\Gamma q(z) = k \left[-U(z) q(z) + U''(z) \int_{-\infty}^{\infty} \frac{e^{-k|z-\zeta|}}{-2k} q(\zeta) d\zeta \right] \qquad (112)$$

for the unbounded model. It has been imposed that $U(z)$ be real and that k be real and positive.

Equation (112) may be put into a standard form,

$$(\Gamma/k)\, q(z) = \int_{-\infty}^{\infty} \left\{ U(z)\, I(z,\zeta) - U''(z)\, \frac{e^{-k|z-\zeta|}}{-2k} \right\} q(\zeta)\, d\zeta \,, \tag{113}$$

where

$$I(z,\zeta) \equiv \underset{a \to 0+}{\mathcal{L}imit} \ \frac{a/\pi}{a^2 + (\zeta - z)^2} \,. \tag{114}$$

The proof that Eq. (113) is a valid expression of Eq. (112) requires that

$$\int_{-\infty}^{\infty} I(z,\zeta)\, q(\zeta)\, d\zeta \equiv q(z) \,. \tag{115}$$

For sufficiently small positive a, $I(z,\zeta) \approx 0$ except for a narrow region of half-width 2a about $\zeta = z$. This permits us to take a mean value of $q(\zeta)$, for this region, outside of the integral in Eq. (115). This value is $q(z)$. It follows that

$$\int_{-\infty}^{\infty} I(z,\zeta)\, q(\zeta)\, d\zeta \equiv q(z) \int_{-\infty}^{\infty} I(z,\zeta)\, d\zeta \equiv q(z) \,.$$

The second integral may be found in tables. It is unity for all z and positive a. It should be noted that the limit is not taken all the way to a = 0 but rather to 0+ which can be as close to zero from above as desired.

The form, Eq. (113), classifies our integral equation as a singular homogeneous Fredholm equation of the second kind. The determination of the Γ possessed by Eq. (113) for the profile, Eq. (94), for the real positive range of k is beyond the scope of the present work. We shall deal only with some salient points.

We may begin by indicating some of the similarities which Eqs. (112) or (113) has with the space-discretized system. It can be demonstrated directly that if λ and $q(z)$ satisfy Eq. (112) then also do λ_c and $q_c(z)$, where the subscript c denotes the complex conjugate. Because of the profile's skew-symmetry it can also be demonstrated that if λ and $q = X(z)$ satisfy Eq. (112) then also do $-\lambda$ and $q = X(-z)$. It follows that the two eigenfunctions corresponding to a Γ^2 which is real and negative (if such is admitted) may be expressed by

$$i\nu, \quad q(z) = \begin{cases} P(z) + iQ(z) & \text{for } z > 0 \\ P(-z) - iQ(-z) & \text{for } z < 0 \end{cases}$$
$$-i\nu, \quad q(z) = \begin{cases} P(z) - iQ(z) & \text{for } z > 0 \\ P(-z) + iQ(-z) & \text{for } z < 0 \end{cases} \tag{116}$$

which is the counterpart of Eq. (102).

The counterpart of Eq. (101) is also readily developed:

$$\left(\frac{\Gamma}{k}\right)^2 Y(z) = \int_0^\infty \int_0^\infty \left[K_1(z,y) - K_2(z,y)\right]\left[K_1(y,\zeta) + K_2(y,\zeta)\right] Y(\zeta)\, dy\, d\zeta \,, \tag{117}$$

where

$$Y(z) = q_u(z) + q_\ell(-z) \,,$$
$$K_1(y,\zeta) = U(y)\, I(y,\zeta) + U''(y)\, \frac{e^{-k|y-\zeta|}}{2k} \,, \tag{118}$$
$$K_2(y,\zeta) = U''(y)\, \frac{e^{-k(y+\zeta)}}{2k} \,.$$

There is one very significant difference between the linearized system and the space-discretized system. It has been shown* that the zeros of $U(z) - \Gamma/k$ (Γ on the real axis; neutral wave) must coincide with the zeros of $U''(z)$. For the profile, Eq. (94), there is only one level where $U''(z)$ is zero, and that is at the level $z = 0$ where $U = 0$. Hence the only value of Γ on the real axis which may be admissible is $\Gamma = 0$. Garcia has shown further that $\Gamma = 0$ is only admissible for $k = 1$.

With this knowledge it can be shown that the eigensolutions of Eq. (112) are not complete. Equation (112) evaluated at $z = 0$ gives: $-\Gamma q(0) = 0$. For $k \neq 1$, $\Gamma = 0$ is not admissible. All eigenfunctions must then be zero at $z = 0$ and it follows that we cannot fit a value of $q(0) \neq 0$ by combining eigensolutions if $k \neq 1$.

We must conclude that all the real positive λ^2, which are admitted by Eq. (101), yield space-discretized eigensolutions which are extraneous. They are not approximations of eigensolutions of the linearized system because the linearized system can have no such counterpart.

The extraneous eigensolutions appear because the space-discretized system must yield a complete set. The system can evolve all arbitrary initial fields with the aid of these eigensolutions but the approximations necessarily deteriorate with time. The extraneous eigensolutions cannot stand alone; either they rely on gross-truncation-error or they are not capable of satisfying the boundary conditions in the limit as we approach the continuous system.

It seems reasonable to believe that the real negative value of $\lambda^2(k)$, $0 < k < 1$, yields eigensolutions which are legitimate counterparts of corresponding eigensolutions of the linearized system. This implies that Eq. (117) admits only one value of $\Gamma^2(k)$

---

*See, e.g., Garcia[1] p. 90, or Lin[6] p. 118.

which is real and negative for $0 < k < 1$ and which is zero and terminates at $k = 1$ (Garcia's solution); and that there are no Γ admitted for $k > 1$.

Having accepted the two eigensolutions with eigenvalues $\pm i\nu$ for $0 < k < 1$ as true eigensolutions of the linearized system, it remains to determine their significance in the finite-amplitude system.

It is well known that the total energy (kinetic) is separable into the energy of the mean flow defined by $\bar{U} = \frac{1}{L}\int_0^L \mathbb{V} \cdot \mathbb{i}\, dx$ where L is the wave length of the perturbation, and the energy of the remainder of the flow (the eddy). This separation is possible because the space-integral of the product term is zero by definition of the mean flow. During evolution the finite-amplitude barotropic mechanism may transfer energy between the mean flow and the eddy but the sum of the two partial energies remains constant.

The linearized system violates this energy conservation. The perturbation remains sinusoidal in x and hence remains the eddy; the straight parallel flow which is held constant by choice, remains the mean flow. Thus the energy of the mean flow is constant even as the eddy grows.

The inclusion of the nonlinear part of the mechanism necessarily rights this situation. The straight parallel flow may still be maintained constant by choice and may make up all or part of the mean flow. The perturbation does not then retain its sinusoidal dependency although it does maintain its periodicity. Consequently the evolving perturbation is made up of the eddy and an addition to the mean flow.

It is of particular interest to determine how the mean flow evolves if the initial profile is dynamically unstable. We can determine this and the significance of the unstable eigensolution by making a finite-amplitude integration. As initial state, we take the straight parallel flow plus a self-excited unstable eigensolution (logically, the most unstable) with a small but finite amplitude.

We shall not further discuss the damped eigensolutions.

10. THE FINITE-AMPLITUDE PROBLEM

The finite-amplitude evolution obeys

$$\frac{\partial}{\partial t} q = -\left(\frac{\partial \psi}{\partial z} + U\right) \frac{\partial q}{\partial x} + \left(\frac{\partial q}{\partial z} + U''\right) \frac{\partial \psi}{\partial x} , \qquad (119)$$

where $q = \nabla^2 \psi$. We shall continue to keep the straight parallel flow, $U = -\tanh z$, constant by choice.

Only one integration is carried out. The perturbation is periodic in x with period 4π . The initial perturbation is based on

$$q(x,z) = D(z) \cos\left[kx - \phi(z)\right] , \qquad (120)$$

where $k = 1/2$ and $D(z)$ and $\phi(z)$ are given in Fig. 3 at $t = 15$ except that $D(z)$ is smoothed through $z = 0$.

A grid is introduced having 272 independent points (16 columns by 17 rows). The 17 rows, at intervals of $\pi/8$, extend the grid from $z = -\pi$ to π , inclusively. The columns divide the period 4π into 16 intervals of $\pi/4$ each.

The grid, plus an ordering, transforms our fields into vectors. The actual initial $\underset{\sim}{q}$ is given in Fig. 7 for one complete wave length. The extremes of the perturbation vorticity are approximately one-fourth as big as those of the profile.

We may refer to a grid point by its <u>coordinates</u> relative to the central leftmost point (0, 0):

$$\begin{aligned} x &= l\pi/4 , \qquad & l &= 0, 1, 2 \ldots 15 \\ z &= m\pi/8 , \qquad & m &= 0, \pm 1, \ldots \pm 8 . \end{aligned} \qquad (121)$$

Or we may refer to a point simply by giving <u>its address</u> (l, m).

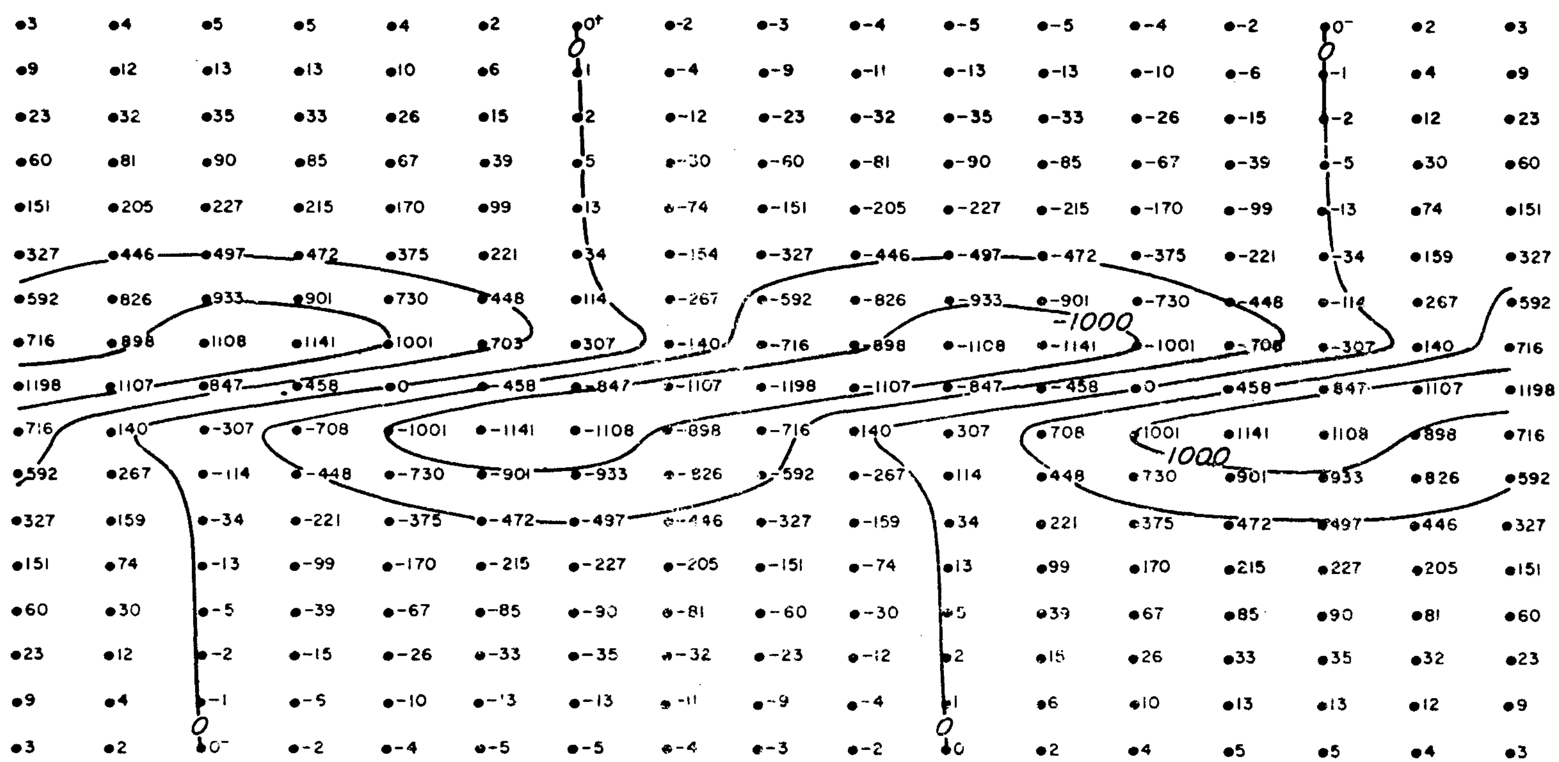

Fig. 7. The initial q-field (amplified by $10^4/1.6$).

The boundary conditions are treated essentially in the same way as they are treated in the unbounded linear integrations. However, instead of using a Green's function-integral type solution over the whole grid, we use it only to determine the values along the two rows $m = \pm 8$. In the interior we may then use the more rapid iterative inversion of the differential operator analogue.

Any particular grid point (l_o , m_o) together with the corresponding point in each of the other periods constitutes a vortex row with uniform strength, S , and uniform interval, $L = 4\pi$. The strength of each vortex is

$$S = q_{l_o m_o} \, \delta A$$

where $\delta A = (\pi/4)(\pi/8)$. The stream function which is compatible with such an unbounded and infinitely extended single row is given at the arbitrary grid point l, m by*

$$\begin{aligned} \psi_{l,m} &= \frac{S}{4\pi} \ln \left[\cosh \frac{\pi^2}{4L} (m - m_o) - \cos \frac{\pi^2}{2L} (l - l_o) \right] \\ &= \frac{\pi}{128} q_{l_o m_o} \ln \left[\cosh \frac{\pi}{16} (m - m_o) - \cos \frac{\pi}{8} (l - l_o) \right] . \end{aligned} \qquad (122)$$

The stream function at the point (l, m), due to the entire distribution, is then given by

$$\psi_{l,m} = \sum_{l_o m_o} \frac{\pi}{128} q_{l_o m_o} \ln \left[\cosh \frac{\pi(m-m_o}{16} \cos \frac{\pi(l-l_o}{8} \right] , \qquad (123)$$

in which the sum is taken over all the grid points as given by Eq. (121). It may be noted that in determining the stream function we are neglecting the vorticity outside our region of attention, as we did in the linear integrations. It is assumed that the vorticity on the outside remains negligible. This is something which will have to be checked by examining the growth at the extreme rows.

---

*See Lamb[5] p. 224.

For economy, Eq. (123) shall be used only for the extreme rows, $m = \pm 8$. The values of ψ, so determined on the extreme rows, then play the role of boundary values for the interior for which we shall invert a finite-difference analogue of $\nabla^2 \psi = q$. At an arbitrary point this analogue has the form

$$\frac{1}{10}\left(\psi_{\ell+1,m} + \psi_{\ell-1,m}\right) + \frac{4}{10}\left(\psi_{\ell,m+1} + \psi_{\ell,m-1}\right) - \psi_{\ell,m} = \frac{\pi^2}{160} q_{\ell,m} \tag{124}$$

The coefficient of $\psi_{\ell,m}$ has intentionally been made -1. If $\ell = 15$ then $\ell + 1$ is taken as 0, and if $\ell = 0$ then $\ell - 1$ is taken as 15 by virtue of the periodicity.

The interior grid is given some order $r = r(\ell, m)$. Equation (124), applied at each point <u>in this order</u>, then yields the system of simultaneous equations

$$\underset{\approx}{C} \, \underset{\sim}{\psi} = \underset{\sim}{d} \, . \tag{125}$$

If $m \neq \pm 7$ then $d_r = \frac{\pi^2}{160} q_{\ell,m}$. If $m = \pm 7$ then the known boundary value which appears on the left-hand side of Eq. (124) is moved to the right-hand side, and $d_r = \frac{\pi^2}{160} q_{\ell,\pm 7} - \frac{4}{10} \psi_{\ell,\pm 8}$

Equation (124) is a partial difference equation of the elliptic type. It is convenient to invert the system, Eq. (125), by an iterative procedure known as the method of successive overrelaxation.* To formally exhibit the method, we first express $\underset{\approx}{C}$ as the sum of three matrices $\underset{\approx}{C} = \underset{\approx}{U} + \underset{\approx}{L} - \underset{\approx}{I}$. In $\underset{\approx}{U}$, nonzero elements appear only above the main diagonal. In $\underset{\approx}{L}$, nonzero elements appear only below the main diagonal. The matrix $\underset{\approx}{I}$ is the identity matrix.

The method is given by

$$\underset{\sim}{\psi}^{(s+1)} = \underset{\sim}{\psi}^{(s)} + \omega \underset{\sim}{R}^{(s+1/2)} \tag{126}$$

*The extrapolated Liebmann method is of this type.

where

$$\underset{\sim}{R}^{(s+1/2)} = \underset{\approx}{L}\,\underset{\sim}{\psi}^{(s+1)} + \underset{\approx}{U}\,\psi^{(s)} - \underset{\sim}{d} - \psi^{(s)} \tag{127}$$

The superscripts in parentheses number the successive approximations of $\underset{\sim}{\psi}$. The operation is carried out in the order r. Hence at a point r_0, the points following, $r > r_0$, are operated on by $\underset{\approx}{U}$, and the points preceding which are once later estimates, $r < r_0$, by $\underset{\approx}{L}$.

If we substitute $\underset{\sim}{\psi}^{(s)} = \underset{\sim}{\psi} + \underset{\sim}{e}^{(s)}$, where $\underset{\sim}{\psi}$ satisfies Eq. (125), in Eq. (126) we find

$$\underset{\sim}{e}^{(s+1)} = \underset{\approx}{T}\,e^{(s)} = \underset{\approx}{T}^{s+1}\,\underset{\sim}{e}^{(0)}, \tag{128}$$

where

$$\underset{\approx}{T} = \left(\underset{\approx}{I} - \omega\underset{\approx}{L}\right)^{-1}\left[(1-\omega)\underset{\approx}{I} + \omega\underset{\approx}{U}\right] \tag{129}$$

This reveals that the convergence depends on the eigenvalues of $\underset{\approx}{T}$ which are given by

$$\left|\underset{\approx}{T} - \lambda\underset{\approx}{I}\right| = 0 \;. \tag{130}$$

The convergence rate is generally dominated by the eigenvalue having the largest magnitude.* Let this magnitude be $\bar{\lambda}$. That $\bar{\lambda} < 1$ is a necessary and sufficient condition for convergence. The rate of convergence may be expressed by $-\ln\bar{\lambda}$.

We are still free to select the ordering, $r(\ell, m)$, and the value of ω. We would like to select these so as to make $\bar{\lambda}$ a minimum. The following analysis of this problem is based on a detailed paper by Young.[10]

*This has been discussed in Section 6 in connection with Eq. (79).

Substituting for $\underset{\approx}{T}$ in Eq. (130) leads to the determinant

$$\left| \left(\underset{\approx}{U} + \lambda \underset{\approx}{L}\right) - \frac{\lambda + \omega - 1}{\omega} \underset{\approx}{I} \right| = 0 \; . \tag{131}$$

In particular instances Eq. (131) is <u>equivalent</u> to

$$\left| \lambda^{1/2} \left(\underset{\approx}{U} + \underset{\approx}{L}\right) - \frac{\lambda + \omega - 1}{\omega} \underset{\approx}{I} \right| = 0 \; . \tag{132}$$

This is so if each term of the formal expansion of the determinant either vanishes because one or more of its elements is zero or, if all its elements are nonzero, then as many come from above the diagonal as from below. The above equivalence is generally latent in elliptic difference equations for most, but not all, grid selections. The equivalence may then be realized by choosing one of a more or less large family of orderings (called "consistent" orderings by Young).

It will be seen that all consistent orderings lead to the same eigenvalues for $\underset{\approx}{T}$. Young then proceeds to determine the best ω for this family of orderings. The possibility remains, however, that there may exist an ordering which is not consistent and which leads to a smaller $\bar{\lambda}$ than can be realized with a consistent ordering. Young's analysis does not rule out this possibility.

The equivalence is latent in our problem if, and only if, we divide the x cycle into an <u>even</u> number of intervals greater than two—as we have done. The simplest consistent ordering and the one we adopt is then:

$$r = 8m + \ell/2 + \begin{cases} 57 & \text{for } \ell \text{ even } m \text{ odd} \\ 176\ 1/2 & \text{" \ " odd " odd} \\ 56\ 1/2 & \text{" \ " odd " even} \\ 177 & \text{" \ " even " even} \end{cases} \tag{133}$$

In effect, this numbers the 240 interior points as one would count checkerboard squares, counting the light squares first and continuing with the dark squares, beginning each traverse at the lower left.

We may now proceed from Eq. (132). Let us denote the eigenvalues of $\underset{\approx}{U} + \underset{\approx}{L} \equiv \underset{\approx}{C} + \underset{\approx}{I}$ by $\mu_1, \mu_2 \cdots \mu_n \cdots \mu_{240}$. These depend on Eq. (124) and the grid dimensions, but not on the ordering. It follows from Eq. (132) that the λ are given by

$$\frac{\lambda_n + \omega - 1}{\omega \lambda_n^{1/2}} = \mu_n . \tag{134}$$

That $\bar{\lambda}$ be less than 1 can be accomplished for some ω only if all μ satisfy $-1 < \mathrm{Re}: \mu < 1$. If in addition all μ are real, then Young has shown that the best ω is given by

$$\omega_b = 1 + \left[\frac{\bar{\mu}^2}{1 + (1-\bar{\mu}^2)^{1/2}} \right]^2 . \tag{135}$$

This yields

$$\bar{\lambda} = \omega_b - 1 \tag{136}$$

The eigensolutions of $\underset{\approx}{C} + \underset{\approx}{I}$ are given by

$$\psi_{l,m}(L,M) = \sin \frac{2\pi L}{16} l \sin \frac{\pi(M+8)}{16} (m+8) , \tag{137}$$

where L and M take on the values

$L = 0, 1, 2, \ldots 15$

$M = -7, -6, \ldots 0, \ldots 6, 7.$

The corresponding eigenvalues are given by

$$\mu(L,M) = \frac{1}{5} \left[\cos \frac{2\pi L}{16} + 4 \cos \frac{\pi(M+8)}{16} \right] \tag{138}$$

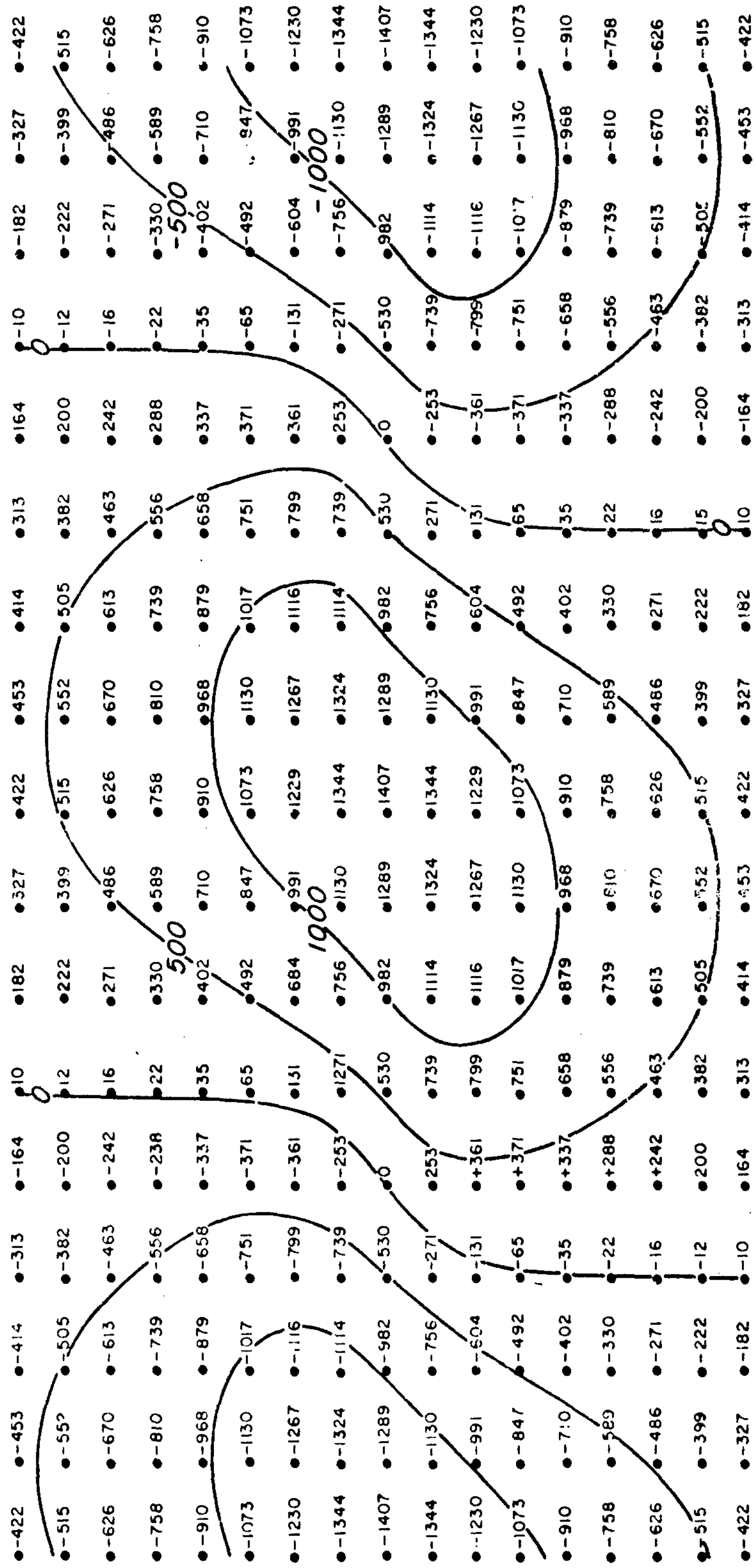

Fig. 6. The initial ψ-field (amplified by $10^4/1.6$).

Hence

$$\bar{\mu} = \frac{1}{5}\left[1 + 4 \cos\frac{\pi}{16}\right] \tag{139}$$
$$= 0.98463$$

For this value of $\bar{\mu}$, Eqs. (135) and (136) yield

$$\omega_b = 1.6812 ; \quad \bar{\lambda} = 0.6812 \tag{140}$$

Determining the rate of convergence by $-\ln \bar{\lambda}$ shows, in this particular application, that using the best ω accelerates convergence by a factor of 12 over and above the factor of 2 gained by relaxing the grid points successively with $\omega = 1$ in a consistent order.

The initial stream function, ψ, as given in Fig. 8 was determined in the manner described, from the initial vorticity given in Fig. 7. The relaxation was continued until Eq. (124) was satisfied at each point within the exacting tolerance of $2^{-28} \simeq 3.68 \times 10^{-8}$, in the same units.

11. THE INTEGRATING PROCEDURE (NONLINEAR PROBLEM)

We shall take up the problem of the time-discretization as the first stage in arriving at a complete numerical analogue for our nonlinear system, Eq. (119), page 68. This will be followed by the space discretization which was begun in Section 10 (for $q = \nabla^2 \psi$).

The system, Eq. (119), is of the first-order in time and may be regarded as a special case of the generalization

$$\frac{\partial}{\partial t} X_i = F_i(X_1, X_2 \ldots), \quad i = 1, 2, 3 \ldots, \tag{141}$$

where X_i is one of a finite number of fields. The F's at any instant are space dependent only.

We shall again use τ to denote our time increment and mark off the instances $t = 0, \tau, 2\tau, \ldots (N-1)\tau, N\tau, (N+1)\tau \ldots$ As the time-discretized form of Eq. (141) we offer

$$(X_i)_{N+1} - (X_i)_N = \tau F_i(\bar{X}_1, \bar{X}_2 \ldots); \quad i = 1, 2 \ldots \tag{142}$$

where the bar implies the mean for the increment, that is,

$$\overline{(\;)} = \frac{1}{2}(\;)_N + \frac{1}{2}(\;)_{N+1} \; . \tag{143}$$

Linearized on <u>any</u> zero-order stationary state, Eq. (142) reduces to the same formula used in our linear integrations. For its solution we shall have to resort to a method of successive approximations (reiterations). Because of the nonlinearity the problem of convergence becomes largely a matter of trial and error.

For propagated effects the domain of dependence (region of influence) using Eq. (142) may be all inclusive for any τ even after space-discretization.

The form, Eq. (119), of our system was arrived at from the governing equation,

$$\frac{\partial}{\partial t} Q = -\mathbb{V} \cdot \nabla Q \;, \tag{144}$$

where $\mathbb{V} = \mathring{\mathbb{j}} \times \nabla \Psi$ and $Q = \nabla^2 \Psi$, by explicit reference to the zero-order straight parallel flow which is kept constant by choice:

$$\mathbb{V} = U\mathring{\mathbb{i}} + \mathbb{v} \Rightarrow Q = U' + q \; \tag{145}$$

We may instead refer to some other state which we shall call the s field and denote by subscript s:

$$\mathbb{V} = \mathbb{V}_s + \mathbb{v} \Rightarrow Q = Q_s + q \,, \tag{146}$$

which satisfies

$$\mathbb{V}_s \cdot \nabla Q_s = 0 \ . \tag{147}$$

This gives

$$\frac{\partial}{\partial t} q = -(\mathbb{V}_s \cdot \nabla) q - (\nabla Q_s) \cdot \mathbb{v} - \mathbb{v} \cdot \nabla q \ . \tag{148}$$

We may postulate that for a given region and particular time interval there exist an s field which minimizes in some prescribed manner the contribution of the nonlinear term of Eq. (148). The amount of linearity exhibited in this manner may be called the inherent linearity during that interval.

The evolution of the large-scale fields of motion in the atmosphere probably exhibit a high degree of inherent linearity even up to periods of a day or so.

The degree of inherent linearity during one time-step (interval) seems pertinent to the problem of convergence of the reiterative process. It may be that if 90 percent or so of the change comes from the linear terms, then the convergence is essentially governed by these terms. This is uncertain; but the smallness of τ must certainly be significant. It may be noted that even in the limit, $\tau \rightarrow 0$, the mechanism generally remains nonlinear.

Another significant feature of the implicit formula, Eq. (142) follows: Applied to the barotropic equation, Eq. (144), this formulation preserves the conservation of total kinetic energy which is inherent in the system for a closed region. It follows that the time-truncation error remains bounded; hence, this form of time-discretization does not introduce any computational instability.

The conservation of total kinetic energy is derived from Eq. (144), in a closed region ($\psi = \psi_b$ on the boundary), in the following manner. Multiply Eq. (144) by ψ and integrate over the region:

$$\int_A \psi \frac{\partial}{\partial t} \nabla^2 \psi \, da = -\int_A \psi \mathbb{V} \cdot \nabla Q \, da \ .$$

To show that the right-hand side is zero, we substitute

$$\psi \mathbb{V} \cdot \nabla Q \equiv \nabla \cdot (\mathbb{V} Q \psi) - Q\psi \nabla \cdot \mathbb{V} - Q \mathbb{V} \cdot \nabla \psi ,$$

where the second and third terms are zero everywhere. Then by Gauss' theorem

$$-\int_A \nabla \cdot (\mathbb{V} Q \psi) \, da = -\oint \mathbb{V} Q \psi \cdot dm$$

which vanishes because there is no outflow.

This leaves us with

$$\int_A \psi \frac{\partial}{\partial t} \nabla^2 \psi \, da = 0$$

$$= \int_A \nabla \cdot \left(\psi \frac{\partial}{\partial t} \nabla \psi\right) da - \int_A \nabla \psi \cdot \frac{\partial}{\partial t} \nabla \psi \, da$$

$$= \oint \psi_b \frac{\partial}{\partial t} \nabla \psi \cdot dm - \int_A \frac{\partial}{\partial t} V^2/2 \, da .$$

The first of the two integrals on the right-hand side is zero because

$$\oint \psi_b \frac{\partial}{\partial t} \nabla \psi \cdot dm = \psi_b \frac{\partial}{\partial t} \int_A \nabla^2 \psi \, da ,$$

and the total contained vorticity remains constant. Thus we have shown

$$\frac{\partial}{\partial t} \int_A V^2/2 \, da = 0 .$$

The proof for the time-discretized form

$$\nabla^2 \psi_{N+1} - \nabla^2 \psi_N = -\tau \overline{\mathbb{V}} \cdot \nabla \overline{Q} \qquad (149)$$

is similar. We multiply by $\overline{\Psi}$ and integrate over the area. As before, the right-hand side drops out and we are left with

$$\int_A \frac{1}{2}\left(\Psi_{N+1} + \Psi_N\right)\left(\nabla^2\Psi_{N+1} - \nabla^2\Psi_N\right) da = 0$$

$$\frac{1}{2}\int_A \left(\nabla\Psi_{N+1}\cdot\nabla\Psi_{N+1} - \nabla\Psi_N\cdot\nabla\Psi_N\right) da + \int_A \nabla\cdot\left[\overline{\Psi}\left(\nabla\Psi_{N+1} - \nabla\Psi_N\right)\right] da = 0 .$$

The second integral is zero because

$$\int_A \nabla\cdot\left[\overline{\Psi}\left(\nabla\Psi_{N+1} - \nabla\Psi_N\right)\right] da = \oint \Psi_b\left(\nabla\Psi_{N+1} - \nabla\Psi_N\right)\cdot dm$$

$$= \Psi_b \int_A \left(\nabla^2\Psi_{N+1} - \nabla^2\Psi_N\right) da = \Psi_b \int_A -\tau\overline{\mathbb{V}}\cdot\nabla\overline{Q}\cdot da = 0 .$$

This leaves us with

$$\int_A V_{N+1}^2 \, da = \int_A V_N^2 \, da$$

which was to be proven.

The preservation of this inherent property after space-discretization leads to an analogue which may be rather difficult to use. To achiev . it we multiply Eq. (149) by $\overline{\Psi}$ and transform the equation into the form

$$\frac{1}{2}\nabla\Psi_{N+1}\cdot\nabla\Psi_{N+1} - \frac{1}{2}\nabla\Psi_N\,\nabla\Psi_N = \tag{150}$$

$$\nabla\cdot\left[\overline{\Psi}\left(\nabla\Psi_{N+1} - \nabla\Psi_N + \tau\overline{\mathbb{V}}\overline{Q}\right)\right] .$$

This is then space-discretized in such a manner that the summation of the term on the right-hand side cancels over all interior grid points. The boundary conditions must have the bracketed term zero at the boundary grid points.

In practice this analogue must then be solved by a reiterative process. This may prove to be difficult.

Because of the nature of our boundary conditions, we have not followed through with the total energy-conserving space-discretization. Instead, for space we have used more conventional finite-differencing. We have already shown in Section 10 how $\nabla^2\psi = q$ and the boundary conditions are to be handled.

Our governing equation, Eq. (119), page 68, time-discretized has the form

$$q_{N+1} - q_N = \tau \left[-\left(\frac{\partial \bar{\psi}}{\partial z} + U \right) \frac{\partial \bar{q}}{\partial x} + \left(\frac{\partial \bar{q}}{\partial z} + U'' \right) \frac{\partial \bar{\psi}}{\partial x} \right]. \qquad (151)$$

This is to be applied to our grid which at a representative <u>interior</u> point has the spacing:

$$\begin{array}{ccccccc} & & & N & & & \\ & & & \circ & & & \\ & & & h & & & \\ W & \circ & 2h & \circ & 2h & \circ & E \\ & & & h & & & \\ & & & \circ & & & \\ & & & S & & & \end{array}$$

Compass directions are used to label neighbouring points relative to the arbitrary point at which Eq. (151) is being applied. We choose to use the analogue

$$q_{N+1} - q_N = \frac{\tau}{8h^2}\left[(\bar{\psi}_E - \bar{\psi}_W)(\beta + \bar{q}_N - \bar{q}_S) - (\bar{q}_E - \bar{q}_W)(\alpha + \bar{\psi}_N - \bar{\psi}_S) \right] , \qquad (152)$$

where $\alpha = 2h U_M$, $\beta = 2h U''_M$ and $h = \pi/8$.
We have one such equation for each interior point. The vorticity changes at the upper and lower boundaries may be obtained by a linear extrapolation of the changes from the interior, or one may

attempt to keep the values of $\underset{\sim}{q}$ constant there in the hope that both the values and gradients at these fringes will remain small anyway. We will try the latter method and will check the validity of this procedure from our results.

The set of equations, Eq. (152), for all interior points may be packaged into the representation

$$\underset{\sim}{q}_{N+1} = \underset{\sim}{q}_N + \tau \underset{\sim}{F}(\bar{\underset{\sim}{q}}, \bar{\underset{\sim}{\psi}})$$

This analogue must also be solved by reiterating. We shall attempt the same procedure used in the linear integrations:

$$\underset{\sim}{q}_{N+1}^{(\Delta+1)} = \underset{\sim}{q}_N + \tau \underset{\sim}{F}(\bar{\underset{\sim}{q}}^{(\Delta)}, \bar{\underset{\sim}{\psi}}^{(\Delta)}), \tag{153}$$

where

$$\bar{\underset{\sim}{q}}^{(\Delta)} = \frac{1}{2}\left[\underset{\sim}{q}_N + \underset{\sim}{q}_{N+1}^{(\Delta)}\right]; \quad \bar{\underset{\sim}{\psi}}^{(\Delta)} = \frac{1}{2}\left[\underset{\sim}{\psi}_N + \underset{\sim}{\psi}_{N+1}^{(\Delta)}\right].$$

$\underset{\sim}{\psi}_{N+1}^{(\Delta+1)}$ is determined from $\underset{\sim}{q}_{N+1}^{(\Delta+1)}$ by the method of Section 10. The iterations are repeated until $\Delta = S$ determined by $\underset{\sim}{q}_{N+1}^{(\Delta)} \approx \underset{\sim}{q}_{N+1}^{(\Delta-1)}$ in that both are compatible with $\underset{\sim}{\psi}_{N+1}^{(\Delta-1)}$ within the prescribed tolerance at all interior points.

As a first guess for $\underset{\sim}{q}_{N+1}$ and for $\underset{\sim}{\psi}_{N+1}$ we choose linear extrapolation in time,

$$\underset{\sim}{q}_{N+1}^{(0)} = 2\underset{\sim}{q}_N - \underset{\sim}{q}_{N-1}, \quad \underset{\sim}{\psi}_{N+1}^{(0)} = 2\underset{\sim}{\psi}_N - \underset{\sim}{\psi}_{N-1}, \tag{154}$$

except for the first time-step where we take

$$\underset{\sim}{q}_1^{(0)} = \underset{\sim}{q}_0, \quad \underset{\sim}{\psi}_1^{(0)} = \underset{\sim}{\psi}_0 \tag{155}$$

We choose $\tau = 1/10$. It is hoped that the inherent linearity will be quite large for so small time-steps (depending as it does on the particular evolution) and that Eq. (153) will converge essentially as if it were linear.

The determination of $\underset{\sim}{\psi}_{N+1}^{(s+1)}$ from $\underset{\sim}{q}_{N+1}^{(s+1)}$ requires the determination of ψ on the upper and lower boundaries by Green's method, followed by the successive overrelaxation of the interior points beginning with $\underset{\sim}{\psi}_{N+1}^{(s)}$ as first guess. We desire compatibility of $\underset{\sim}{\psi}_{N+1}$ and $\underset{\sim}{q}_{N+1}$ to within quite small tolerance, but the successive estimates of these vectors need not be so highly compatible. It would seem wasteful to make them so.

In an attempt to accelerate convergence to $\underset{\sim}{\psi}_{N+1}$ and $\underset{\sim}{q}_{N+1}$, the following scheme is incorporated into the relaxation. After each complete grid traverse in a series of traverses, the tolerance is raised by multiplication with a prescribed factor greater than one. Hence, the more traverses it takes to determine $\underset{\sim}{\psi}_{N+1}^{(s+1)}$ the greater its incompatibility with $\underset{\sim}{q}_{N+1}^{(s+1)}$. The tolerance is then reset at its original small value to begin the next series of traverses. Thus, if convergence (all within tolerance) is found on one traverse (which signals $s = S$) then $\underset{\sim}{\psi}_{N+1}$ and $\underset{\sim}{q}_{N+1}$ have been found to the desired prescribed initial tolerance. This scheme considerably shortened test computations in which a factor of 1.25 was used.

12. THE RESULTS

The initial perturbation field which is superimposed on the unbounded hyperbolic-tangent profile is given in Figs. 7 and 8, pages 69 and 75, respectively. Computations have been carried out which take the evolution to $t = 5$.* Outputs were obtained every five time-steps, that is, at intervals of $t = 1/2$. Figures 9 and 10 show the fields at $t = 2$ and Figs. 11 and 12 at $t = 5$. Six more decimal digits were carried and outputed beyond those shown in the figures.

*See footnote p. 51.

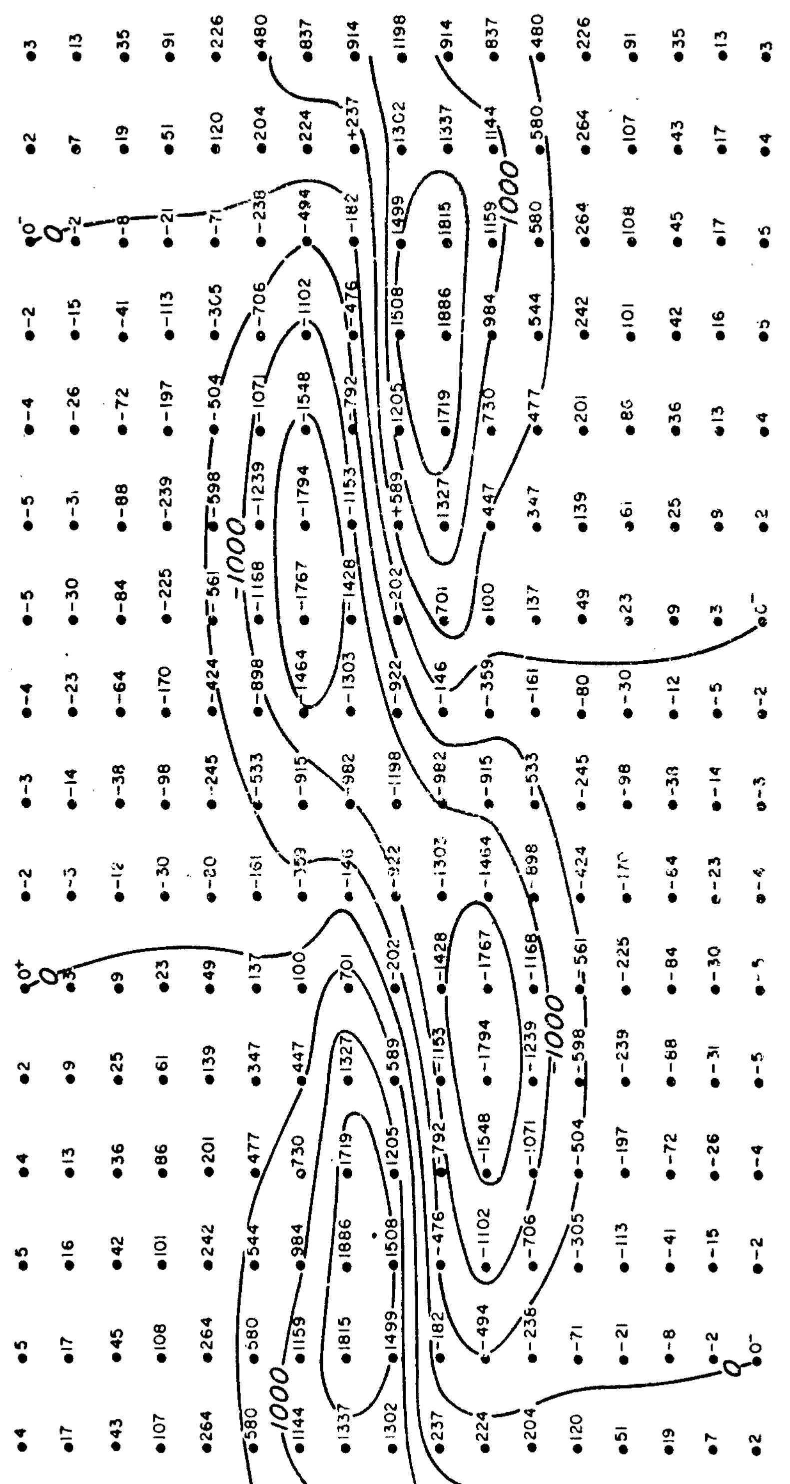

Fig. 9. The q-field at $t = 2$ (amplified by $10^4/1.6$).

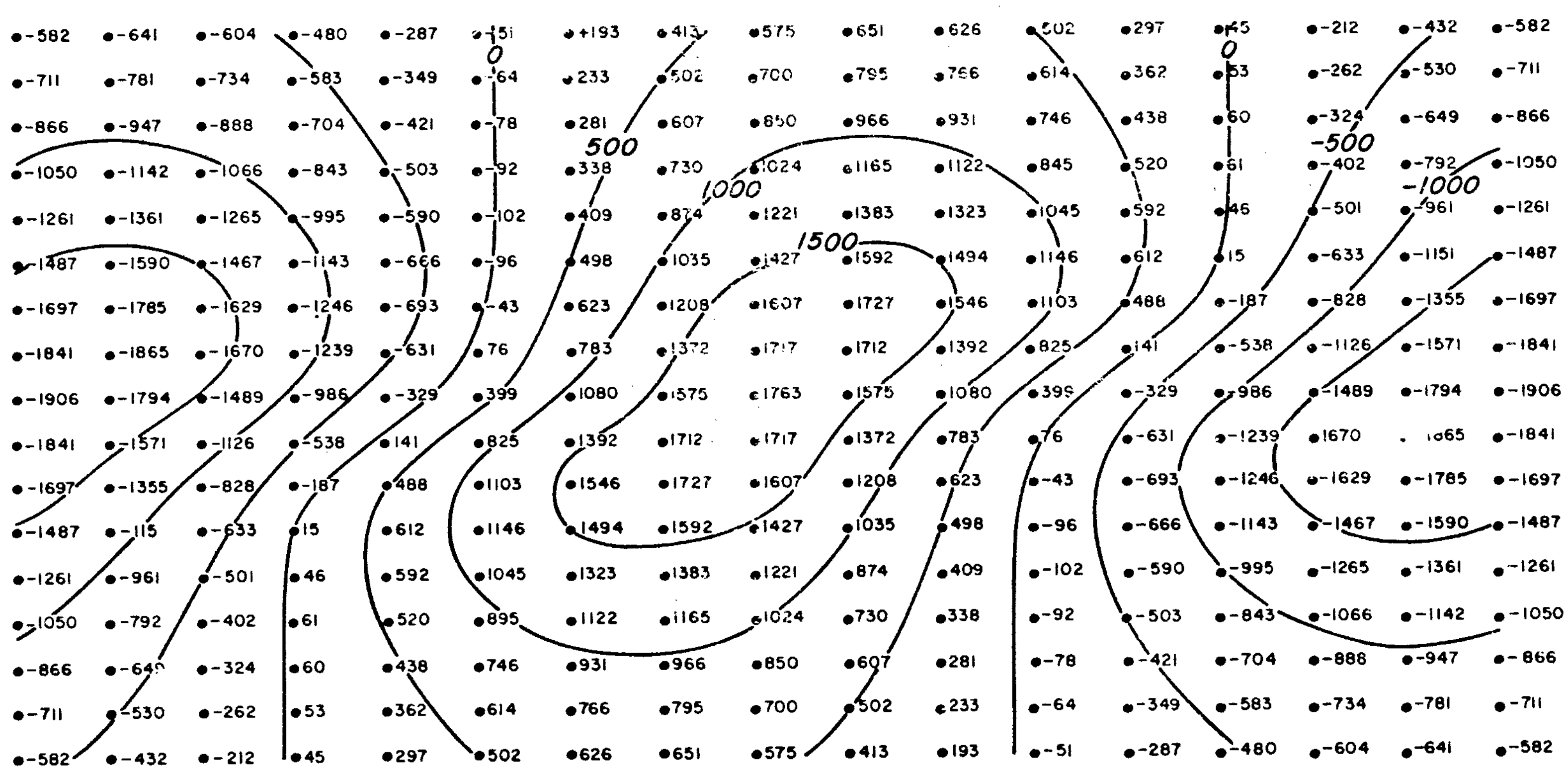

Fig. 10. The ψ-field at $t = 2$ (amplified by $10^4/1.6$).

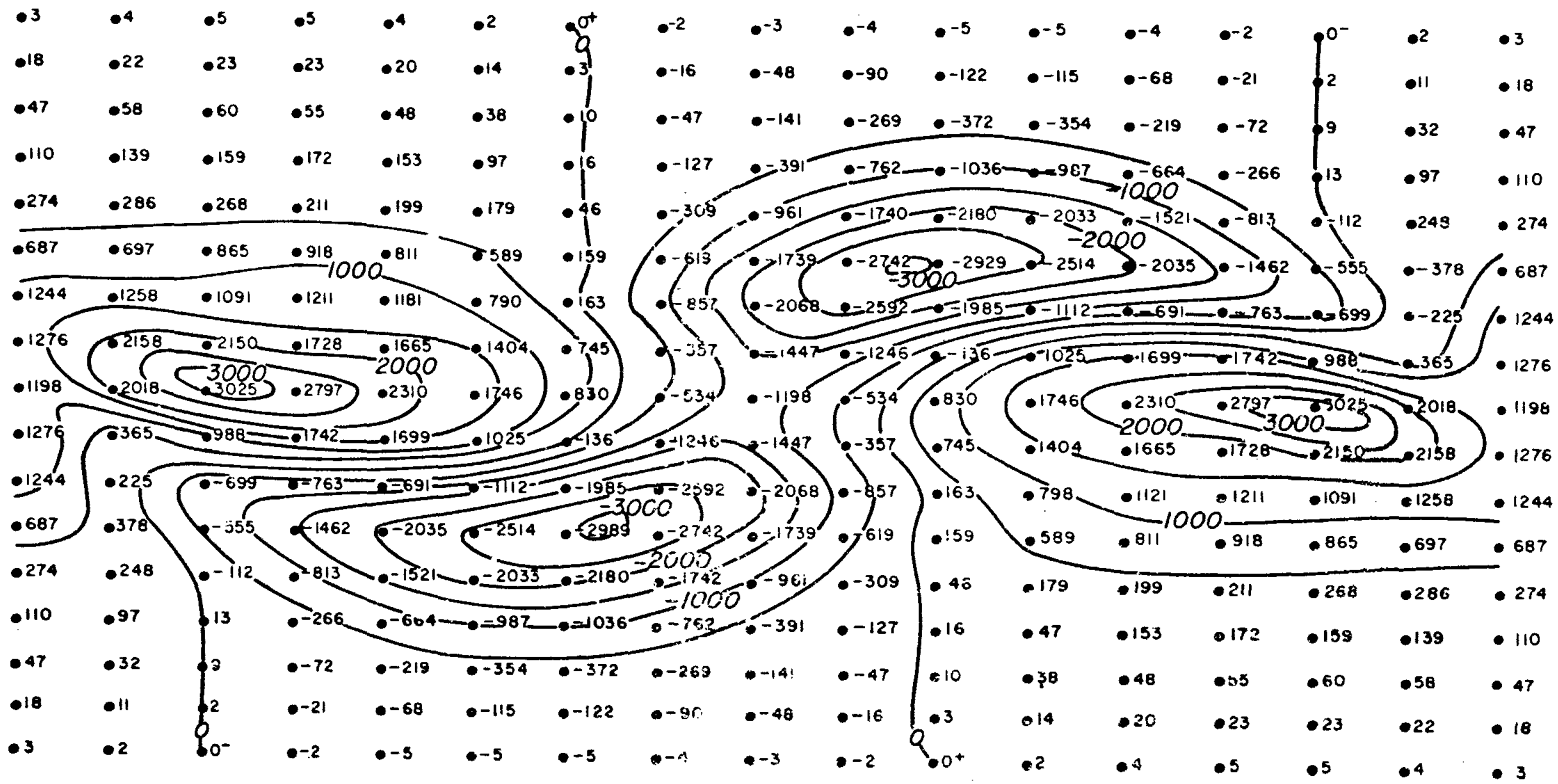

Fig. 11. q -field at t = 5 (amplified by $10^4/1.6$).

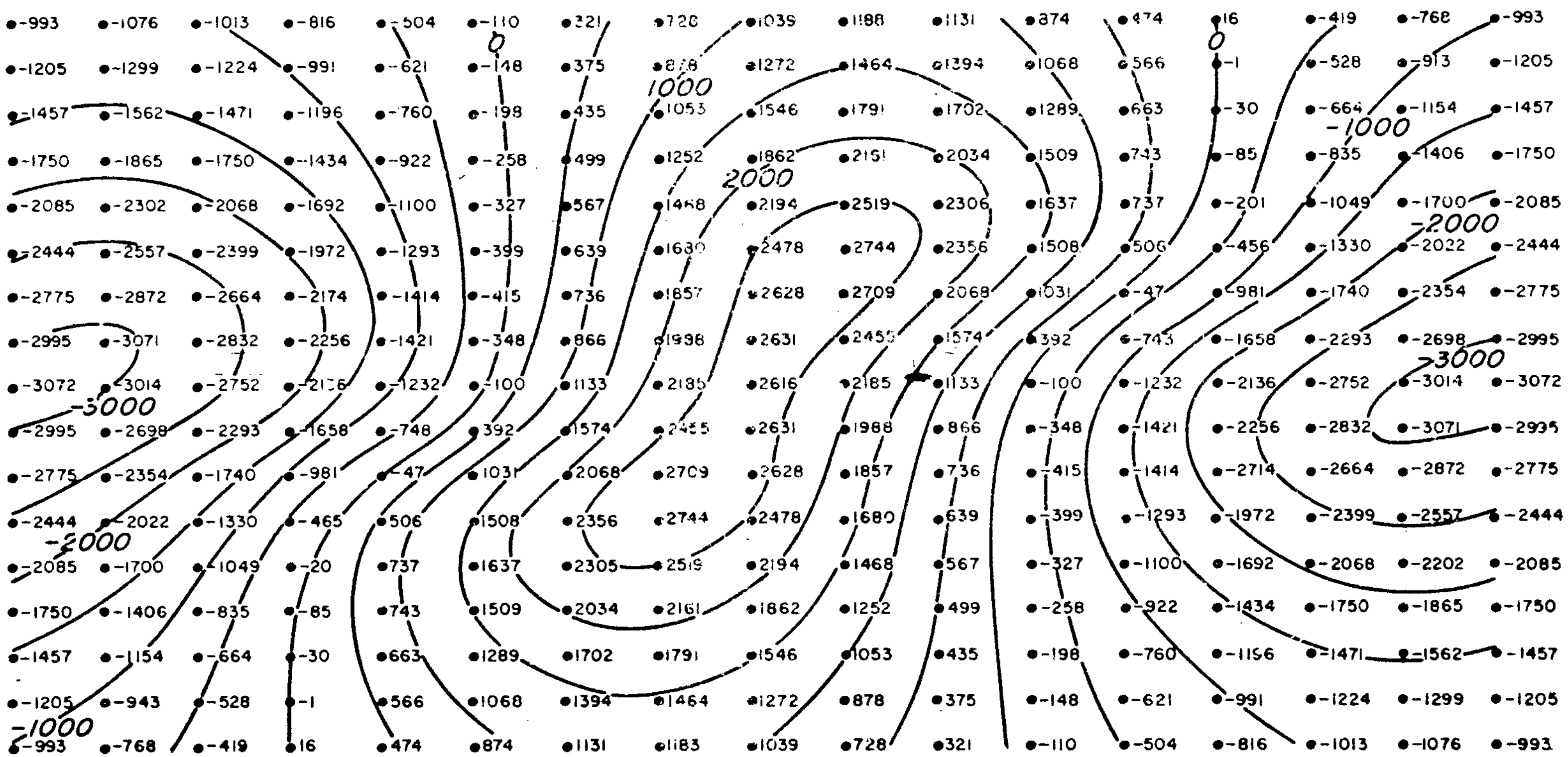

Fig. 12. The ψ-field at $t = 5$ (amplified by $10^4/1.6$).

It is notable that the position and growth develops essentially as predicted by the linear integrations. This shows the significance of the unstable characteristic yielded by the linear theory.

What we call the perturbation is now composed of an eddy and a mean (averaged along x) which when added to our profile gives the mean flow. An examination of Fig. 11 reveals how the mean flow is being modified. The centers of positive perturbation vorticity have moved inward, toward the central level, and the centers of negative vorticity have moved outward, away from the central level.

The profile itself has only negative vorticity with a maximum at the central level. Thus, the eddy is altering the mean flow by transporting mean negative vorticity away from the central level.

The perturbation fields at $t = 5$ are averaged along x to show the following means.

m	q_m	ψ_m
8, -8	0	4
7, -7	- 22	4
6, -6	- 70	- 1
5, -5	-205	- 15
4, -4	- 497	- 62
3, -3	- 593	-186
2, -2	- 229	-400
1, -1	+860	-650
0	+ 1, 524	-768

These values of q_m and ψ_m have been amplified by $10^4/1.6$. The removal of these means from the perturbation yields the eddy shown in Figs. 13 and 14. Figure 15 shows how these perturbation means have altered the mean flow, tending apparently to stabilize it.

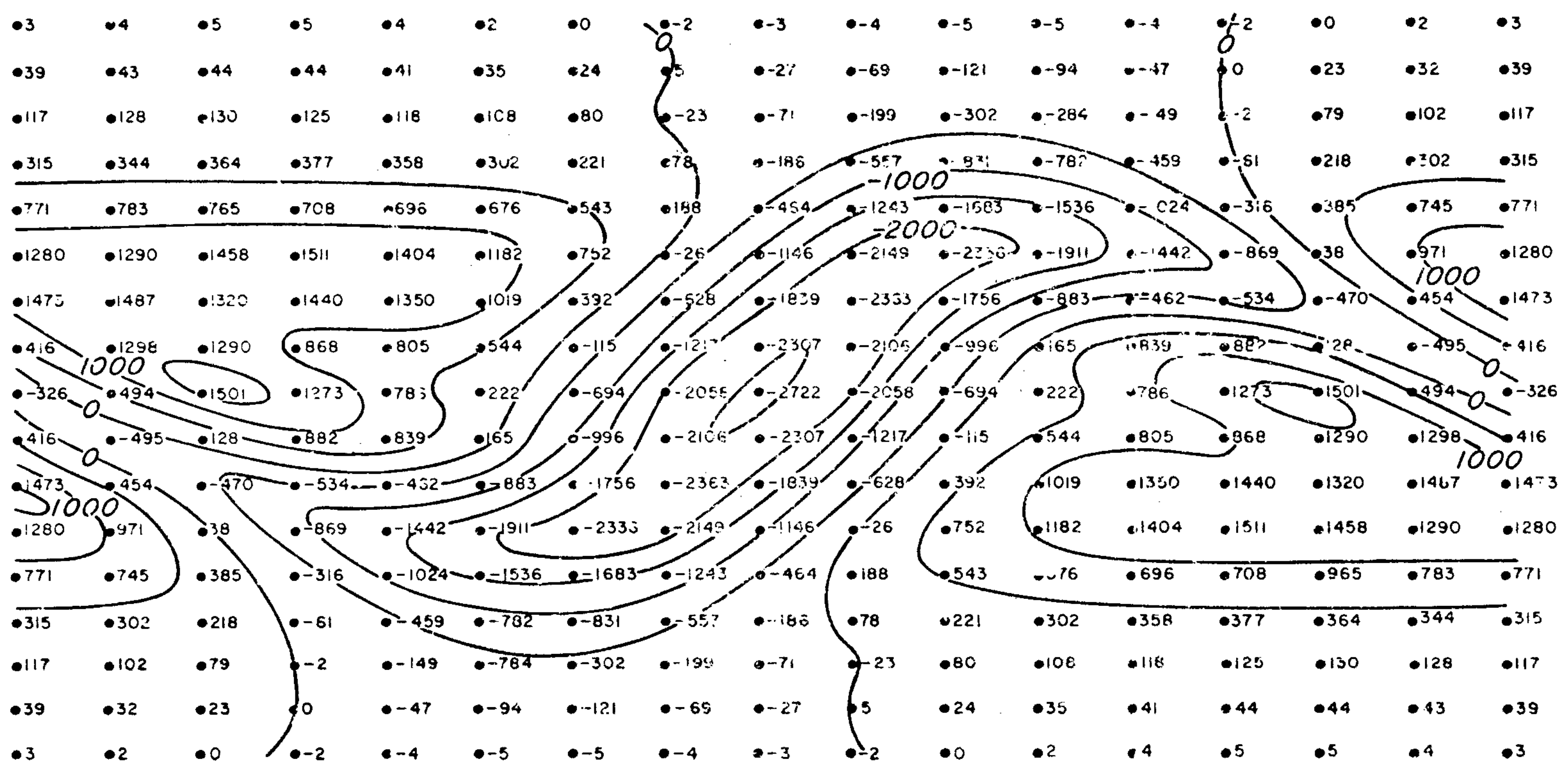

Fig. 13. The eddy vorticity at $t = 5$ (amplified by $10^4/1.6$).

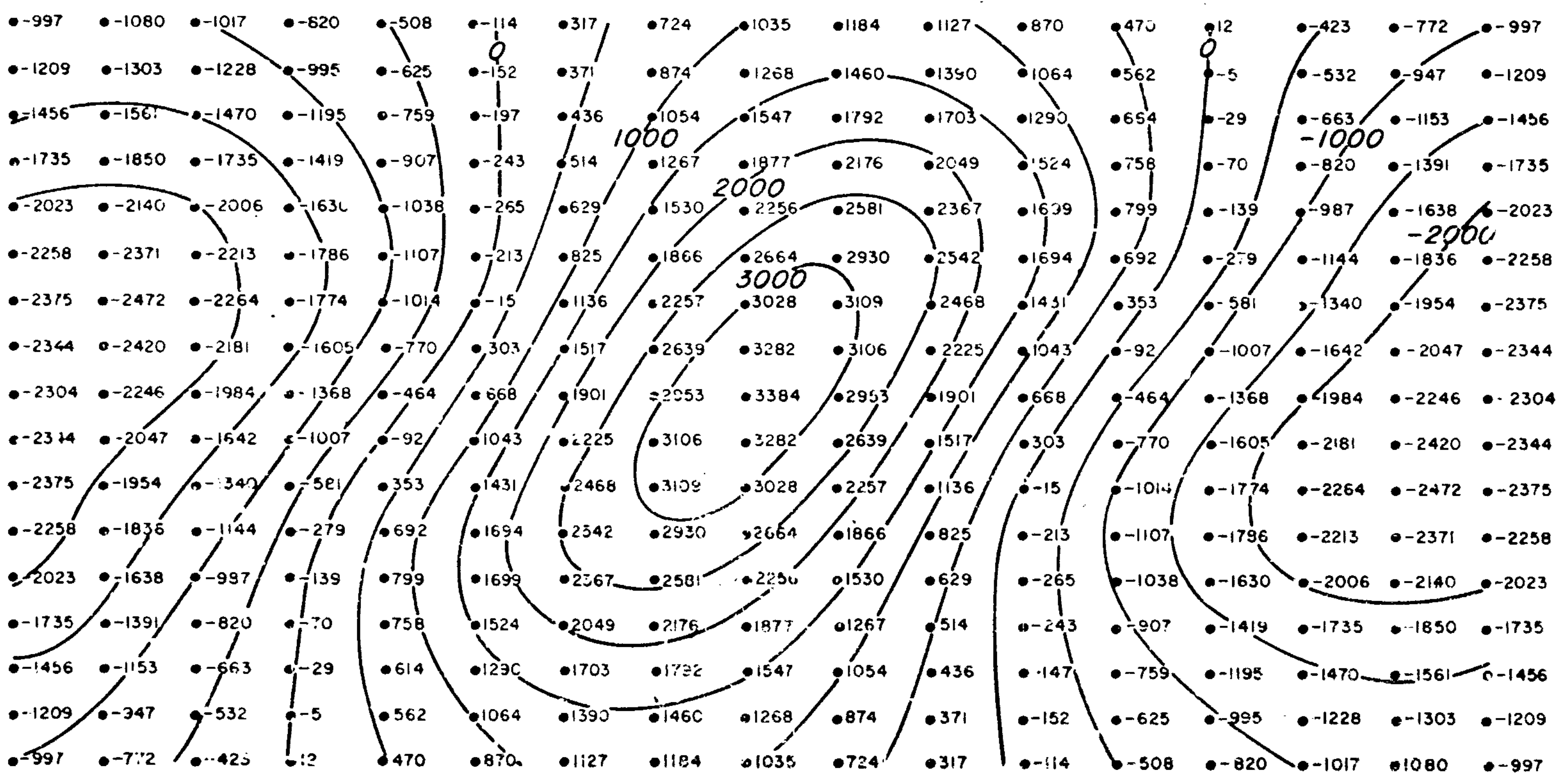

Fig. 14. The eddy streamfunction at $t = 5$ (amplified by $10^4/1.6$).

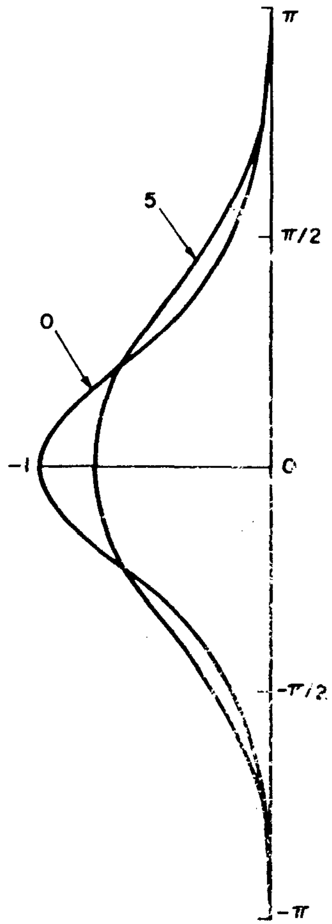

Fig. 15. Vorticity of mean flow at $t = 0$ and $t = 5$.

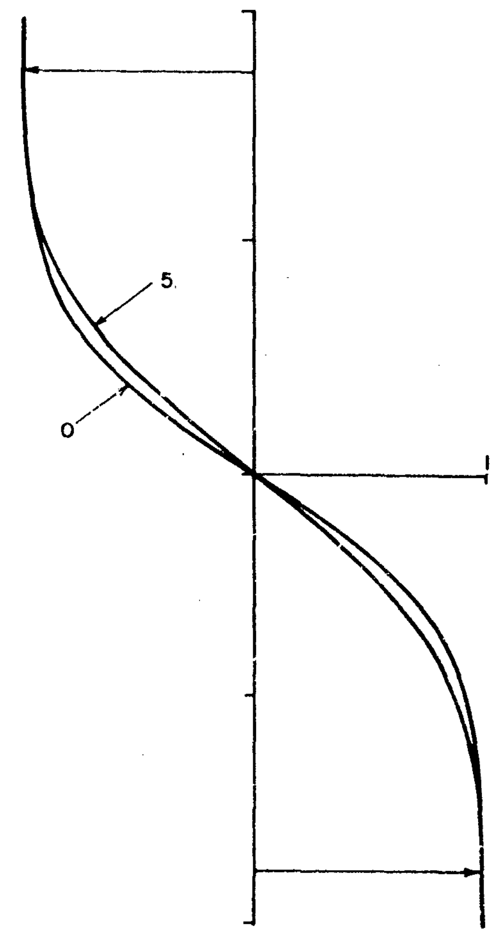

Mean flow at $t = 0$ and $t = 5$.

It is quite noticeable that the error due to space-discretization is becoming more serious as the evolution progresses. This is one reason why the computations have not been carried further with our present grid. Another reason for not continuing is that our initial value lacks generality. We have placed the constraint of periodicity of period 4π on the evolution. As a demonstration of what may develop due to dynamic instability and the presence of noise, we have gone far enough.

13. CONCLUDING REMARKS

The instability mechanism is pertinent to a number of meteorological problems on all scales. However, a more comprehensive approach to any of these problems generally includes the effects of other meteorological parameters.

The results of Section 12 demonstrate the modification of motion on one scale by the formation of eddies on a lower scale, the scale of the eddies being dynamically determined by the causative gradients. It has clearly been revealed that such modification cannot be handled by an empirical eddy viscosity. The profile we have examined contains a vorticity maximum which is flattened by the eddies. If the profile had a vorticity minimum instead, the rate of smoothing would not at all have progressed so rapidly because such a profile is dynamically stable and thus does not favor eddy formation.

Consider the large-scale vertical structure of the atmosphere. At a single locality we may ignore horizontal variations at all levels if it can later be shown that these variations are negligible on the scale of the developing eddies. A comprehensive approach to the stability problem might then be developed which takes account of variations with height in the large-scale density, horizontal velocity, and humidity distributions. It might also be wise to include the modifying effect of the local variation with height in the large-scale fields of vertical motion and horizontal divergence.

The eddies which form due to the vertical structure of the atmosphere are not only significant because they are associated with convective clouds and turbulence but also because they modify the vertical structure.

On the whole, the lapse rate must be the most significant parameter in determining vertical dynamic stability of the atmosphere. Even though it can be shown by a proper selection of units that the eddy in our study grew from having a maximum vertical component of about four meters per second to twelve meters per second in less than eight minutes, this in itself is not significant. Our thinking must be modified by other considerations.

We must also consider the rate at which the dynamic instability of the vertical structure is being built up by large-scale processes including surface heating. As the vertical structure crosses thresholds of instability how much energy becomes available to the eddies? And are the eddies capable of modifying the vertical structure rapidly enough to keep the instability at the threshold? What then is the strength of the eddies? These are questions which may be answerable by numerical integration studies.

Knowledge of how vertical structures are modified by eddies constitutes a prerequisite for making dynamical numerical weather predictions. Consider a model which discretizes the vertical structure by a number of levels, and which has grid spacings of the order of hundreds of kilometers in the horizontal. If no allowance is made for the vertical adjustments by eddies of a smaller scale than the grid, ridiculous profiles and lapse rates may be developed. However, if the mechanism is understood and stratified empirical techniques have been developed, then not only could the vertical structure be adjusted to keep the evolution on the right track, but also useful predictions of turbulence and convective cloud formations may result.

It is hoped that such investigations will be undertaken. The numerical techniques to be used are themselves in need of further development.

If the behavioral properties of a differential system are not known and are being numerically investigated, then finite-difference approximations and the order of truncation error are of primary interest, and the concept of the limit is essential. However, in practice, in numerically integrating partial differential systems such as those which model atmospheric circulations, the precept that we are bound to finite differences generally exists. The differences must be the larger the faster we wish the integration to proceed relative to real time, and the concept of the limit as our increments tend to zero does not enter.

In practice we are concerned with the complete system of finite-difference equations as a numerical analogue of the complete differential system.

The procedure is to construct and modify a numerical analogue, having finite increments, until its behavioral properties resemble as closely as possible those of the given differential system. This requires a pretty good understanding of the differential system.

For some systems, exact numerical analogues can be derived. To illustrate this, let us take another look at the linear system

$$\frac{d}{dt}\, \underset{\sim}{q}(t) = -i\, \underset{\approx}{C}\, \underset{\sim}{q}(t) \tag{156}$$

We arrived, in Section 5, by what we shall call the finite-difference approach, at the analogue

$$\underset{\sim}{q}_{N+1} - \underset{\sim}{q}_N = -i\,\frac{\tau}{2}\,\underset{\approx}{C}\left[\underset{\sim}{q}_N + \underset{\sim}{q}_{N+1}\right], \tag{157}$$

which may be written in explicit form,

$$\underset{\sim}{q}_{N+1} = \underset{\approx}{D}\,\underset{\sim}{q}_N = \underset{\approx}{D}^{N+1}\,\underset{\sim}{q}_0, \tag{158}$$

where

$$\underset{\approx}{D} = \left(2\underset{\approx}{I} + i\tau\underset{\approx}{C}\right)^{-1}\left(2\underset{\approx}{I} - i\tau\underset{\approx}{C}\right). \tag{159}$$

Our analysis showed us that this analogue has <u>similar</u> properties to the differential system but that the prediction deteriorates with length of forecast.

If we abandon for the moment the finite-difference approach, we can, by a full appreciation of the properties of the differential system as revealed by its eigensolutions, arrive at a numerical analogue which exactly expresses the evolution. In terms of the eigenvectors and eigenvalues of the matrix $\underset{\approx}{C}$,

$$\underset{\sim}{q}_N = \sum_n \alpha_n \underset{\sim}{q}_n e^{-i\lambda_n N\tau} \tag{160}$$

gives the evolution of the initial vector

$$\underset{\sim}{q}_0 = \sum_n \alpha_n \underset{\sim}{q}_n$$

at intervals τ . If we now construct a matrix $\underset{\approx}{M}$ which has these same eigenvectors but has eigenvalues $e^{-i\lambda_n\tau}$, then

$$\underset{\sim}{q}_N = \underset{\approx}{M}^N \underset{\sim}{q}_0 = \underset{\approx}{M}\, \underset{\sim}{q}_{N-1} \tag{161}$$

which expresses Eq. (160) exactly, no matter the magnitude of τ .*

---

*It may be noticed that the expression, Eq. (161), resembles a linear regression formula in which the same set of parameters enters both as predictor and predictand. If it is justifiable to assume that the set of parameters is governed by an expression such as Eq. (156) then from an analysis of the matrix, which has been determined statistically, one may construct both the tendency matrix and a matrix to be used for any other time interval. Some difficulty, however, will be encountered in interpreting those stable eigensolutions which have undergone more than one oscillation in the data interval.

We have demonstrated that for certain simple differential systems exact (except for random round-off) numerical analogues are possible. We have also indicated that we should not be constrained by the finite-difference approach and the limit concept.

When dealing with nonlinear partial differential systems the problem becomes rather nebulous. We have no eigensolutions to guide us and we may know very little about the system. An attempt should be made to learn as much as possible about the behavioral properties of the systems. If limit cycles are understood these could perhaps be modeled by the analogue.

With little else to guide us in complicated systems, then perhaps the best we can do is to attempt to preserve physical continuity principals which may be inherent in the system. An example of this is Eq. (150), page 80, which attempts to preserve the conservation of total energy in a closed system. It is not yet clear how many such principals one can preserve simultaneously.

This last approach may lead to considerable success for General Circulation models (models which contain atmospheric forcing and friction terms and which are integrated to times far removed from the initial values). The problems are many.

ACKNOWLEDGEMENTS

Much of the work that has gone into this report, including the computations, was carried out while the author was associated with the "Dynamics of Simple Atmosphere Flow" project directed by Professor J. Holmboe, Department of Meteorology, University of California at Los Angeles (UCLA). This project has been supported by the Geophysics Research Directorate, Air Force Cambridge Research Center. The computations were carried out on the Standards Western Automatic Computer (SWAC), Numerical Analysis Research, UCLA. The support by the Office of Naval Research of the SWAC facility at UCLA is acknowledged.

The author is indebted to Professor Holmboe for his stimulation and interest in this work. Mr. F. Strauss of the project capably assisted in the calculations, the computing and the preparation of the figures.

BIBLIOGRAPHY

1. Garcia, R. V., Barotropic Waves in Straight Parallel Flow with Curved Velocity Profile. Tellus 8, pp. 82-93, (1956).
2. Holl, M. M., The Evolution of Perturbations Superimposed on Straight Parallel Flow, Dissertation, UCLA, (1956).
3. Holmboe, J., Straight Parallel Flow with Linear Profiles, Unpublished Technical Report, Final Report, Contr. W28-099 ac-403, Air Force Cambridge Research Center, (1953).
4. Hyman, M. A., On the Numerical Solution of Partial Differential Equations, Dissertation, Delft, (1953).
5. Lamb, H., Hydrodynamics, Sixth Edition, New York, Dover Publications, (1932).
6. Lin, C. C., The Theory of Hydrodynamic Stability, Cambridge University Press, (1955).
7. Milne, W. E., Numerical Solution of Differential Equations, New York, Wiley, (1953).
8. Rayleigh, Lord, On the Stability, or Instability, of Certain Fluid Motions, Scientific Papers, I, 474-87, Cambridge University Press, (1880).
9. Tollmien, W., Ein allgemeines Kriterium der Instabilitat laminarer Gesch windigkeitsverteilungen, Nachr. Geo. Wiss. Gottingen, Math. - phys. Klasse, 50, 79-114, (1935).
10. Young, D., Iterative Methods for Solving Partial Difference Equations of Elliptic Type, Amer. Math. Soc. Transactions, v 76, no. 1, (1954).

GEOPHYSICAL RESEARCH PAPERS

No. 1. Isotropic and Non-Isotropic Turbulence in the Atmospheric Surface Layer, Heinz Lettau, Geophysics Research Directorate, December 1949.

No. 2. Effective Radiation Temperatures of the Ozonosphere over New Mexico, Adel, Geophysics R-D, December 1949.

No. 3. Diffraction Effects in the Propagation of Compressional Waves in the Atmosphere, Norman A. Haskell, Geophysics Research Directorate, March 1950.

No. 4. Evaluation of Results of Joint Air Force-Weather Bureau Cloud Seeding Trials Conducted During Winter and Spring 1949, Charles E. Anderson, Geophysics Research Directorate, May 1950.

No. 5. Investigation of Stratosphere Winds and Temperatures From Acoustical Propagation Studies, Albert P. Crary, Geophysics Research Directorate, June 1950.

No. 6. Air-Coupled Flexural Waves in Floating Ice, F. Press, M. Ewing, A. P. Crary, S. Katz, and J. Oliver, Geophysics Research Directorate, November 1950.

No. 7. Proceedings of the Conference on Ionospheric Research (June 1949), edited by Bradford B. Underhill and Ralph J. Donaldson, Jr., Geophysics Research Directorate, December 1950.

No. 8. Proceedings of the Colloquium on Mesospheric Physics, edited by N. C. Gerson, Geophysics Research Directorate, July 1951.

No. 9. The Dispersion of Surface Waves on Multi-Layered Media, Norman A. Haskell, Geophysics Research Directorate, August 1951.

No. 10. The Measurement of Stratospheric Density Distribution with the Searchlight Technique, L. Elterman, Geophysics Research Directorate, December 1951.

No. 11. Proceedings of the Conference on Ionospheric Physics (July 1950) Part A, edited by N. C. Gerson and Ralph J. Donaldson, Jr., Geophysics Research Directorate, April 1952.

No. 12. Proceedings of the Conference on Ionospheric Physics (July 1950) Part B, edited by Ludwig Katz and N. C. Gerson, Geophysics Research Directorate, April 1952.

No. 13. Proceedings of the Colloquium on Microwave Meteorology, Aerosols and Cloud Physics, edited by Ralph J. Donaldson, Jr., Geophysics Research Directorate, May 1952.

No. 14. Atmospheric Flow Patterns and Their Representation by Spherical-Surface Harmonics, B. Haurwitz and Richard A. Craig, Geophysics Research Directorate, July 1952.

No. 15. Back-Scattering of Electromagnetic Waves From Spheres and Spherical Shells, A. L. Aden, Geophysics Research Directorate, July 1952.

No. 16. Notes on the Theory of Large-Scale Disturbances in Atmospheric Flow With Applications to Numerical Weather Prediction, Philip Duncan Thompson, Major, U. S. Air Force, Geophysics Research Directorate, July 1952.

GEOPHYSICAL RESEARCH PAPERS (Continued)

No. 17. The Observed Mean Field of Motion of the Atmosphere, Yale Mintz and Gordon Dean, Geophysics Research Directorate, August 1952.

No. 18. The Distribution of Radiational Temperature Change in the Northern Hemisphere During March, Julius London, Geophysics Research Directorate, December 1952.

No. 19. International Symposium on Atmospheric Turbulence in the Boundary Layer, Massachusetts Institute of Technology, 4-8 June 1951, edited by E. W. Hewson, Geophysics Research Directorate, December 1952.

No. 20. On the Phenomenon of the Colored Sun, Especially the "Blue" Sun of September 1950, Rudolf Penndorf, Geophysics Research Directorate, April 1953.

No. 21. Absorption Coefficients of Several Atmospheric Gases, K. Watanabe, Murray Zelikoff and Edward C. Y. Inn, Geophysics Research Directorate, June 1953.

No. 22. Asymptotic Approximation for the Elastic Normal Modes in a Stratified Solid Medium, Norman A. Haskell, Geophysics Research Directorate, August 1953.

No. 23. Forecasting Relationships Between Upper Level Flow and Surface Meteorological Processes, J. J. George, R. O. Roche, H. B. Visscher, R. J. Shafer, P. W. Funke, W. R. Biggers and R. M. Whiting, Geophysics Research Directorate, August 1953.

No. 24. Contributions to the Study of Planetary Atmospheric Circulations, edited by Robert M. White, Geophysics Research Directorate, November 1953.

No. 25. The Vertical Distribution of Mie Particles in the Troposphere, R. Penndorf, Geophysics Research Directorate, March 1954.

No. 26. Study of Atmospheric Ions in a Nonequilibrium System, C. G. Stergis, Geophysics Research Directorate, April 1954.

No. 27. Investigation of Microbarometric Oscillations in Eastern Massachusetts, E. A. Flauraud, A. H. Mears, F. A. Crowley, Jr., and A. P. Crary, Geophysics Research Directorate, May 1954.

No. 28. The Rotation-Vibration Spectra of Ammonia in the 6- and 10-Micron Regions, R. G. Breene, Jr., Capt., USAF, Geophysics Research Directorate, June 1954.

No. 29. Seasonal Trends of Temperature, Density, and Pressure in the Stratosphere Obtained With the Searchlight Probing Technique, Louis Elterman, July 1954.

No. 30. Proceedings of the Conference on Auroral Physics, edited by N. C. Gerson, Geophysics Research Directorate, July 1954.

No. 31. Fog Modification by Cold-Water Seeding, Vernon G. Plank, Geophysics Research Directorate, August 1954.

No. 32. Adsorption Studies of Heterogeneous Phase Transitions, S. J. Birstein, Geophysics Research Directorate, December 1954.

No. 33. The Latitudinal and Seasonal Variations of the Absorption of Solar Radiation by Ozone, J. Pressman, Geophysics Research Directorate, December 1954

No. 34. Synoptic Analysis of Convection in a Rotating Cylinder, D. Fultz and J. Corn, Geophysics Research Directorate, January 1955.

No. 35. Balance Requirements of the General Circulation, V. P. Starr and R. M. White, Geophysics Research Directorate, December 1954.

No. 36. The Mean Molecular Weight of the Upper Atmosphere, Warren E. Thompson, Geophysics Research Directorate, May 1955.

No. 37. Proceedings on the Conference on Interfacial Phenomena and Nucleation.
I. Conference on Nucleation.
II. Conference on Nucleation and Surface Tension.
III. Conference on Adsorption.
Edited by H. Reiss, Geophysics Research Directorate, July 1955.

No. 38. The Stability of a Simple Baroclinic Flow With Horizontal Shear, Leon S. Pocinki, Geophysics Research Directorate, July 1955.

No. 39. The Chemistry and Vertical Distribution of the Oxides of Nitrogen in the Atmosphere, L. Miller, Geophysics Research Directorate, April 1955.

No. 40. Near Infrared Transmission Through Synthetic Atmospheres, J. N. Howard, Geophysics Research Directorate, November 1955.

No. 41. The Shift and Shape of Spectral Lines, R. G. Breene, Geophysics Research Directorate, October 1955.

No. 42. Proceedings on the Conference on Atmospheric Electricity, R. Holzer, W. Smith, Geophysics Research Directorate, December 1955.

No. 43. Methods and Results of Upper Atmospheric Research, J. Kaplan, G. Schilling, H. Kallman, Geophysics Research Directorate, November 1955.

No. 44. Luminous and Spectral Reflectance as Well as Colors of Natural Objects, R. Penndorf, Geophysics Research Directorate, February 1956.

No. 45. New Tables of Mie Scattering Functions for Spherical Particles, R. Penndorf, B. Goldberg, Geophysics Research Directorate, March 1956.

No. 46. Results of Numerical Forecasting With the Barotropic and Thermotropic Models, W. Gates, L. S. Pocinki, C. F. Jenkins, Geophysics Research Directorate, April 1956.

No. 47. A Meteorological Analysis of Clear Air Turbulence (A Report on the U. S. Synoptic High-Altitude Gust Program), H. Lake, Geophysics Research Directorate, February 1956.

No. 48. A Review of Charge Transfer Processes in Gases, S. N. Ghosh, W. F. Sheridan, J. A. Dillon, Jr., and H. D. Edwards, Geophysics Research Directorate, July 1955.

No. 49. Theory of Motion of a Thin Metallic Cylinder Carrying a High Current, C. W. Dubs, Geophysics Research Directorate, October 1955.

No. 50. Hurricane Edna, 1954: Analysis of Radar, Aircraft, and Synoptic Data, E. Kessler, III and D. Atlas, Geophysics Research Directorate, July 1956.

No. 51. Cloud Refractive Index Studies, R. M. Cunningham, V. G. Plank, and C. F. Campen, Jr. Geophysics Research Directorate, October 1956.

No. 52. A Meteorological Study of Radar Angels, V. G. Plank, Geophysics Research Directorate, August 1956.

No. 53. The Construction and Use of Forecast Rejisters, I. Gringorten, I. Lund, M. Miller, Geophysics Research Directorate, June, 1956.

No. 54. Solar Geomagnetic Ionospheric Parameters as Indices of Solar Activity, F. Ward Jr., Geophysics Research Directorate, November, 1955.

No. 55. Preparation of Mutually Consistent Magnetic Charts, Paul Fougere, J. McClay, Geophysics Research Directorate, June 1957.

No. 56. Radar Synoptic Analysis of an Intense Winter Storm, Edwin Kessler III, Geophysics Research Directorate, October 1957.

No. 57. Mean Monthly 300- and 200-mb Contours and 500-, 300-, and 200-mb Temperatures for the Northern Hemisphere, E. W. Wahl, Geophysics Research Directorate, April 1958.

No. 58. Vol. I. Theory of Large-Scale Atmospheric Diffusion and its Application to Air Trajectories.
Vol. II. The Downstream Probability Density Function for Various Constant Values of Mean Zonal Wind.
Vol. III. The Downstream Probability Density Fucntion for North America and Eurasia by S. B. Solot and E. M. Darling, Jr., Geophysics Research Directorate, June 1958.

No. 59. Project Prairie Grass, A Field Program in Diffusion, edited by M. L. Barad, Geophysics Research Directorate, July 1958.

No. 60. Observations on Heavy Primary Cosmic Ray Nuclei Above the Atmosphere, H. Yagoda, Geophysics Research Directorate, July 1958.

UNCLASSIFIED

AD 209171

Air Force Cambridge Research Center
Geophysics Research Directorate
Bedford, Mass.

A NUMERICAL INVESTIGATION OF THE BAROTROPIC DEVELOPMENT OF EDDIES, by M. M. Holl, December 1958. 98 p. incl illus. (Geophysical Research Papers No. 61; AFCRC-TR-58-276). Unclassified Report

This paper deals with the formation of eddies in a straight parallel or zonal flow and with the subsequent modification of the flow profile. The fluid is taken to be homogeneous and inviscid. Numerical analogues for the physical equations are developed in detail and are analyzed.

The work begins with the linear theory of dynamic stability. Numerical analogues are developed to determine the evolution of perturbations, sinusoidal along the flow, which are initially prescribed with arbitrary wave number, amplitude, and tilt variations, and which are superimposed on arbitrary flows. These flows are straight-parallel and (over)

1. Weather forecasting -- numerical
2. Meteorology - Dynamic

I. Holl, M. M.

UNCLASSIFIED

UNCLASSIFIED

AD 209171

Air Force Cambridge Research Center
Geophysics Research Directorate
Bedford, Mass.

A NUMERICAL INVESTIGATION OF THE BAROTROPIC DEVELOPMENT OF EDDIES, by M. M. Holl, December 1958. 98 p. incl illus. (Geophysical Research Papers No. 61; AFCRC-TR-58-276). Unclassified Report

This paper deals with the formation of eddies in a straight parallel or zonal flow and with the subsequent modification of the flow profile. The fluid is taken to be homogeneous and inviscid. Numerical analogues for the physical equations are developed in detail and are analyzed.

The work begins with the linear theory of dynamic stability. Numerical analogues are developed to determine the evolution of perturbations, sinusoidal along the flow, which are initially prescribed with arbitrary wave number, amplitude, and tilt variations, and which are superimposed on arbitrary flows. These flows are straight-parallel and (over)

1. Weather forecasting -- numerical
2. Meteorology - Dynamic

I. Holl, M. M.

UNCLASSIFIED

UNCLASSIFIED

AD 209171

Air Force Cambridge Research Center
Geophysics Research Directorate
Bedford, Mass.

A NUMERICAL INVESTIGATION OF THE BAROTROPIC DEVELOPMENT OF EDDIES, by M. M. Holl, December 1958. 98 p. incl. illus. (Geophysical Research Papers No. 61; AFCRC-TR-58-276). Unclassified Report

This paper deals with the formation of eddies in a straight parallel or zonal flow and with the subsequent modification of the flow profile. The fluid is taken to be homogeneous and inviscid. Numerical analogues for the physical equations are developed in detail and are analyzed.

The work begins with the linear theory of dynamic stability. Numerical analogues are developed to determine the evolution of perturbations, sinusoidal along the flow, which are initially prescribed with arbitrary wave number, amplitude, and tilt vari

1. Weather forecasting -- numerical
2. Meteorology - Dynamic

I. Holl, M. M.

UNCLASSIFIED

AD 209171

Air Force Cambridge Research Center
Geophysics Research Directorate
Bedford, Mass.

A NUMERICAL INVESTIGATION OF THE BAROTROPIC DEVELOPMENT OF EDDIES, by M. M. Holl, December 1958. 98 p. incl. illus. (Geophysical Research Papers No. 61; AFCRC-TR-58-276). Unclassified Report

This paper deals with the formation of eddies in a straight parallel or zonal flow and with the subsequent modification of the flow profile. The fluid is taken to be homogeneous and inviscid. Numerical analogues for the physical equations are developed in detail and are analyzed.

The work begins with the linear theory of dynamic stability. Numerical analogues are developed to determine the evolution of perturbations, sinusoidal along the flow, which are initially prescribed with arbitrary wave number, amplitude, and tilt vari

1. Weather forecasting -- numerical
2. Meteorology - Dynamic

I. Holl, M. M.

AD 209171

are unbounded, or are half-bounded or bounded by plane surfaces. Integrations are carried out for an unbounded flow profile with an inflection point. Unstable perturbations are isolated and the unstable spectrum is determined.

A numerical analogue for the finite-amplitude problem, by which one can study the transfer of energy from the mean flow to the eddy is then developed. The most unstable perturbation, linearly determined, is taken as a small but finite disturbance. The integration is carried out and reveals the continued growth of the eddy and the modification of the mean flow.

This method of investigation with added lapse rate and compressibility is discussed as an approach to turbulence, and to the modification of wind shear and lapse rate by the developed eddies. The general problem of numerical analogues for integrations requiring finite time-steps is also briefly discussed.

UNCLASSIFIED

UNCLASSIFIED

AD 209171

are unbounded, or are half-bounded or bounded by plane surfaces. Integrations are carried out for an unbounded flow profile with an inflection point. Unstable perturbations are isolated and the unstable spectrum is determined.

A numerical analogue for the finite-amplitude problem, by which one can study the transfer of energy from the mean flow to the eddy is then developed. The most unstable perturbation, linearly determined, is taken as a small but finite disturbance. The integration is carried out and reveals the continued growth of the eddy and the modification of the mean flow.

This method of investigation with added lapse rate and compressibility is discussed as an approach to turbulence, and to the modification of wind shear and lapse rate by the developed eddies. The general problem of numerical analogues for integrations requiring finite time-steps is also briefly discussed.

UNCLASSIFIED

UNCLASSIFIED

AD 209171

are unbounded, or are half-bounded or bounded by plane surfaces. Integrations are carried out for an unbounded flow profile with an inflection point. Unstable perturbations are isolated and the unstable spectrum is determined.

A numerical analogue for the finite-amplitude problem, by which one can study the transfer of energy from the mean flow to the eddy is then developed. The most unstable perturbation, linearly determined, is taken as a small but finite disturbance. The integration is carried out and reveals the continued growth of the eddy and the modification of the mean flow.

This method of investigation with added lapse rate and compressibility is discussed as an approach to turbulence, and to the modification of wind shear and lapse rate by the developed eddies. The general problem of numerical analogues for integrations requiring finite time-steps is also briefly discussed.

UNCLASSIFIED

UNCLASSIFIED

AD 209171

are unbounded, or are half-bounded or bounded by plane surfaces. Integrations are carried out for an unbounded flow profile with an inflection point. Unstable perturbations are isolated and the unstable spectrum is determined.

A numerical analogue for the finite-amplitude problem, by which one can study the transfer of energy from the mean flow to the eddy is then developed. The most unstable perturbation, linearly determined, is taken as a small but finite disturbance. The integration is carried out and reveals the continued growth of the eddy and the modification of the mean flow.

This method of investigation with added lapse rate and compressibility is discussed as an approach to turbulence, and to the modification of wind shear and lapse rate by the developed eddies. The general problem of numerical analogues for integrations requiring finite time-steps is also briefly discussed.

UNCLASSIFIED

UNCLASSIFIED